



TOXICOLOGICAL REVIEW OF FORMALDEHYDE - INHALATION ASSESSMENT

(CAS No. 50-00-0)

**In Support of Summary Information on the
Integrated Risk Information System (IRIS)**

VOLUME I of IV

**Introduction, Background,
and Toxicokinetics**

June 2, 2010

NOTICE

This document is an *External Review draft*. This information is distributed solely for the purpose of pre-dissemination peer review under applicable information quality guidelines. It has not been formally disseminated by EPA. It does not represent and should not be construed to represent any Agency determination or policy. It is being circulated for review of its technical accuracy and science policy implications.

U.S. Environmental Protection Agency
Washington, DC

DISCLAIMER

This document is a preliminary draft for review purposes only. This information is distributed solely for the purpose of pre-dissemination peer review under applicable information quality guidelines. It has not been formally disseminated by EPA. It does not represent and should not be construed to represent any Agency determination or policy. Mention of trade names or commercial products does not constitute endorsement or recommendation for use.

This document is a draft for review purposes only and does not constitute Agency policy.

CONTENTS IN BRIEF

VOLUME I: INTRODUCTION, BACKGROUND, AND TOXICOKINETICS

- Chapter 1: Introduction
- Chapter 2: Background
- Chapter 3: Toxicokinetics

VOLUME II: HAZARD CHARACTERIZATION

- Chapter 4: Hazard Characterization

VOLUME III: QUANTITATIVE ASSESSMENT, MAJOR CONCLUSIONS IN THE CHARACTERIZATION OF HAZARD AND DOSE RESPONSE, AND REFERENCES

- Chapter 5: Quantitative Assessment: Inhalation Exposure
- Chapter 6: Major Conclusions in the Characterization of Hazard and Dose-Response
- References

VOLUME IV: APPENDICES

- Appendix A: Summary of External Peer Review and Public Comments and Dispositions
- Appendix B: Simulations of Interindividual and Adult-to-Child Variability in Reactive Gas Uptake in a Small Sample of People (Garcia et al., 2009)
- Appendix C: Lifetable Analysis
- Appendix D: Model Structure & Calibration in Conolly et al. (2003, 2004)
- Appendix E: Evaluation of BBDR Modeling of Nasal Cancer in the F344 Rat: Conolly et al. (2003) and Alternative Implementations
- Appendix F: Sensitivity Analysis of BBDR Model for Formaldehyde Induced Respiratory Cancer in Humans
- Appendix G: Evaluation of the Cancer Dose-Response Modeling of Genomic Data for Formaldehyde Risk Assessment
- Appendix H: Expert Panel Consultation on Quantitative Evaluation of Animal Toxicology Data for Analyzing Cancer Risk Due to Inhaled Formaldehyde

**CONTENTS—TOXICOLOGICAL REVIEW OF FORMALDEHYDE
(CAS No. 50-00-0)**

VOLUME I

LIST OF TABLES	I-xiv
LIST OF FIGURES	I-xxiv
LIST OF ABBREVIATIONS AND ACRONYMS.....	I-xxxii
FOREWORD	I-xxxvi
AUTHORS, CONTRIBUTORS, AND REVIEWERS.....	I-xxxvii
1. INTRODUCTION.....	1-1
2. BACKGROUND.....	2-1
2.1. PHYSICOCHEMICAL PROPERTIES OF FORMALDEHYDE	2-1
2.2. PRODUCTION, USES, AND SOURCES OF FORMALDEHYDE.....	2-1
2.3. ENVIRONMENTAL LEVELS AND HUMAN EXPOSURE	2-4
2.3.1. Inhalation	2-5
2.3.2. Ingestion.....	2-11
2.3.3. Dermal Contact	2-12
3. TOXICOKINETICS.....	3-1
3.1. CHEMICAL PROPERTIES AND REACTIVITY	3-1
3.1.1. Hydration of Formaldehyde.....	3-1
3.1.2. Binding of Formaldehyde to Proteins	3-2
3.2. ABSORPTION	3-4
3.2.1. Oral	3-4
3.2.2. Dermal.....	3-4
3.2.3. Inhalation	3-4
3.2.3.1. Formaldehyde Uptake Can Be Affected by Effects at the Portal of Entry	3-5
3.3. DISTRIBUTION	3-7
3.3.1. Transport of Methylene Glycol.....	3-7
3.3.2. Formaldehyde-GSH Conjugate as a Method of Systemic Distribution.....	3-8
3.3.3. Levels in Blood	3-8
3.3.4. Levels in Various Tissues	3-10
3.3.4.1. Disposition of Formaldehyde: Differentiating Covalent Binding and Metabolic Incorporation.....	3-12
3.4. METABOLISM.....	3-15
3.4.1. In Vitro and In Vivo Characterization of Formaldehyde Metabolism.....	3-15
3.4.2. Formaldehyde Exposure and Perturbation of Metabolic Pathways.....	3-19
3.4.3. Evidence for Susceptibility in Formaldehyde Metabolism.....	3-20
3.5. ENDOGENOUS SOURCES OF FORMALDEHYDE.....	3-21
3.5.1.1. Normal Cellular Metabolism (Enzymatic)	3-21
3.5.1.2. Normal Metabolism (Nonenzymatic)	3-23

This document is a draft for review purposes only and does not constitute Agency policy.

CONTENTS (continued)

- 3.5.1.3. Exogenous Sources of Formaldehyde Production 3-23
- 3.5.1.4. Metabolic Products of Formaldehyde Metabolism..... 3-24
- 3.5.1.5. Levels of Endogenous Formaldehyde in Animal and Human
Tissues 3-24
- 3.6. EXCRETION 3-26
 - 3.6.1. Formaldehyde Excretion in Rodents..... 3-27
 - 3.6.2. Formaldehyde Excretion in Exhaled Human Breath 3-28
 - 3.6.3. Formaldehyde Excretion in Human Urine..... 3-34
- 3.7. MODELING THE TOXICOKINETICS OF FORMALDEHYDE AND DPX 3-35
 - 3.7.1. Motivation..... 3-35
 - 3.7.2. Species Differences in Anatomy: Consequences for Gas Transport and Risk.. 3-35
 - 3.7.3. Modeling Formaldehyde Uptake in Nasal Passages..... 3-41
 - 3.7.3.1. Flux Bins..... 3-42
 - 3.7.3.2. Flux Estimates..... 3-42
 - 3.7.3.3. Mass Balance Errors 3-43
 - 3.7.4. Modeling Formaldehyde Uptake in the Lower Respiratory Tract..... 3-43
 - 3.7.5. Uncertainties in Formaldehyde Dosimetry Modeling 3-45
 - 3.7.5.1. Verification of Predicted Flow Profiles 3-45
 - 3.7.5.2. Level of Confidence in Formaldehyde Uptake Simulations..... 3-46
 - 3.7.6. PBPK Modeling of DNA Protein Cross-Links (DPXs) Formed by
Formaldehyde 3-49
 - 3.7.6.1. PBPK Models for DPXs 3-49
 - 3.7.6.2. A PBPK Model for DPXs in the F344 Rat and Rhesus Monkey
that Uses Local Tissue Dose of Formaldehyde 3-51
 - 3.7.6.3. Uncertainties in Modeling the Rat and Rhesus DPX Data 3-52
 - 3.7.7. Uncertainty in Prediction of Human DPX Concentrations..... 3-54
 - 3.7.8. Modeling Interindividual Variability in the Nasal Dosimetry of Reactive
and Soluble Gases..... 3-56

VOLUME II

- 4. HAZARD CHARACTERIZATION 4-1
 - 4.1. HUMAN STUDIES..... 4-1
 - 4.1.1. Noncancer Health Effects..... 4-1
 - 4.1.1.1. Sensory Irritation (Eye, Nose, Throat Irritation)..... 4-1
 - 4.1.1.2. Pulmonary Function 4-11
 - 4.1.1.3. Asthma..... 4-50
 - 4.1.1.4. Respiratory Tract Pathology..... 4-65
 - 4.1.1.5. Immunologic Effects 4-69
 - 4.1.1.6. Neurological/Behavioral 4-82
 - 4.1.1.7. Developmental and Reproductive Toxicity..... 4-85

This document is a draft for review purposes only and does not constitute Agency policy.

CONTENTS (continued)

4.1.1.8.	Oral Exposure Effects on the Gastrointestinal Tract.....	4-96
4.1.1.9.	Summary: Noncarcinogenic Hazard in Humans	4-96
4.1.2.	Cancer Health Effects.....	4-97
4.1.2.1.	Respiratory Tract Cancer.....	4-98
4.1.2.2.	Nonrespiratory Tract Cancer	4-134
4.1.2.3.	Summary: Carcinogenic Hazard in Humans	4-188
4.2.	ANIMAL STUDIES.....	4-191
4.2.1.	Reflex Bradypnea	4-192
4.2.1.1.	Tolerance	4-195
4.2.1.2.	Cross-Species Differences in Inhaled Dose	4-195
4.2.1.3.	Cross-Tolerance.....	4-198
4.2.1.4.	Formaldehyde Binding and Activation of Trigeminal Nerve Afferent Activity	4-199
4.2.2.	Respiratory Tract Pathology.....	4-201
4.2.2.1.	Mucociliary Clearance	4-202
4.2.2.2.	Cell Proliferation	4-209
4.2.2.3.	Short-Term Studies.....	4-226
4.2.2.4.	Subchronic Studies	4-240
4.2.2.5.	Chronic Inhalation Bioassays.....	4-260
4.2.2.6.	Summary of Respiratory Pathology and Carcinogenic Potential.....	4-286
4.2.3.	Gastrointestinal Tract Pathology	4-291
4.2.3.1.	Short-Term and Subchronic Ingestion Studies.....	4-291
4.2.3.2.	Chronic Ingestion Studies	4-294
4.2.3.3.	Summary of Gastrointestinal Effects and Evaluation of Carcinogenic Potential	4-300
4.2.4.	Immune Function	4-300
4.2.5.	Hypersensitivity and Atopic Reactions	4-309
4.2.5.1.	Inhalation Studies in Experimental Animals.....	4-311
4.2.5.2.	Dermal Sensitization	4-331
4.2.5.3.	Summary of Sensitization Studies.....	4-333
4.2.6.	Neurological and Neurobehavioral Function	4-338
4.2.6.1.	Inhalation Exposure.....	4-338
4.2.6.2.	Oral Exposure.....	4-367
4.2.6.3.	Summary.....	4-369
4.2.6.4.	Other Considerations	4-369
4.2.7.	Reproductive and Developmental Toxicity.....	4-370
4.2.7.1.	Inhalation Studies Addressing Developmental and Reproductive Toxicity	4-370
4.2.7.2.	Oral Exposure Studies Addressing Developmental and Reproductive Toxicity	4-387

This document is a draft for review purposes only and does not constitute Agency policy.

CONTENTS (continued)

- 4.2.7.3. Intraperitoneal Studies Addressing Developmental and Reproductive Toxicity 4-390
- 4.2.7.4. Dermal Exposure Studies Addressing Developmental and Reproductive Toxicity 4-392
- 4.2.7.5. Summary of Reproductive and Developmental Effects 4-393
- 4.3. GENOTOXICITY 4-406
 - 4.3.1. Formaldehyde-DNA Reactions 4-406
 - 4.3.1.1. DNA-Protein Cross-Links (DPXs)..... 4-409
 - 4.3.1.2. DNA Adducts 4-415
 - 4.3.1.3. DNA-DNA Cross-Links (DDXs)..... 4-418
 - 4.3.1.4. Single Strand Breaks 4-418
 - 4.3.1.5. Other Genetic Effects of Formaldehyde in Mammalian Cells 4-420
 - 4.3.2. In Vitro Clastogenicity 4-421
 - 4.3.3. In Vitro Mutagenicity 4-424
 - 4.3.3.1. Mutagenicity in Bacterial Systems..... 4-424
 - 4.3.3.2. Mutagenicity in Other Nonmammalian Cell Systems..... 4-429
 - 4.3.3.3. Mutagenicity in Mammalian Cell Systems 4-429
 - 4.3.4. In Vivo Mammalian Genotoxicity 4-435
 - 4.3.4.1. Genotoxicity in Laboratory Animals..... 4-435
 - 4.3.4.2. Genotoxicity in Humans..... 4-438
 - 4.3.5. Summary of Genotoxicity 4-448
- 4.4. SYNTHESIS AND MAJOR EVALUATION OF NONCARCINOGENIC EFFECTS 4-449
 - 4.4.1. Sensory Irritation..... 4-449
 - 4.4.2. Pulmonary Function 4-456
 - 4.4.3. Hypersensitivity and Atopic Reactions 4-460
 - 4.4.4. Upper Respiratory Tract Histopathology 4-465
 - 4.4.5. Toxicogenomic and Molecular Data that may Inform MOAs 4-467
 - 4.4.6. Noncancer Modes of Actions 4-468
 - 4.4.7. Immunotoxicity 4-471
 - 4.4.8. Effects on the Nervous System 4-472
 - 4.4.8.1. Irritant Threshold Detection 4-472
 - 4.4.8.2. Behavioral Effects 4-472
 - 4.4.8.3. Neurochemistry, Neuropathology, and Mechanistic Studies 4-473
 - 4.4.8.4. Summary..... 4-474
 - 4.4.8.5. Data Gaps 4-474
 - 4.4.9. Reproductive and Developmental Toxicity..... 4-475
 - 4.4.9.1. Spontaneous Abortion and Fetal Death..... 4-475
 - 4.4.9.2. Congenital Malformations..... 4-478
 - 4.4.9.3. Low Birth Weight and Growth Retardation 4-478
 - 4.4.9.4. Functional Developmental Outcomes 4-479
 - 4.4.9.5. Male Reproductive Toxicity..... 4-479

This document is a draft for review purposes only and does not constitute Agency policy.

CONTENTS (continued)

- 4.4.9.6. Female Reproductive Toxicity 4-481
- 4.4.9.7. Mode of Action 4-482
- 4.4.9.8. Data Gaps 4-484
- 4.5. SYNTHESIS AND EVALUATION OF CARCINOGENICITY 4-484
 - 4.5.1. Cancers of the Respiratory Tract..... 4-484
 - 4.5.2. Lymphohematopoietic Malignancies 4-489
 - 4.5.2.1. Background 4-489
 - 4.5.2.2. All LHP Malignancies..... 4-490
 - 4.5.2.3. All Leukemia..... 4-494
 - 4.5.2.4. Subtype Analysis..... 4-496
 - 4.5.2.5. Myeloid Leukemia 4-497
 - 4.5.2.6. Solid Tumors of Lymphoid Origin..... 4-500
 - 4.5.2.7. Supporting Evidence from Animal Bio-Assays for
Formaldehyde-Induced Lymphohematopoietic Malignancies 4-504
 - 4.5.3. Carcinogenic Mode(s) of Action..... 4-508
 - 4.5.3.1. Mechanistic Data for Formaldehyde 4-510
 - 4.5.3.2. Mode of Action Evaluation for Upper Respiratory Tract
Cancer (Nasopharyngeal Cancer, Sino-nasal)..... 4-521
 - 4.5.3.3. Mode(s) of Action for Lymphohematopoietic Malignancies..... 4-527
 - 4.5.4. Hazard Characterization for Formaldehyde Carcinogenicity..... 4-533
- 4.6. SUSCEPTIBLE POPULATIONS..... 4-535
 - 4.6.1. Life Stages 4-535
 - 4.6.1.1. Early Life Stages 4-536
 - 4.6.1.2. Later Life Stages 4-540
 - 4.6.1.3. Conclusions on Life-Stage Susceptibility 4-540
 - 4.6.2. Health/Disease Status 4-541
 - 4.6.3. Nutritional Status..... 4-542
 - 4.6.4. Gender Differences..... 4-543
 - 4.6.5. Genetic Differences..... 4-543
 - 4.6.6. Coexposures 4-545
 - 4.6.6.1. Cumulative Risk 4-545
 - 4.6.6.2. Aggregate Exposure 4-546
 - 4.6.7. Uncertainties of Database..... 4-546
 - 4.6.7.1. Uncertainties of Exposure 4-546
 - 4.6.7.2. Uncertainties of Effect..... 4-547
 - 4.6.8. Summary of Potential Susceptibility 4-548

This document is a draft for review purposes only and does not constitute Agency policy.

CONTENTS (continued)

VOLUME III

5. QUANTITATIVE ASSESSMENT: INHALATION EXPOSURE 5-1

5.1. INHALATION REFERENCE CONCENTRATION (RfC) 5-2

5.1.1. Candidate Critical Effects by Health Effect Category 5-3

5.1.1.1. Sensory Irritation of the Eyes, Nose, and Throat 5-3

5.1.1.2. Upper Respiratory Tract Pathology 5-5

5.1.1.3. Pulmonary Function Effects 5-6

5.1.1.4. Asthma and Allergic Sensitization (Atopy) 5-10

5.1.1.5. Immune Function 5-17

5.1.1.6. Neurological and Behavioral Toxicity 5-17

5.1.1.7. Developmental and Reproductive Toxicity 5-26

5.1.2. Summary of Critical Effects and Candidate RfCs 5-34

5.1.2.1. Selection of Studies for Candidate RfC Derivation 5-34

5.1.2.2. Derivation of Candidate RfCs from Key Studies 5-40

5.1.2.3. Evaluation of the Study-Specific Candidate RfCs 5-66

5.1.3. Database Uncertainties in the RfC Derivation 5-70

5.1.4. Uncertainties in the RfC Derivation 5-72

5.1.4.1. Point of Departure 5-73

5.1.4.2. Extrapolation from Laboratory Animal Data to Humans 5-74

5.1.4.3. Human Variation 5-74

5.1.4.4. Subchronic-to-Chronic Extrapolation 5-74

5.1.5. Previous Inhalation Assessment 5-75

5.2. QUANTITATIVE CANCER ASSESSMENT BASED ON THE NATIONAL
CANCER INSTITUTE COHORT STUDY 5-75

5.2.1. Choice of Epidemiology Study 5-76

5.2.2. Nasopharyngeal Cancer 5-78

5.2.2.1. Exposure-Response Modeling of the National Cancer
Institute Cohort 5-78

5.2.2.2. Prediction of Lifetime Extra Risk of Nasopharyngeal Cancer
Mortality 5-81

5.2.2.3. Prediction of Lifetime Extra Risk of Nasopharyngeal Cancer
Incidence 5-83

5.2.2.4. Sources of Uncertainty 5-85

5.2.3. Lymphohematopoietic Cancer 5-90

5.2.3.1. Exposure-Response Modeling of the National Cancer
Institute Cohort 5-90

5.2.3.2. Prediction of Lifetime Extra Risks for Hodgkin Lymphoma
and Leukemia Mortality 5-93

5.2.3.3. Prediction of Lifetime Extra Risks for Hodgkin Lymphoma
and Leukemia Incidence 5-96

5.2.3.4. Sources of Uncertainty 5-98

This document is a draft for review purposes only and does not constitute Agency policy.

CONTENTS (continued)

5.2.4.	Conclusions on Cancer Unit Risk Estimates Based on Human Data.....	5-102
5.3.	DOSE-RESPONSE MODELING OF RISK OF SQUAMOUS CELL CARCINOMA IN THE RESPIRATORY TRACT USING ANIMAL DATA	5-104
5.3.1.	Long-Term Bioassays in Laboratory Animals	5-108
5.3.1.1.	Nasal Tumor Incidence Data.....	5-108
5.3.1.2.	Mechanistic Data.....	5-110
5.3.2.	The CIIT Biologically Based Dose-Response Modeling	5-111
5.3.2.1.	Major Results of the CIIT Modeling Effort	5-115
5.3.3.	This Assessment’s Conclusions from Evaluation of Dose-Response Models of DPX, Cell-Replication and Genomics Data, and of BBDR Models for Risk Estimation.....	5-115
5.3.4.	Benchmark Dose Approaches to Rat Nasal Tumor Data	5-122
5.3.4.1.	Benchmark Dose Derived from BBDR Rat Model and Flux as Dosimeter	5-122
5.3.4.2.	Comparison with Other Benchmark Dose Modeling Efforts	5-129
5.3.4.3.	Kaplan-Meier Adjustment.....	5-132
5.3.4.4.	EPA Time-to-Tumor Statistical Modeling.....	5-132
5.4.	CONCLUSIONS FROM THE QUANTITATIVE ASSESSMENT OF CANCER RISK FROM FORMALDEHYDE EXPOSURE BY INHALATION ..	5-138
5.4.1.	Inhalation Unit Risk Estimates Based on Human Data.....	5-138
5.4.2.	Inhalation Unit Risk Estimates Based on Rodent Data.....	5-138
5.4.3.	Summary of Inhalation Unit Risk Estimates	5-139
5.4.4.	Application of Age-Dependent Adjustment Factors (ADAFs).....	5-140
5.4.5.	Conclusions: Cancer Inhalation Unit Risk Estimates	5-142
6.	MAJOR CONCLUSIONS IN THE CHARACTERIZATION OF HAZARD AND DOSE-RESPONSE	6-1
6.1.	SUMMARY OF HUMAN HAZARD POTENTIAL.....	6-1
6.1.1.	Exposure.....	6-1
6.1.2.	Absorption, Distribution, Metabolism, and Excretion	6-1
6.1.3.	Noncancer Health Effects in Humans and Laboratory Animals	6-4
6.1.3.1.	Sensory Irritation.....	6-4
6.1.3.2.	Respiratory Tract Pathology.....	6-6
6.1.3.3.	Effects on Pulmonary Function.....	6-8
6.1.3.4.	Asthmatic Responses and Increased Atopic Symptoms.....	6-9
6.1.3.5.	Effects on the Immune System.....	6-11
6.1.3.6.	Neurological Effects.....	6-11
6.1.3.7.	Reproductive and Developmental Effects.....	6-12
6.1.3.8.	Effects on General Systemic Toxicity.....	6-14
6.1.3.9.	Summary.....	6-14
6.1.4.	Carcinogenicity in Humans and Laboratory Animals	6-14
6.1.4.1.	Carcinogenicity in Humans	6-15

This document is a draft for review purposes only and does not constitute Agency policy.

CONTENTS (continued)

6.1.4.2.	Carcinogenicity in Laboratory Animals	6-21
6.1.4.3.	Carcinogenic Mode(s) of Action	6-22
6.1.5.	Cancer Hazard Characterization.....	6-25
6.2.	DOSE-RESPONSE CHARACTERIZATION.....	6-25
6.2.1.	Noncancer Toxicity: Reference Concentration (RfC).....	6-25
6.2.1.1.	Assessment Approach Employed.....	6-26
6.2.1.2.	Derivation of Candidate Reference Concentrations.....	6-26
6.2.1.3.	Adequacy of Overall Data Base for RfC Derivation.....	6-27
6.2.1.4.	Uncertainties in the Reference Concentration (RfC)	6-29
6.2.1.5.	Conclusions	6-32
6.2.2.	Cancer Risk Estimates.....	6-33
6.2.2.1.	Choice of Data.....	6-33
6.2.2.2.	Analysis of Epidemiologic Data.....	6-34
6.2.2.3.	Analysis of Laboratory Animal Data	6-36
6.2.2.4.	Extrapolation Approaches	6-37
6.2.2.5.	Inhalation Unit Risk Estimates for Cancer.....	6-41
6.2.2.6.	Early-Life Susceptibility	6-41
6.2.2.7.	Uncertainties in the Quantitative Risk Estimates.....	6-42
6.2.2.8.	Conclusions	6-44
6.3.	SUMMARY AND CONCLUSIONS.....	6-45
REFERENCES	R-1

VOLUME IV

APPENDIX A:	SUMMARY OF EXTERNAL PEER REVIEW AND PUBLIC COMMENTS AND DISPOSITIONS	A-2
APPENDIX B:	SIMULATIONS OF INTERINDIVIDUAL AND ADULT-TO-CHILD VARIABILITY IN REACTIVE GAS UPTAKE IN A SMALL SAMPLE OF PEOPLE (Garcia et al., 2009).....	B-2
APPENDIX C:	LIFETABLE ANALYSIS	C-2
APPENDIX D:	MODEL STRUCTURE & CALIBRATION IN CONOLLY ET AL. (2003, 2004).....	D-2
D.1.	DPX AND MUTATIONAL ACTION.....	D-4
D.2.	CALIBRATION OF MODEL.....	D-4
D.3.	FLUX BINS	D-5
D.4.	USE OF LABELING DATA	D-5
D.5.	UPWARD EXTRAPOLATION OF NORMAL CELL DIVISION RATE.....	D-5

This document is a draft for review purposes only and does not constitute Agency policy.

CONTENTS (continued)

D.6. INITIATED CELL DIVISION AND DEATH RATES	D-7
D.7. STRUCTURE OF THE CIIT HUMAN MODEL.....	D-7
APPENDIX E: EVALUATION OF BBDR MODELING OF NASAL CANCER IN THE F344 RAT: CONOLLY ET AL. (2003) AND ALTERNATIVE IMPLEMENTATIONS.....	
E-2	E-2
E.1. TABULATION OF ALL ISSUES EVALUATED IN THE RAT MODELS.....	E-2
E.2. STATISTICAL METHODS USED IN EVALUATION.....	E-7
E.3. PRIMARY UNCERTAINTIES IN BBDR MODELING OF THE F344 RAT DATA.....	E-8
E.3.1. Sensitivity to Use of Historical Controls.....	E-9
E.3.1.1. Use of Historical Controls.....	E-9
E.3.1.2. Influence of Historical Controls on Model Calibration and on Human Model.....	E-10
E.3.1.3. Influence of Historical Controls on Dose-Response Curve	E-13
E.3.1.4. Problem Including 1976 Study for Inhalation Historical Control.....	E-13
E.3.1.5. Effect of Control Data on MOA Inferences	E-14
E.3.2. Characterization of Uncertainty-Variability in Cell Replication Rates	E-14
E.3.2.1. Dose-Response for \square_N as Used in the CIIT Clonal Growth Modeling	E-14
E.3.2.2. Time Variability in Labeling Data	E-17
E.3.2.3. Site and Time Variability in Derived Cell Replication Rate.....	E-18
E.3.2.4. Alternate Dose-Response Curves for Cell Replication	E-22
E.3.3. Uncertainty in Model Specification of Initiated Cell Replication and Death	E-30
E.3.3.1. Biological Implications of Assumptions in Conolly et al. (2003)	E-30
E.3.3.2. Plausible Alternative Assumptions for α_I and β_I	E-32
E.3.4. Results of Sensitivity Analyses on α_N , α_I , and β_I	E-33
E.3.4.1. Further Constraints	E-33
E.3.4.2. Sensitivity of Risk Estimates for the F344 Rat	E-34
E.3.4.3. MOA Inferences Revisited.....	E-41
E.3.4.4. Confidence Bounds: Model Uncertainty Versus Statistical Uncertainty	E-42
APPENDIX F: SENSITIVITY ANALYSIS OF BBDR MODEL FOR FORMALDEHYDE INDUCED RESPIRATORY CANCER IN HUMANS	
F-2	F-2
F.1. MAJOR UNCERTAINTIES IN THE FORMALDEHYDE HUMAN BBDR MODEL.....	F-2

This document is a draft for review purposes only and does not constitute Agency policy.

CONTENTS (continued)

F.2. SENSITIVITY ANALYSIS OF HUMAN BBDR MODELING..... F-4

 F.2.1. Effect of Background Rates of Nasal Tumors in Rats on Human Risk
 Estimates F-4

 F.2.2. Alternative Assumptions Regarding the Rate of Replication of Initiated
 Cells..... F-6

 F.2.3. Biological Plausibility of Alternate Assumptions F-10

 F.2.4. Effect of Alternate Assumptions for Initiated Cell Kinetics on Human
 Risk Estimates F-13

APPENDIX G: EVALUATION OF THE CANCER DOSE-RESPONSE MODELING..... G-2

 G.1. MAJOR CONCLUSIONS IN ANDERSEN ET AL. (2008) G-2

 G.2. USE OF MULTIPLE FILTERS ON THE DATA G-3

 G.3. DATA FOR LOW-DOSE CANCER RESPONSE G-4

 G.4. DIFFICULTIES IN INTERPRETING THE BENCHMARK MODELING G-5

 G.5. STATISTICAL SENSITIVITY OF THE DATA FOR DOSE-RESPONSE..... G-6

 G.6. LENGTH OF THE STUDY AND STOCHASTIC EVENTS G-6

 G.7. OVERALL CONCLUSION..... G-7

APPENDIX H: EXPERT PANEL CONSULTATION ON QUANTITATIVE
EVALUATION OF ANIMAL TOXICOLOGY DATA FOR
ANALYZING CANCER RISK DUE TO INHALED
FORMALDEHYDE H-2

LIST OF TABLES

Table 2-1.	Physicochemical properties of formaldehyde	2-2
Table 2-2.	Ambient air levels by land use category	2-6
Table 2-3.	Studies on residential indoor air levels of formaldehyde (nonoccupational)	2-9
Table 3-1.	Formaldehyde kinetics in human and rat tissue samples	3-17
Table 3-2.	Allelic frequencies of ADH3 in human populations	3-18
Table 3-3.	Endogenous formaldehyde levels in animal and human tissues and body fluids .	3-25
Table 3-4.	Percent distribution of airborne [¹⁴ C]-formaldehyde in F344 rats.....	3-27
Table 3-5.	Measurements of exhaled formaldehyde concentrations in the mouth and nose, and in the oral cavity after breath holding in three healthy male laboratory workers	3-31
Table 3-6.	Formaldehyde, methanol and ethanol levels reported in the exhaled breath of 34 subjects	3-32
Table 3-7.	Apparent formaldehyde levels (ppb) in exhaled breath of individuals attending a health fair, adjusted for methanol and ethanol levels which contribute to the detection of the protonated species with a mass to charge ratio of 31 reported as formaldehyde ($m/z = 31$)	3-33
Table 3-8.	Extrapolation of parameters for enzymatic metabolism to the human	3-55
Table 4-1.	Epidemiologic studies of formaldehyde and pulmonary function	4-14
Table 4-2.	Major cohort studies of formaldehyde exposure and nasopharyngeal cancer	4-99
Table 4-3.	Case-control studies of formaldehyde exposure and nasopharyngeal cancer	4-102
Table 4-4.	Case-control studies of formaldehyde exposure and nasal and paranasal (sinonasal) cancers	4-122
Table 4-5.	Epidemiologic studies of formaldehyde and pharyngeal cancer.....	4-136
Table 4-6.	Comparison of SMRs in the exposed workers to the SMRs in the unexposed workers from NCI cohort reported by Beane-Freeman et al. (2009)	4-146
Table 4-7.	Epidemiologic studies of formaldehyde and lymphohematopoietic cancers	4-152

LIST OF TABLES (continued)

This document is a draft for review purposes only and does not constitute Agency policy.

Table 4-8. Respiratory effects of formaldehyde-induced reflex bradypnea in various strains of mice	4-193
Table 4-9. Respiratory effects of formaldehyde-induced reflex bradypnea in various strains of rats	4-194
Table 4-10. Inhaled dose of formaldehyde to nasal mucosa of F344 rats and B6C3F1 mice exposed to 15 ppm.....	4-197
Table 4-11. Exposure regimen for cross-tolerance study	4-198
Table 4-12. Summary of formaldehyde effects on mucociliary function in the upper respiratory tract	4-208
Table 4-13. Cell proliferation in nasal mucosa, trachea, and free lung cells isolated from male Wistar rats after inhalation exposures to formaldehyde	4-214
Table 4-14. The effect of repeated formaldehyde inhalation exposures for 3 months on cell count, basal membrane length, proliferation cells, and two measures of cell proliferation, LI and ULLI, in male F344 rats.....	4-217
Table 4-15. Formaldehyde-induced changes in cell proliferation (ULLI) in the nasal passages of male F344 rats exposed 6 hours/day	4-219
Table 4-16. Cell population and surface area estimates in untreated male F344 rats and regional site location of squamous cell carcinomas in formaldehyde-exposed rats for correlation to cell proliferation rates.....	4-220
Table 4-17. Summary of formaldehyde effects on cell proliferation in the upper respiratory tract	4-222
Table 4-18. Concentration regimens for ultrastructural evaluation of male CDF rat nasoturbinates	4-227
Table 4-19. Enzymatic activities in nasal respiratory epithelium of male Wistar rats exposed to formaldehyde, ozone, or both.....	4-229
Table 4-20. Lipid analysis of lung tissue and lung lavage from male F344 rats exposed to 0, 15, or 145.6 ppm formaldehyde for 6 hours.....	4-236
Table 4-21. Formaldehyde effects on biochemical parameters in nasal mucosa and lung tissue homogenates from male F344 rats exposed to 0, 15, or 145.6 ppm formaldehyde for 6 hours	4-237

LIST OF TABLES (continued)

This document is a draft for review purposes only and does not constitute Agency policy.

Table 4-22. Mast cell degranulation and neutrophil infiltration in the lung of rats exposed to formaldehyde via inhalation.....	4-238
Table 4-23. Summary of respiratory tract pathology from inhalation exposures to formaldehyde—short-term studies	4-241
Table 4-24. Location and incidence of respiratory tract lesions in B6C3F1 mice exposed to formaldehyde.....	4-244
Table 4-25. Formaldehyde effects (incidence and severity) on histopathologic changes in the noses and larynxes of male and female albino SPF Wistar rats exposed to formaldehyde 6 hours/day for 13 weeks.....	4-246
Table 4-26. Formaldehyde-induced nonneoplastic histopathologic changes in male albino SPF Wistar rats exposed to 0, 10, or 20 ppm formaldehyde and examined at the end of 130 weeks inclusive of exposure	4-247
Table 4-27. Formaldehyde-induced nasal tumors in male albino SPF Wistar rats exposed to formaldehyde (6 hours/day, 5 days/week for 13 weeks) and examined at the end of 130 weeks inclusive of exposure	4-248
Table 4-28. Formaldehyde effects on nasal epithelium for various concentration-by-time products in male albino Wistar rats.....	4-251
Table 4-29. Rhinitis observed in formaldehyde-treated animals; data pooled for male and female animals.....	4-253
Table 4-30. Epithelial lesions found in the middle region of nasoturbinates of formaldehyde-treated and control animals; data pooled for males and females.....	4-253
Table 4-31. Cellular and molecular changes in nasal tissues of F344 rats exposed to formaldehyde.....	4-255
Table 4-32. Percent body weight gain and concentrations of iron, zinc, and copper in cerebral cortex of male Wistar rats exposed to formaldehyde via inhalation for 4 and 13 weeks.....	4-256
Table 4-33. Zinc, copper, and iron content of lung tissue from formaldehyde-treated male Wistar rats.....	4-257
Table 4-34. Total lung cytochrome P450 measurements of control and formaldehyde-treated male Sprague-Dawley rats.....	4-258

LIST OF TABLES (continued)

Table 4-35. Cytochrome P450 levels in formaldehyde-treated rats 4-258

Table 4-36. Summary of respiratory tract pathology from inhalation exposures to formaldehyde, subchronic studies 4-261

Table 4-37. Histopathologic findings and severity scores in the naso- and maxilloturbinates of female Sprague-Dawley rats exposed to inhaled formaldehyde and wood dust for 104 weeks 4-265

Table 4-38. Histopathologic changes (including tumors) in nasal cavities of male Sprague-Dawley rats exposed to inhaled formaldehyde or HCl alone and in combination for a lifetime 4-269

Table 4-39. Summary of neoplastic lesions in the nasal cavity of F344 rats exposed to inhaled formaldehyde for 2 years 4-273

Table 4-40. Apparent sites of origin for the SCCs in the nasal cavity of F344 rats exposed to 14.3 ppm of formaldehyde gas in the Kerns et al. (1983) bioassay ... 4-273

Table 4-41. Incidence and location of nasal squamous cell carcinoma in male F344 rats exposed to inhaled formaldehyde for 2 years 4-275

Table 4-42. Summary of respiratory tract pathology from chronic inhalation exposures to formaldehyde 4-282

Table 4-43. Summary of lesions observed in the gastrointestinal tracts of Wistar rats after drinking-water exposure to formaldehyde for 4 weeks 4-293

Table 4-44. Incidence of lesions observed in the gastrointestinal tracts of Wistar rats after drinking-water exposure to formaldehyde for 2 years 4-296

Table 4-45. Effect of formaldehyde on gastroduodenal carcinogenesis initiated by MNNG and NaCl in male Wistar rats exposed to formaldehyde in drinking water for 8 weeks 4-299

Table 4-46. Battery of immune parameters and functional tests assessed in female B6C3F1 mice after a 3 week, 15-ppm formaldehyde exposure 4-302

Table 4-47. Summary of the effects of formaldehyde inhalation on the mononuclear phagocyte system (MPS) in female B6C3F1 mice after a 3 week, 15 ppm formaldehyde exposure (6 hours/day, 5 days/week) 4-303

Table 4-48. Formaldehyde exposure regimens for determining the effects of formaldehyde exposure on pulmonary *S. aureus* infection 4-305

This document is a draft for review purposes only and does not constitute Agency policy.

LIST OF TABLES (continued)

Table 4-49. Summary of immune function changes due to inhaled formaldehyde exposure in experimental animals 4-310

Table 4-50. Study design for guinea pigs exposed to formaldehyde through different routes of exposure: inhalation, dermal, and injection 4-316

Table 4-51. Sensitization response of guinea pigs exposed to formaldehyde through inhalation, topical application, or footpad injection..... 4-317

Table 4-52. Cytokine and chemokine levels in lung tissue homogenate supernatants in formaldehyde-exposed male ICR mice with and without Der f sensitization..... 4-324

Table 4-53. Correlation coefficients among ear swelling responses and skin mRNA levels in contact hypersensitivity to formaldehyde in mice 4-333

Table 4-54. Summary of sensitization and atopy studies by inhalation or dermal sensitization due to formaldehyde in experimental animals 4-335

Table 4-55. Fluctuation of behavioral responses when male AB mice inhaled formaldehyde in a single 2-hour exposure: effects after 2 hours 4-343

Table 4-56. Fluctuation of behavioral responses when male AB mice inhaled formaldehyde in a single 2-hour exposure: effects after 24 hours 4-343

Table 4-57. Effects of formaldehyde exposure on completion of the labyrinth test by male and female LEW.1K rats 4-347

Table 4-58. Summary of neurological and neurobehavioral studies of inhaled formaldehyde in experimental animals 4-363

Table 4-59. Effects of formaldehyde on body and organ weights in rat pups from dams exposed via inhalation from mating through gestation..... 4-373

Table 4-60. Formaldehyde effects on Leydig cell quantity and nuclear damage in adult male Wistar rats..... 4-382

Table 4-61. Formaldehyde effects on adult male albino Wistar rats 4-383

Table 4-62. Formaldehyde effects on testosterone levels and seminiferous tubule diameters in Wistar rats following 91 days of exposure 4-384

Table 4-63. Effects of formaldehyde exposure on seminiferous tubule diameter and epithelial height in Wistar rats following 18 weeks of exposure 4-386

This document is a draft for review purposes only and does not constitute Agency policy.

LIST OF TABLES (continued)

Table 4-64. Incidence of sperm abnormalities and dominant lethal effects in formaldehyde-treated mice..... 4-386

Table 4-65. Body weights of pups born to beagles exposed to formaldehyde during gestation..... 4-388

Table 4-66. Testicular weights, sperm head counts, and percentage incidence of abnormal sperm after oral administration of formaldehyde to male Wistar rats 4-389

Table 4-67. Effect of formaldehyde on spermatogenic parameters in male Wistar rats exposed intraperitoneally..... 4-391

Table 4-68. Incidence of sperm head abnormalities in formaldehyde-treated rats..... 4-392

Table 4-69. Dominant lethal mutations after exposure of male rats to formaldehyde 4-393

Table 4-70. Summary of reported developmental effects in formaldehyde inhalation exposure studies 4-395

Table 4-71. Summary of reported developmental effects in formaldehyde oral exposure studies 4-401

Table 4-72. Summary of reported developmental effects in formaldehyde dermal exposure studies 4-402

Table 4-73. Summary of reported reproductive effects in formaldehyde inhalation studies 4-403

Table 4-74. Summary of reported reproductive effects in formaldehyde oral studies 4-407

Table 4-75. Summary of reported reproductive effects in formaldehyde intraperitoneal studies 4-408

Table 4-76. Formaldehyde-DNA reactions (DPX formation)..... 4-410

Table 4-77. Formaldehyde-DNA reactions (DNA adduct formation)..... 4-416

Table 4-78. Formaldehyde-DNA interactions (single strand breaks)..... 4-419

Table 4-79. Other genetic effects of formaldehyde in mammalian cells..... 4-420

Table 4-80. In vitro clastogenicity of formaldehyde 4-422

LIST OF TABLES (continued)

This document is a draft for review purposes only and does not constitute Agency policy.

Table 4-81. Summary of mutagenicity of formaldehyde in bacterial systems	4-426
Table 4-82. Mutagenicity in mammalian cell systems	4-430
Table 4-83. Genotoxicity in laboratory animals	4-436
Table 4-84. MN frequencies in buccal mucosa cells of volunteers exposed to formaldehyde.....	4-440
Table 4-85. MN and SCE formation in mortuary science students exposed to formaldehyde for 85 days.....	4-441
Table 4-86. Incidence of MN formation in mortuary students exposed to formaldehyde for 90 days.....	4-442
Table 4-87. Multivariate repression models linking genomic instability/occupational exposures to selected endpoints from the MN assay.....	4-447
Table 4-88. Genotoxicity measures in pathological anatomy laboratory workers and controls	4-447
Table 4-89. Summary of human cytogenetic studies.....	4-450
Table 4-90. Summary of cohort and case-control studies which evaluated the incidence of all LHP cancers in formaldehyde-exposed populations and all leukemias.....	4-491
Table 4-91. Secondary analysis of published mortality statistics to explore alternative disease groupings within the broad category of all lymphohematopoietic malignancies	4-493
Table 4-92. Summary of studies which provide mortality statistics for myeloid leukemia subtypes	4-498
Table 4-93. Summary of mortality statistics for Hodgkin’s lymphoma, lymphoma and multiple myeloma from cohort analyses of formaldehyde exposed workers.....	4-501
Table 4-94. Leukemia incidence in Fischer 344 rats surviving at least 21 months.....	4-506
Table 4-95. Available evidence for susceptibility factors of concern for formaldehyde exposure.....	4-549
Table 5-1. Candidate points of departure (PODs) including duration adjustments for nervous system toxicity in key human and animal studies	5-7

LIST OF TABLES (continued)

This document is a draft for review purposes only and does not constitute Agency policy.

Table 5-2. Effects of formaldehyde exposure on completion of the labyrinth test by male and female LEW.1K rats	5-23
Table 5-3. Candidate PODs including duration adjustments for developmental and reproductive toxicity in key animal studies.....	5-28
Table 5-4. Summary of candidate studies for formaldehyde RfC development by health endpoint category	5-37
Table 5-5. Adjustment for nonoccupational exposures to formaldehyde.....	5-63
Table 5-6. Summary of reference concentration (RfC) derivation from critical study and supporting studies	5-67
Table 5-6. Summary of reference concentration (RfC) derivation from critical study and supporting studies (continued)	5-68
Table 5-7. Relative risk estimates for mortality from nasopharyngeal malignancies (ICD 8 code 147) by level of formaldehyde exposure for different exposure metrics	5-80
Table 5-8. Regression coefficients from NCI log-linear trend test models for NPC mortality from cumulative exposure to formaldehyde.....	5-81
Table 5-9. Extra risk estimates for NPC mortality from various levels of continuous exposure to formaldehyde	5-82
Table 5-10. EC0005, LEC0005, and inhalation unit risk estimates for NPC mortality from formaldehyde exposure based on the Hauptmann et al. (2004) log-linear trend analyses for cumulative exposure	5-83
Table 5-11. EC0005, LEC0005, and inhalation unit risk estimates for NPC incidence from formaldehyde exposure based on the Hauptmann et al. (2004) trend analyses for cumulative exposure.....	5-84
Table 5-12. Relative risk estimates for mortality from Hodgkin lymphoma (ICD 8 code 201) and leukemia (ICD 8 codes 204–207) by level of formaldehyde exposure for different exposure metrics	5-92
Table 5-13. Regression coefficients for Hodgkin lymphoma and leukemia mortality from NCI trend test models	5-93
Table 5-14. Extra risk estimates for Hodgkin lymphoma mortality from various levels of continuous exposure to formaldehyde	5-94

This document is a draft for review purposes only and does not constitute Agency policy.

LIST OF TABLES (continued)

Table 5-15. Extra risk estimates for leukemia mortality from various levels of continuous exposure to formaldehyde..... 5-94

Table 5-16. EC0005, LEC0005, and inhalation unit risk estimates for Hodgkin lymphoma mortality from formaldehyde exposure based on Beane Freeman et al. (2009) log-linear trend analyses for cumulative exposure 5-95

Table 5-17. EC005, LEC005, and inhalation unit risk estimates for leukemia mortality from formaldehyde exposure based on Beane Freeman et al. (2009) log-linear trend analyses for cumulative exposure 5-96

Table 5-18. EC0005, LEC0005, and inhalation unit risk estimates for Hodgkin lymphoma incidence from formaldehyde exposure, based on Beane Freeman et al. (2009) log-linear trend analyses for cumulative exposure 5-97

Table 5-19. EC005, LEC005, and inhalation unit risk estimates for leukemia incidence from formaldehyde exposure based on Beane Freeman et al. (2009) log-linear trend analyses for cumulative exposure 5-97

Table 5-20. Calculation of combined cancer mortality unit risk estimate at 0.1 ppm..... 5-103

Table 5-21. Calculation of combined cancer incidence unit risk estimate at 0.1 ppm 5-103

Table 5-22. Summary of tumor incidence in long-term bioassays on F344 rats 5-109

Table 5-23. BMD modeling of unit risk of SCC in the human respiratory tract 5-129

Table 5-24. Human benchmark extrapolations of nasal tumors in rats by using formaldehyde flux and DPX..... 5-132

Table 5-25. Formaldehyde-induced rat tumor incidences 5-133

Table 5-26. Summary of inhalation unit risk estimates 5-139

Table 5-27. Extra risk estimates per ppm based on ECs 5-140

Table 5-28. Total cancer risk from exposure to a constant formaldehyde exposure level of 1 µg/m³ from ages 0–70 years 5-141

Table 6-1. Summary of candidate reference concentrations (RfC) for cocritical studies..... 6-27

Table 6-2. Effective concentrations (lifetime continuous exposure levels) predicted for specified extra cancer risk levels for selected formaldehyde-related cancers..... 6-35

LIST OF TABLES (continued)

This document is a draft for review purposes only and does not constitute Agency policy.

Table 6-3. Inhalation unit risk estimates based on epidemiological and experimental animal data	6-41
Table B-1. Variations in overall nasal uptake, whole nose flux, and key parameters	B-4
Table C-1. Extra risk calculation for environmental exposure to 0.0461 ppm formaldehyde (the LEC0005 for NPC incidence) using a log-linear exposure-response model based on the cumulative exposure trend results of Hauptmann et al. (2004), as described in Section 5.2.2	C-3
Table E-1. Evaluation of assumptions and uncertainties in the CIIT model for nasal tumors in the F344 rat	E-3
Table E-2. Influence of control data in modeling formaldehyde-induced cancer in the F344 rat.....	E-11
Table E-3. Variation in number of cells across nasal sites in the F344 rat	E-20
Table E-4. Parameter specifications and estimates for clonal growth models of nasal SCC in the F344 rat using alternative characterization of cell replication and death rates	E-39
Table E-5. Parameter specifications and estimates for clonal growth models of nasal SCC in the F344 rat using cell replication and death rates as characterized in Conolly et al. (2003).....	E-40
Table E-6. Comparison of statistical confidence bounds on added risk for two models	E-42
Table F-1. Summary of evaluation of major assumptions and results in CIIT human BBDR model	F-3

LIST OF FIGURES

Figure 2-1. Chemical structure of formaldehyde.....	2-1
Figure 2-2. Locations of hazardous air pollutant monitors.	2-6
Figure 2-3. Modeled ambient air concentrations based on 1999 emissions.....	2-7
Figure 2-4. Range of formaldehyde air concentrations (ppb) in different environments.....	2-10
Figure 3-1. Formaldehyde-mediated protein modifications.	3-3
Figure 3-2. $^3\text{H}/^{14}\text{C}$ ratios in macromolecular extracts from rat tissues following exposure to ^{14}C - and ^3H -labeled formaldehyde	3-14
Figure 3-3. Formaldehyde clearance by ALDH2 (GSH-independent) and ADH3 (GSH-dependent).....	3-16
Figure 3-4. Metabolism of formate.....	3-18
Figure 3-5. Detection of the characteristic analytical product ion for formaldehyde by proton transfer reaction mass spectrometry (PTR-MS) in gas samples spiked with only methanol and ethanol	3-29
Figure 3-6. Reconstructed nasal passages of F344 rat, rhesus monkey, and human.....	3-37
Figure 3-7. Illustration of interspecies differences in airflow and verification of CFD simulations with water-dye studies.....	3-38
Figure 3-8. Lateral view of nasal wall mass flux of inhaled formaldehyde simulated in the F344 rat, rhesus monkey, and human.	3-39
Figure 3-9. CFD simulations of formaldehyde flux to human nasal lining at different inspiratory flow rates.	3-40
Figure 3-10. Single-path model simulations of surface flux per ppm of formaldehyde exposure concentration in an adult male human.....	3-44
Figure 3-11. Pressure drop vs. volumetric airflow rate predicted by the CIIT CFD model compared with pressure drop measurements made in two hollow molds of the rat nasal passage or in rats in vivo.....	3-46
Figure 3-12. Formaldehyde-DPX dosimetry in the F344 rat.....	3-48

LIST OF FIGURES (continued)

Figure 4-1. Delayed asthmatic reaction following the inhalation of formaldehyde after “painting” 100% formalin for 20 minutes	4-51
Figure 4-2. McGwin Forest plot of relative risk estimates and 95% CIs from studies included in a meta-analysis of formaldehyde exposure and asthma in children based on the random effects models.....	4-60
Figure 4-3. Association between peak formaldehyde exposure and the risk of lymphohematopoietic malignancy.....	4-148
Figure 4-4. Association between average intensity of formaldehyde exposure and the risk of lymphohematopoietic malignancy.....	4-149
Figure 4-5. Formaldehyde effects on minute volume in naïve and formaldehyde-pretreated male B6C3F1 mice and F344 rats.....	4-196
Figure 4-6. Sagittal view of the rat nose (nares oriented to the left).....	4-202
Figure 4-7. Main components of the nasal respiratory epithelium.....	4-203
Figure 4-8. Decreased mucus clearance and ciliary beat in isolated frog palates exposed to formaldehyde after 3 days in culture.....	4-207
Figure 4-9. Effect of formaldehyde exposure on cell proliferation of the respiratory mucosa of rats and mice.....	4-211
Figure 4-10. Diagram of nasal passages, showing section levels chosen for morphometry and autoradiography in male rhesus monkeys exposed to formaldehyde.....	4-233
Figure 4-11. Formaldehyde-induced cell proliferation in male rhesus monkeys exposed to formaldehyde.....	4-234
Figure 4-12. Formaldehyde-induced lesions in male rhesus monkeys exposed to formaldehyde.....	4-235
Figure 4-13. Frequency and location by cross-section level of squamous metaplasia in the nasal cavity of F344 rats exposed to formaldehyde via inhalation.....	4-272
Figure 4-14. Mortality corrected cumulative incidences of nasal carcinomas in the indicated exposure groups.....	4-290
Figure 4-15. Alveolar MP Fc-mediated phagocytosis from mice exposed to 5 ppm formaldehyde, 10 mg/m ³ carbon black, or both.....	4-307

This document is a draft for review purposes only and does not constitute Agency policy.

LIST OF FIGURES (continued)

Figure 4-16. Compressed air in milliliters as parameter for airway obstruction following formaldehyde exposure in guinea pigs after OVA sensitization and OVA challenge.....	4-319
Figure 4-17. OVA-specific IgG1 (1B) in formaldehyde-treated sensitized guinea pigs prior to OVA challenge.....	4-319
Figure 4-18. Anti-OVA titers in female Balb/C mice exposed to 6.63 ppm formaldehyde for 10 consecutive days or once a week for 7 weeks.....	4-320
Figure 4-19. Vascular permeability in the trachea and bronchi of male Wistar rats after 10 minutes of formaldehyde inhalation.....	4-322
Figure 4-20. Effect of select receptor antagonists on formaldehyde-induced vascular permeability in the trachea and bronchi male of Wistar rats.	4-323
Figure 4-21. The effects of formaldehyde inhalation exposures on eosinophil infiltration and goblet cell proliferation after Der f challenge in the nasal mucosa of male ICR mice after sensitization and challenge.	4-325
Figure 4-22. NGF in BAL fluid from formaldehyde-exposed female C3H/He mice with and without OVA sensitization.....	4-328
Figure 4-23. Plasma substance P levels in formaldehyde-exposed female C3H/He mice with and without OVA sensitization.....	4-329
Figure 4-24. Motor activity in male and female rats 2 hours after exposure to formaldehyde expressed as mean number of crossed quadrants \pm SEM.....	4-340
Figure 4-25. Habituation of motor activity was observed in control rats during the second observation period	4-341
Figure 4-26. Motor activity was reduced in male and female LEW.1K rats 2 hours after termination of 10-minute formaldehyde exposure.	4-342
Figure 4-27. The effects of the acute formaldehyde exposures on the ambulatory and vertical components of SLMA.....	4-344
Figure 4-28. Effects of formaldehyde exposure on the error rate of female LEW.1K rats performing the water labyrinth learning test.....	4-348
Figure 4-29. Basal and stress-induced trunk blood corticosterone levels in male LEW.1K rats after formaldehyde inhalation exposures.....	4-353

This document is a draft for review purposes only and does not constitute Agency policy.

LIST OF FIGURES (continued)

Figure 4-30. NGF production in the brains of formaldehyde-exposed mice.....	4-358
Figure 4-31. DNA-protein cross-links (DPX) and thymidine kinase (<i>tk</i>) mutants in TK6 human lymphoblasts exposed to formaldehyde for 2 hours.....	4-433
Figure 4-32. Developmental origins for cancers of the lymphohematopoietic system	4-489
Figure 4-33. Unscheduled deaths in female F344 rats exposed to formaldehyde for 24 months.....	4-506
Figure 4-34. Cumulative incidence of tumor bearing animals for lymphoma in female B6C3F1 mice exposed to formaldehyde for 24 months ($p < 0.05$).	4-507
Figure 4-35. Effect of various doses of formaldehyde on cell number in (A) HT-29 human colon carcinoma cells and in (B) human umbilical vein epithelial cells (HUVEC).....	4-515
Figure 4-36. Integrated MOA scheme for respiratory tract tumors.....	4-527
Figure 4-37. Location of intraepithelial lymphocytes along side epithelial cells in the human adenoid.	4-530
Figure 5-1. Change in number of additions made in 10 minutes following formaldehyde exposure at 0.04, 0.21, 0.48, or 1.1 mg/m ³	5-22
Figure 5-2. Effects of formaldehyde exposure on the error rate of female LEW.1K rats performing the water labyrinth learning test.....	5-25
Figure 5-3. Fecundity density ratio among women exposed to formaldehyde in the high exposure index category with 8 hour time-weighted average formaldehyde exposure concentration of 219 ppb.....	5-31
Figure 5-4. Estimated reduction in peak expiratory flow rate in children in relation to indoor residential formaldehyde concentrations.....	5-42
Figure 5-5. Odds ratios for physician-diagnosed asthma in children associated with in-home formaldehyde levels in air.	5-46
Figure 5-6. Prevalence of asthma and respiratory symptom scores in children associated with in-home formaldehyde levels.....	5-50
Figure 5-7. Prevalence and severity of allergic sensitization in children associated with in-home formaldehyde levels.....	5-50

This document is a draft for review purposes only and does not constitute Agency policy.

LIST OF FIGURES (continued)

Figure 5-8. Positive exposure-response relationships reported for in-home formaldehyde exposures and sensory irritation (eye irritation)	5-53
Figure 5-9. Positive exposure-response relationships reported for in-home formaldehyde exposures and sensory irritation (burning eyes)	5-54
Figure 5-10. Age-specific mortality and incidence rates for myeloid, lymphoid, and all leukemia.....	5-101
Figure 5-11. Schematic of integration of pharmacokinetic and pharmacodynamic components in the CIIT model.	5-106
Figure 5-12. Fit to the rat tumor incidence data using the model and assumptions in Conolly et al. (2003).	5-110
Figure 5-13. Spatial distribution of formaldehyde over the nasal lining, as characterized by partitioning the nasal surface by formaldehyde flux to the tissue per ppm of exposure concentration, resulting in 20 flux bins.....	5-124
Figure 5-14. Distribution of cells at risk across flux bins in the F344 rat nasal lining.....	5-124
Figure 5-15. MLE and upper bound added risk of SCC in the human nose for two BBDR models.	5-127
Figure 5-16. Replot of log-probit fit of the combined Kerns et al. and Monticello et al. data on tumor incidence showing BMC10 and BMCL10.	5-130
Figure 5-17. EPA Multistage Weibull modeling: nasal tumor dose response.....	5-135
Figure 5-18. Multistage Weibull model fit.	5-136
Figure 5-19. Multistage Weibull model fit of tumor incidence data compared with KM estimates of spontaneous tumor incidence.....	5-136
Figure B-1. Gas flux across the nasal lining for the case of a “maximum uptake” gas in Garcia et al. (2009) as a function of axial distance from the nostril	B-5
Figure D-1. Dose response of normal (α_N) and initiated (α_I) cell division rate in Conolly et al. (2003).....	D-6
Figure D-2. Flux dependence of ratio of initiated and normal cell replication rates (α_I/α_N) in CIIT model.	D-8
Figure E-1. ULLI data for pulse and continuous labeling studies.....	E-16

This document is a draft for review purposes only and does not constitute Agency policy.

LIST OF FIGURES (continued)

Figure E-2.	Logarithm of normal cell replication rate α_N versus formaldehyde flux or the F344 rat nasal epithelium.	E-19
Figure E-3A.	Logarithm of normal cell replication rate versus formaldehyde flux with simultaneous confidence limits for the ALM.	E-20
Figure E-3B.	Logarithm of normal cell replication rate versus formaldehyde flux with simultaneous confidence limits for the PLM	E-21
Figure E-4, N1.	Various dose-response modeling of normal cell replication rate.	E-25
Figure E-4, N2.	Various dose-response modeling of normal cell replication rate	E-25
Figure E-4, N3.	Various dose-response modeling of normal cell replication rate	E-26
Figure E-4, N4.	Various dose-response modeling of normal cell replication rate	E-26
Figure E-4, N5.	Various dose-response modeling of normal cell replication rate	E-27
Figure E-4, N6.	Various dose-response modeling of normal cell replication rate	E-28
Figure E-5A.	BBDR models for the rat—models with positive added risk.	E-35
Figure E-5B.	BBDR rat models resulting in negative added risk	E-36
Figure E-6A.	Models resulting in positive added rat risk: Dose-response for normal and initiated cell replication.	E-37
Figure E-6B.	Models resulting in negative added rat risk: Dose-response for normal and initiated cell replication	E-38
Figure F-1.	Effect of choice of NTP bioassays for historical controls on human risk.	F-5
Figure F-2.	Conolly et al. (2003) hockey-stick model for division rates of initiated cells in rats and two modified models.	F-7
Figure F-3.	Conolly et al. (2003) J shape model for division rates of initiated cells in rats and two modified models.	F-8
Figure F-4.	Very similar model estimates of probability of fatal tumor in rats for three models in Figure F-2.	F-9
Figure F-5.	Cell proliferation data from Meng et al. (2010).	F-12

LIST OF FIGURES (continued)

This document is a draft for review purposes only and does not constitute Agency policy.

Figure F-6. Graphs of the additional human risks estimated by applying these modified models for α_1 , using all NTP controls, compared to those obtained using the original Conolly et al. (2004) model.....F-13

Figure G-1. Graphs of epithelial hyperplasia versus formaldehyde concentration with 95% confidence intervals. G-7

LIST OF ABBREVIATIONS AND ACRONYMS

ACGIH	American Conference of Governmental Industrial Hygienists		response
ADAF	age-dependent adjustment factors	BC	bronchial construction
ADH	alcohol dehydrogenase	BCME	bis(chloromethyl)ether
ADS	anterior dorsal septum	BDNF	brain-derived neurotrophic factor
AGT	O ⁶ -alkylguanyl-DNA alkyltransferase	BEIR	biologic effects of ionizing radiation
AIC	Akaike Information Criterion	BfR	German Federal Institute for Risk Assessment
AIE	average intensity of exposure	BHR	bronchial hyperresponsiveness
AIHA	American Industrial Hygiene Association	BMC	benchmark concentration
ALB	albumin	BMCL	95% lower bound on the benchmark concentration
ALDH	aldehyde dehydrogenase	BMCR	binucleated micronucleated cell rate fluoresce
ALL	acute lymphocytic leukemia	BMD	benchmark dose
ALM	anterior lateral meatus	BMDL	95% lower bound on the benchmark dose
ALP	alkaline phosphatase	BMR	benchmark response
ALS	amyotrophic lateral sclerosis	BN	Brown-Norway
ALT	alanine aminotransferase	BrdU	bromodeoxyuridine
AML	acute myelogenous leukemia	BUN	blood urea nitrogen
AMM	anterior medial maxilloturbinate	BW	body weight
AMPase	adenosine monophosphatase	CA	chromosomal aberrations
AMS	anterior medial septum	CalEPA	California Environmental Protection Agency
ANAE	alpha-naphthylacetate esterase	CAP	College of American Pathologists
ANOVA	analysis of variance	CASRN	Chemical Abstracts Service Registry Number
APA	American Psychiatric Association	CAT	catalase
ARB	Air Resources Board	CBMA	cytokinesis-blocked micronucleus assay
AST	aspartate aminotransferase	CBMN	cytokinesis-blocked micronucleus
ATCM	airborne toxic control measure	CDC	U.S. Centers for Disease Control and Prevention
ATP	adenosine triphosphate	CDHS	California Department of Health Services
ATPase	adenosine triphosphatase	CFD	computational fluid dynamics
ATS	American Thoracic Society	CGM	clonal growth model
ATSDR	Agency for Toxic Substances and Disease Registry	CHO	Chinese hamster ovary
AUC	area under the curve		
BAL	bronchoalveolar lavage		
BALT	bronchus associated lymphoid tissue		
BBDR	biologically based dose		

This document is a draft for review purposes only and does not constitute Agency policy.

LIST OF ABBREVIATIONS AND ACRONYMS (continued)

CI	confidence interval	FEMA	Federal Emergency Management Agency
CIIT	Chemical Industry Institute of Toxicology	FEV1	forced expiratory volume in 1 second
CLL	chronic lymphocytic leukemia	FISH	fluorescent in situ hybridization
CML	chronic myelogenous leukemia	FSH	follicle-stimulating hormone
CNS	central nervous system	FVC	forced vital capacity
CO ₂	carbon dioxide	GALT	gut-associated lymphoid tissue
COEHHA	California Office of Environmental Health Hazard Assessment	GC-MS	gas chromatography-mass spectrometry
CREB	cyclic AMP responsive element binding proteins	GD	gestation day
CS	conditioned stimulus	GI	gastrointestinal
C × t	concentration times time	GO	gene ontology
DA	Daltons	G6PDH	glucose-6-phosphate dehydrogenase
DAF	dosimetric adjustment factor	GPX	glutathione peroxidase
DDC/DDX	DNA-DNA cross-links	GR	glutathione reductase
DEI	daily exposure index	GM-CSF	granulocyte macrophage-colony-stimulating factor
DEN	diethylnitrosamine	GSH	reduced glutathione
Der f	common dust mite allergen	GSNO	S-nitrosoglutathione
DMG	dimethylglycine	GST	glutathione S-transferase
DMGDH	dimethylglycine dehydrogenase	HAP	hazardous air pollutant
DNA	deoxyribonucleic acid	Hb	hemoglobin
DOPAC	3,4-dihydroxyphenylacetic acid	HCl	hydrochloric acid
DPC/DPX	DNA-protein cross-links	HCT	hematocrit
EBV	Epstein-Barr virus	HEC	human equivalent concentration
EC	effective concentration	5-HIAA	5-hydroxyindoleacetic acid
ED	effective dose	hm	hydroxymethyl
EHC	Environmental Health Committee	HMGSH	S-hydroxymethylglutathione
ELISA	enzyme-linked immunosorbent assay	HPA	hypothalamic-pituitary adrenal
EPA	U.S. Environmental Protection Agency	HPG	hypothalamo-pituitary-gonadal
ERPG	emergency response planning guideline	HPLC	high-performance liquid chromatography
ET	ethmoid turbinates	HPRT	hypoxanthine-guanine phosphoribosyltransferase
FALDH	formaldehyde dehydrogenase	HR	high responders
FDA	U.S. Food and Drug Administration	HSA	human serum albumin
FDR	fecundability density ratio	HSDB	Hazardous Substances Data Bank
FEF	forced expiratory flow	Hsp	heat shock protein
		HUVEC	human umbilical vein

This document is a draft for review purposes only and does not constitute Agency policy.

LIST OF ABBREVIATIONS AND ACRONYMS (continued)

	endothelial cell	MEF	maximal expiratory flow
HWE	healthy worker effect	ML	myeloid leukemia
I cell	initiated cell	MLE	maximum likelihood estimate
		MMS	methyl methane sulfonate
IARC	International Agency for Research on Cancer	MMT	medial maxilloturbinate
ICD	International Classification of Diseases	MN	micronucleus, micronuclei
IF	interfacial	MNNG	N-methyl-N'-nitro-N- nitrosoguanidine
IFN	interferon	MOA	mode of action
Ig	immunoglobulin	MoDC	monocyte-derived dendritic cell
IL	interleukin	MP	macrophage
I.P.	intraperitoneal	MPD	multistage polynomial degree
IPCS	International Programme on Chemical Safety	MPS	mononuclear phagocyte system
IRIS	Integrated Risk Information System	MRL	minimum risk level
K_m	Michaels-Menton constant	mRNA	messenger ribonucleic acid
KM	Kaplan-Meier	MVE-2	Murray Valley encephalitis virus
LD ₅₀	median lethal dose	MVK	Moolgavkar, Venzon, and Knudson
LDH	lactate dehydrogenase	N cell	normal cell
LEC	95% lower bound on the effective concentration	NaCl	sodium chloride
LED	95% lower bound on the effective dose	NAD+	nicotinamide adenine dinucleotide
LHP	lymphohematopoietic	NADH	reduced nicotinamide adenine dinucleotide
LI	labeling index	NALT	nasally associated lymphoid tissue
LM	Listeria monocytogenes	NATA	National-Scale Air Toxics Assessment
LMS	linearized multistage	NCEA	National Center for Environmental Assessment
LLNA	local lymph node assay	NCHS	National Center for Health Statistics
LOAEL	lowest-observed-adverse-effect level	NCI	National Cancer Institute
LPS	lipopolysaccharide	NEG	Nordic Expert Group
LR	low responders	NER	nucleotide excision repair
LRT	lower respiratory tract	NGF	nerve growth factor
MA	methylamine	NHL	non-Hodgkin's lymphoma
MALT	mucus-associated lymph tissues	NHMRC/ARMCANZ	National Health and Medical Research Council/Agriculture and Resource Management Council of Australia and New Zealand
MCH	mean corpuscular hemoglobin		
MCHC	mean corpuscular hemoglobin concentration		
MCS	multiple chemical sensitivity		
MCV	mean corpuscular volume		
MDA	malondialdehyde		

This document is a draft for review purposes only and does not constitute Agency policy.

LIST OF ABBREVIATIONS AND ACRONYMS (continued)

NNK	4-(methylnitrosamino)- 1-(3-pyridyl)-butanone	PEF	adhesion molecule peak expiratory flow
N ⁶ -hmdA	N ⁶ -hydroxymethyldeoxy- adenosine	PEFR	peak expiratory flow rates
N ⁴ -hmdC	N ⁴ -hydroxymethyldeoxy- cytidine	PEL	permissible exposure limit
N ² -hmdG	N ² -hydroxymethyldeoxy- guanosine	PFC	plaque-forming cell
NICNAS	National Industrial Chemicals Notification and Assessment Scheme	PG	periglomerular
NIOSH	National Institute for Occupational Safety and Health	PHA	phytohemagglutinin
NLM	National Library of Medicine	PLA2	phospholipase A2
NMDA	N-methyl-D-aspartate	PI	phagocytic index
NMU	N-methyl-N-nitrosourea	PLM	posterior lateral meatus
NNK	nitrosamine, 4- (methylnitrosamino)- 1-(3- pyridyl)-1-butanone	PMA	phorbol 12-myristate 13- acetate
NO	nitric oxide	PMR	proportionate mortality ratio
NOAEL	no-observed-adverse-effect level	PMS	posterior medial septum
NPC	nasopharyngeal cancer	PND	postnatal day
NRBA	neutrophil respiratory burst activity	POD	point of departure
NRC	National Research Council	POE	portal of entry
NTP	National Toxicology Program	PTZ	pentilenetetrazole
OR	odds ratio	PUFA	polyunsaturated fatty acids
OSHA	Occupational Safety and Health Administration	PWULLI	population weighted unit length labeling index
OTS	Office of Toxic Substances	RA	reflex apnea
OVA	ovalbumin	RANTES	regulated upon activation, normal T-cell expressed and secreted
PBPK	physiologically based pharmacokinetic	RB	reflex bradypnea
PC	Philadelphia chromosome	RBC	red blood cells
PCA	passive cutaneous anaphylaxis	RD ₅₀	exposure concentration that results in a 50% reduction in respiratory rate
PCMR	proportionate cancer mortality ratio	REL	recommended exposure limit
PCNA	proliferating cell nuclear antigen	RfC	reference concentration
PCR	polymerase chain reaction	RfD	reference dose
PCV	packed cell volume	RGD	regional gas dose
PECAM	platelet endothelial cell	RGDR	regional gas dose ratio
		RR	relative risk
		RT	reverse transcriptase
		SAB	Science Advisory Board
		SCC	squamous cell carcinoma
		SCE	sister chromatid exchange
		SCG	sodium cromoglycate
		SD	standard deviation
		SDH	succinate dehydrogenase; sarcosine dehydrogenase

This document is a draft for review purposes only and does not constitute Agency policy.

LIST OF ABBREVIATIONS AND ACRONYMS (continued)

SEER	Surveillance, Epidemiology, and End Results	TL	tail length
SEM	standard error of the mean	TLV	threshold limit value
SEN	sensitizer	TNF	tumor necrosis factor
SH	sulfhydryl	TP	total protein
SHE	Syrian hamster embryo	TRI	Toxic Release Inventory
SI	sensory irritation	TRPV	transient receptor potential vanilloid
SLMA	spontaneous locomotor activity	TWA	time-weighted average
SMR	standardized mortality ratio	TZCA	thiazolidine-4-carboxylate
SNP	single nucleotide polymorphism	UCL	upper confidence limit
SOD	superoxide dismutase	UDS	unscheduled DNA synthesis
SOMedA	N ⁶ -sulfomethyldeoxyadenosine	UF	uncertainty factor
SOMedG	N ² -sulfomethyldeoxyguanosine	UFFI	urea formaldehyde foam insulation
Sp1	specificity protein	ULLI	unit length labeling index
SPIR	standardized proportionate incidence ratio	URT	upper respiratory tract
SSAO	semicarbazide-sensitive amine oxidase	USDA	U.S. Department of Agriculture
SSB	single strand breaks	VC	vital capacity
STEL	short-term exposure limit	VOC	volatile organic compound
TBA	tumor bearing animal	WBC	white blood cell
TH	T-lymphocyte helper	WDS	wet dog shake
THF	tetrahydrofolate	WHO	World Health Organization
TK	toxicokinetics	WHOROE	World Health Organization Regional Office for Europe

FOREWORD

The purpose of this Toxicological Review is to provide scientific support and rationale for the hazard and dose-response assessment in IRIS pertaining to chronic inhalation exposure to formaldehyde. It is not intended to be a comprehensive treatise on the chemical or toxicological nature of formaldehyde.

In Chapter 6, *Major Conclusions in the Characterization of Hazard and Dose Response*, EPA has characterized its overall confidence in the qualitative and quantitative aspects of hazard and dose response by addressing knowledge gaps, uncertainties, quality of data, and scientific controversies. The discussion is intended to convey the limitations of the assessment and to aid and guide the risk assessor in the ensuing steps of the risk assessment process.

For other general information about this assessment or other questions relating to IRIS, the reader is referred to EPA's IRIS Hotline at (202) 566-1676 (phone), (202) 566-1749 (fax), or hotline.iris@epa.gov (email address).

AUTHORS, CONTRIBUTORS, AND REVIEWERS

CHEMICAL MANAGERS

John E. Whalan¹
EPA-ORD-NCEA

Danielle DeVoney²
EPA-ORD-NCEA

AUTHORS

Thomas Bateson
EPA-ORD-NCEA

Sue Makris
EPA-ORD-NCEA

Ravi Subramaniam
EPA-ORD-NCEA

Susan Euling
EPA-ORD-NCEA

Kathleen Raffaele
EPA-ORD-NCEA

Suryanarayana Vulimiri
EPA-ORD-NCEA

Jennifer Jinot
EPA-ORD-NCEA

John Schaum
EPA-ORD-NCEA

CONTRIBUTORS

Gillian Backus³
EPA-ORD-NCEA

John Fox
EPA-ORD-NCEA

Larry Valcovic³
EPA-ORD-NCEA

Stanley Barone
EPA-ORD-NCEA

Barbara Glenn
EPA-ORD-NCEA

John J. Vandenberg
EPA-ORD-NCEA

David Bayliss³
EPA-ORD-NCEA

Rosemarie Hakim³
EPA-ORD-NCEA

Lisa Vinikoor
EPA-ORD-NCEA

Ted Berner
EPA-ORD-NCEA

Karen Hogan
EPA-ORD-NCEA

Paul White
EPA-ORD-NCEA

David Bussard
EPA-ORD-NCEA

Babasaheb Sonawane
EPA-ORD-NCEA

David Farrar
EPA-ORD-NCEA

Chad Thompson³
EPA-ORD-NCEA

AUTHORS, CONTRIBUTORS, AND REVIEWERS (continued)

¹ Chemical Manager since July 2003.

² Chemical Manager since June 2009.

CONTRACTOR SUPPORT

The literature search and preliminary drafts of this document as well as support for editing and formatting were provided by Oak Ridge Institute for Science and Education (ORISE), Oak Ridge Associated Universities (ORAU), Department of Energy, under Interagency Agreement (IAG) Project No. 03-18. The ORISE individuals who contributed to this effort include Sheri Hester, George Holdsworth, Bobette D. Nourse, Wanda Olson, and Lutz W. Weber.

Assistance with the biologically based dose response model evaluation was provided by ENVIRON International Corporation of Monroe, Louisiana (subcontractors to ORISE; Project No. 03-18). The primary scientists involved in the work were Kenny S. Crump and Cynthia Van Landingham.

REVIEWERS

This document has been provided for review to EPA scientists and interagency reviewers from other federal agencies and White House Offices.

³ Separated from the Agency prior to final revisions to document.

AUTHORS, CONTRIBUTORS, AND REVIEWERS (continued)

INTERNAL EPA REVIEWERS

Daniel Axelrad, PhD
Office of Policy, Economics, and Innovation

Elizabeth Margosches, PhD
Office of Pollution Prevention and Toxics

Iris Camacho, PhD
Office of Pollution Prevention and Toxics

Timothy McMahon, PhD
Office of Pesticide Programs

Christina Cinalli, PhD
Office of Pollution Prevention and Toxics

Julie Migrin-Sturza, PhD
Office of Policy, Economics, and Innovation

Rebecca Edelstein, PhD
Office of Pollution Prevention and Toxics

Greg Miller, PhD
Office of Children's Health Protection and
Environmental Education

Ernest Falke, PhD
Office of Pollution Prevention and Toxics

Deirdre Murphy, PhD
Office of Air and Radiation

Stiven Foster, PhD
Office of Solid Waste and Emergency
Response

Marion Olson, PhD
EPA Region 2

Greg Fritz
Office of Pollution Prevention and Toxics

Andrea Pfahles-Hutchens, PhD
Office of Pollution Prevention and Toxics

Susan Griffin, PhD
EPA Region 8

Jennifer Seed, PhD
Office of Pollution Prevention and Toxics

Timothy Leighton, PhD
Office of Pesticide Programs

This document is a draft for review purposes only and does not constitute Agency policy.

I-xxxix DRAFT—DO NOT CITE OR QUOTE

This page intentionally left blank

1. INTRODUCTION

1
2
3 This document presents background information and justification for the Integrated Risk
4 Information System (IRIS) Summary of the hazard and dose-response assessment of
5 formaldehyde. IRIS Summaries may include oral reference dose (RfD) and inhalation reference
6 concentration (RfC) values for chronic and other exposure durations, and a carcinogenicity
7 assessment.

8 The RfD and RfC, if derived, provide quantitative information for use in risk assessments
9 for health effects known or assumed to be produced through a nonlinear (presumed threshold)
10 mode of action. The RfD (expressed in units of mg/kg-day) is defined as an estimate (with
11 uncertainty spanning perhaps an order of magnitude) of a daily exposure to the human
12 population (including sensitive subgroups) that is likely to be without an appreciable risk of
13 deleterious effects during a lifetime. The inhalation RfC (expressed in units of mg/m³) is
14 analogous to the oral RfD, but provides a continuous inhalation exposure estimate. The
15 inhalation RfC considers toxic effects for both the respiratory system (portal of entry [POE]) and
16 for effects peripheral to the respiratory system (extrarespiratory or systemic effects). Reference
17 values are generally derived for chronic exposures (up to a lifetime), but may also be derived for
18 acute (≤ 24 hours), short-term (> 24 hours up to 30 days), and subchronic (> 30 days up to 10% of
19 lifetime) exposure durations, all of which are derived based on an assumption of continuous
20 exposure throughout the duration specified. Unless specified otherwise, the RfD and RfC are
21 derived for chronic exposure duration.

22 The carcinogenicity assessment provides information on the carcinogenic hazard
23 potential of the substance in question and quantitative estimates of risk from oral and inhalation
24 exposure may be derived. The information includes a weight-of-evidence judgment of the
25 likelihood that the agent is a human carcinogen and the conditions under which the carcinogenic
26 effects may be expressed. Quantitative risk estimates may be derived from the application of a
27 low-dose extrapolation procedure. If derived, the oral slope factor is a plausible upper bound on
28 the estimate of risk per mg/kg-day of oral exposure. Similarly, an inhalation unit risk is a
29 plausible upper bound on the estimate of risk per $\mu\text{g}/\text{m}^3$ air breathed.

30 Development of these hazard identification and dose-response assessments for
31 formaldehyde has followed the general guidelines for risk assessment as set forth by the National
32 Research Council (NRC) (1983). EPA Guidelines and Risk Assessment Forum Technical Panel
33 Reports that may have been used in the development of this assessment include the following:
34 *Guidelines for the Health Risk Assessment of Chemical Mixtures* (U.S. EPA, 1986a), *Guidelines*
35 *for Mutagenicity Risk Assessment* (U.S. EPA, 1986b), *Recommendations for and Documentation*

This document is a draft for review purposes only and does not constitute Agency policy.

1 *of Biological Values for Use in Risk Assessment* (U.S. EPA, 1988), *Guidelines for*
2 *Developmental Toxicity Risk Assessment* (U.S. EPA, 1991), *Interim Policy for Particle Size and*
3 *Limit Concentration Issues in Inhalation Toxicity* (U.S. EPA, 1994a), *Methods for Derivation of*
4 *Inhalation Reference Concentrations and Application of Inhalation Dosimetry* (U.S. EPA,
5 1994b), *Use of the Benchmark Dose Approach in Health Risk Assessment* (U.S. EPA, 1995),
6 *Guidelines for Reproductive Toxicity Risk Assessment* (U.S. EPA, 1996), *Guidelines for*
7 *Neurotoxicity Risk Assessment* (U.S. EPA, 1998), *Science Policy Council Handbook: Risk*
8 *Characterization* (U.S. EPA, 2000a), *Benchmark Dose Technical Guidance Document* (U.S.
9 EPA, 2000b), *Supplementary Guidance for Conducting Health Risk Assessment of Chemical*
10 *Mixtures* (U.S. EPA, 2000c), *A Review of the Reference Dose and Reference Concentration*
11 *Processes* (U.S. EPA, 2002a), *Guidelines for Carcinogen Risk Assessment* (U.S. EPA, 2005a),
12 *Supplemental Guidance for Assessing Susceptibility from Early-Life Exposure to Carcinogens*
13 (U.S. EPA, 2005b), *Science Policy Council Handbook: Peer Review* (U.S. EPA, 2006a), and A
14 *Framework for Assessing Health Risks of Environmental Exposures to Children* (U.S. EPA,
15 2006b).

16 The literature search strategy employed for this compound was based on the Chemical
17 Abstracts Service Registry Number (CASRN) and at least one common name. Any pertinent
18 scientific information submitted by the public to the IRIS Submission Desk was also considered
19 in the development of this document. This assessment includes a comprehensive review of
20 literature through April 2009. As periodic literature searches are conducted by EPA for the
21 formaldehyde assessment, additional literature identified through December 2009 is included
22 where that literature was determined to be critical to the assessment. This included a few articles
23 which were identified through PubMed[®] searches and publically available as “e-publications” in
24 2009, but have final publication dates of 2010.

2. BACKGROUND

This chapter provides an overview of the physical and chemical characteristics of formaldehyde. Also provided in this chapter are a description of the production, uses, and sources of formaldehyde and information regarding environmental levels and human exposure. A description of the toxicokinetics and toxicodynamic processes involved in formaldehyde toxicity for the inhalation, oral, and dermal routes can be found in Chapter 3 (Toxicokinetics).

2.1. PHYSICOCHEMICAL PROPERTIES OF FORMALDEHYDE

Formaldehyde (CASRN 50-00-0) is the first of the series of aliphatic aldehydes and is a gas at room temperature. Its molecular structure is depicted in Figure 2-1. It is noted for its reactivity and versatility as a chemical intermediate. It readily undergoes polymerization, is highly flammable, and can form explosive mixtures with air. It decomposes at temperatures above 150°C.

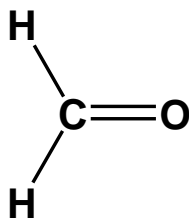


Figure 2-1. Chemical structure of formaldehyde.

At room temperature, pure formaldehyde is a colorless gas with a strong, pungent, suffocating, and highly irritating odor. Formaldehyde is readily soluble in water, alcohols, ether, and other polar solvents. A synopsis of its physicochemical properties is given in Table 2-1.

2.2. PRODUCTION, USES, AND SOURCES OF FORMALDEHYDE

Formaldehyde has been produced commercially since the early 1900s and, in recent years, has been ranked in the top 25 highest volume chemicals produced in the U.S. (National Toxicology Program [NTP], 2002). In 2003, 4.33 million metric tons of formaldehyde were produced in the U.S. (Global Insight, 2006). In 2000, worldwide formaldehyde production was estimated to be 21.5 million metric tons (International Agency for Research on Cancer [IARC], 2006).

This document is a draft for review purposes only and does not constitute Agency policy.

Table 2-1. Physicochemical properties of formaldehyde

Name	Formaldehyde
International Union for Pure and Applied Chemistry name	Formaldehyde
Synonyms	Formic aldehyde Methanal Methyl aldehyde Methylene oxide Oxomethane Oxymethylene
Chemical Abstracts Service Index name	Formaldehyde
Chemical Abstracts Service Registry Number	50-00-0
Formula	HCHO
Molecular weight	30.03
Density	Gas: 1.067 (air = 1) Liquid: 0.815 g/mL at -20°C
Vapor pressure	3,883 mm Hg at 25°C
Log K _{ow}	-0.75 to 0.35
Henry's law constant	3.4×10^{-7} atm-m ³ /mol at 25°C 2.2×10^{-2} Pa-m ³ /mol at 25°C
Conversion factors (25°C, 760 mm Hg)	1 ppm = 1.23 mg/m ³ (v/v) 1 mg/m ³ = 0.81 ppm (v/v)
Boiling point	-19.5°C at 760 mm Hg
Melting point	-92°C
Flash point	60°C; 83°C, closed cup for 37%, methanol-free aqueous solution; 50°C closed cup for 37% aqueous solution with 15% methanol
Explosive limits	73% upper; 7% lower by volume in air
Autoignition temperature	300°C
Solubility	Very soluble in water; soluble in alcohols, ether, acetone, benzene
Reactivity	Reacts with alkalis, acids and oxidizers

Sources: American Conference of Governmental Industrial Hygienists (ACGIH) (2002); International Programme on Chemical Safety (IPCS) (2002); Agency for Toxic Substances and Disease Registry (ATSDR) (1999); Gerberich and Seaman (1994); Walker (1975).

This document is a draft for review purposes only and does not constitute Agency policy.

1 Formaldehyde is a chemical intermediate used in the production of some plywood
2 adhesives, abrasive materials, insulation, foundry binders, brake linings made from phenolic
3 resins, surface coatings, molding compounds, laminates, wood adhesives made from melamine
4 resins, phenolic thermosetting, resin curing agents, explosives made from
5 hexamethylenetetramine, urethanes, lubricants, alkyd resins, acrylates made from
6 trimethylolpropane, plumbing components from polyacetal resins, and controlled-release
7 fertilizers made from urea formaldehyde concentrates (IPCS, 1989). Formaldehyde is used in
8 smaller quantities for the preservation and embalming of biological specimens. It is also used as
9 a germicide, an insecticide, and a fungicide in some products. It is found (as an ingredient or
10 impurity) in some cosmetics/personal hygiene products, such as some soaps, shampoos, hair
11 preparations, deodorants, sunscreens, dry skin lotions, and mouthwashes, mascara and other eye
12 makeup, cuticle softeners, nail creams, vaginal deodorants, and shaving cream (IPCS, 2002;
13 ATSDR, 1999).

14 Formaldehyde is commonly produced as an aqueous solution called formalin, which
15 usually contains about 37% formaldehyde and 12–15% methanol. Methanol is added to
16 formalin to slow polymerization that leads eventually to precipitation as paraformaldehyde.
17 Paraformaldehyde has the formula $(\text{CH}_2\text{O})_n$ where n is 8 to 100. It is essentially a solid form of
18 formaldehyde and therefore has some of the same uses as formaldehyde (Kiernan, 2000). When
19 heated, paraformaldehyde sublimates as formaldehyde gas. This characteristic makes it useful as a
20 fumigant, disinfectant, and fungicide, such as for the decontamination of laboratories,
21 agricultural premises, and barbering equipment. Long-chain polymers (e.g., Delrin plastic) are
22 less inclined to release formaldehyde, but they have a formaldehyde odor and require additives
23 to prevent decomposition (U.S. EPA, 2008).

24 The major sources of anthropogenic emissions of formaldehyde are motor vehicle
25 exhaust, power plants, manufacturing plants that produce or use formaldehyde or substances that
26 contain formaldehyde (i.e., adhesives), petroleum refineries, coking operations, incineration,
27 wood burning, and tobacco smoke. Among these anthropogenic sources, the greatest volume
28 source of formaldehyde is automotive exhaust from engines not fitted with catalytic converters
29 (NEG, 2003). The Toxic Release Inventory (TRI) data for 2007 show total releases of
30 21.9 million pounds with about half to the air and half to underground injection (EPA TRI
31 Explorer, <http://www.epa.gov/triexplorer/>) (U.S. EPA, 2009a).

32 Formaldehyde is formed in the lower atmosphere by photochemical oxidation of
33 hydrocarbons or other formaldehyde precursors that are released from combustion processes
34 (ATSDR, 1999). Formaldehyde can also be formed by a variety of other natural processes such

1 as decomposition of plant residues in the soil, photochemical processes in sea water and forest
2 fires (National Library of Medicine, 2001).

3 During smog episodes, indirect production of formaldehyde may be greater than direct
4 emissions (Fishbein, 1992). Grosjean et al. (1983) estimated the relative contributions of direct
5 emissions and atmospheric photochemistry to levels of formaldehyde and other carbonyls in Los
6 Angeles. They found that photochemical production predominates over direct emissions in
7 controlling formaldehyde levels in Los Angeles air. Using two models, their data were
8 translated into formaldehyde photochemical production rates of 12–161 tons per day.

9 Oxidation of methane is the dominant source of formaldehyde in regions remote from
10 hydrocarbon emissions (Staffelbach et al., 1991). Based on atmospheric measurements at a rural
11 site in Ontario, Canada and principal component analysis, Li et al. (1994) estimated that
12 formaldehyde production by atmospheric photochemical oxidation of hydrocarbons is
13 approximately 16 times that from primary emissions.

14 The input of formaldehyde into the environment is counterbalanced by its removal by
15 several pathways. Formaldehyde is removed from the air by direct photolysis and oxidation by
16 photochemically produced hydroxyl and nitrate radicals. Measured or estimated half-lives for
17 formaldehyde in the atmosphere range from 1.6 to 19 hours, depending upon estimates of radiant
18 energy, the presence and concentrations of other pollutants, and other factors (ATSDR, 1999).
19 Given the generally short daytime residence times for formaldehyde, there is limited potential for
20 long-range transport (IPCS, 2002). In cases where organic precursors are transported long
21 distances, however, secondary formation of formaldehyde may occur far from the anthropogenic
22 sources of the precursors.

23 Formaldehyde is released to water from the discharges of both treated and untreated
24 industrial wastewater from its production and from its use in the manufacture of formaldehyde-
25 containing resins (ATSDR, 1999). Formaldehyde is also a possible drinking-water disinfection
26 by-product from the use of ozone and/or hydrogen peroxide. In water, formaldehyde is rapidly
27 hydrated to form a glycol, and the equilibrium favors the glycol.

29 **2.3. ENVIRONMENTAL LEVELS AND HUMAN EXPOSURE**

30 General population exposure to formaldehyde can occur via inhalation, ingestion and
31 dermal contact. Each of these pathways and associated media levels are discussed below.
32 Formaldehyde exposure can also occur occupationally via three main scenarios:

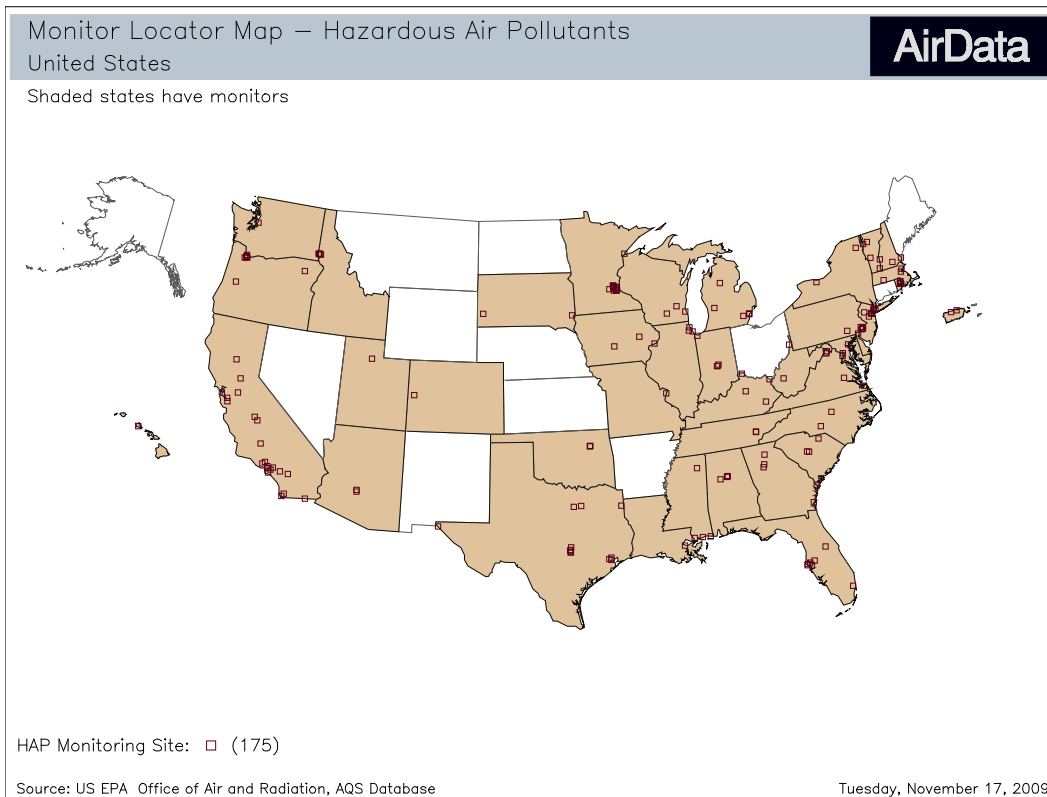
- 1 • The production of aqueous solutions of formaldehyde (formalin) and their use in the
2 chemical industry (e.g., for the synthesis of various resins, as a preservative in medical
3 laboratories and embalming fluids, and as a disinfectant).
- 4 • Release from formaldehyde-based resins in which it is present as a residue and/or
5 through their hydrolysis and decomposition by heat (e.g., during the manufacture of
6 wood products, textiles, synthetic vitreous insulation products, and plastics). In general,
7 the use of phenol-formaldehyde resins results in much lower emissions of formaldehyde
8 than those of urea- based resins.
- 9 • The pyrolysis or combustion of organic matter (e.g., in engine exhaust gases or during
10 firefighting) (IARC, 2006).

11
12 Industries with the greatest potential for exposure include health services, business
13 services, printing and publishing, manufacture of chemicals and allied products, manufacture of
14 apparel and allied products, manufacture of paper and allied products, personal services,
15 machinery (except clerical), transport equipment, and furniture and fixtures (IARC, 1995).

16 17 **2.3.1. Inhalation**

18 The most current ambient air monitoring data for formaldehyde come from EPA's air
19 quality system database (EPA's AirData Web site: <http://www.epa.gov/air/data/index.html>)
20 (U.S. EPA, 2009b). These data have been collected from a wide variety of sources, including
21 state and local environmental agencies, but have not been collected from a statistically based
22 survey. The most recent data, for the year 2007, come from 188 monitors located in 33 states as
23 shown in Figure 2-2 (U.S. EPA, 2008). The annual means for these monitors range from
24 0.7–45.03 $\mu\text{g}/\text{m}^3$ (0.56–36.31 ppb) and have an overall average of 3.44 $\mu\text{g}/\text{m}^3$ (2.77 ppb). The
25 annual means are derived by EPA by averaging all available daily data from each monitor.
26 Table 2-2 shows a breakout of the data by land use category based on the annual means from
27 each monitor for 2005, 2006, and 2007. The land use is established on the basis of the most
28 prevalent land use within 0.25 miles of the monitor. The mobile category (land near major
29 highways or interstates such that it is primarily impacted by mobile sources) has the highest
30 mean levels, and agricultural lands have the lowest.

31 Under the National-Scale Air Toxics Assessment (NATA) program, EPA has conducted
32 an emissions inventory for a variety of hazardous air pollutants (HAPs), including formaldehyde
33 (U.S. EPA, 2006c). The NATA uses the emissions inventory data to model nationwide air
34 concentrations/exposures (U.S. EPA, 2006c). The results of the 1999 ambient air concentration
35 modeling for formaldehyde suggest that county median air levels range from 0 to 6.94 $\mu\text{g}/\text{m}^3$
36 (0–5.59 ppb) with a national median of 0.56 $\mu\text{g}/\text{m}^3$ (0.45 ppb) (see Figure 2-3). Similar results



1 **Figure 2-2. Locations of hazardous air pollutant monitors.**
Dasgupta et al. (2005) measured formaldehyde levels in 5 U.S. cities during 1999–2002. Samples were collected over approximately a one month period in the spring or summer. Mean levels were 5.05 ppb in Nashville, TN; 7.96 ppb in Atlanta, GA; 4.49 ppb in Houston, TX; 3.12 ppb in Philadelphia, PA; and 2.63 in Sydney, FL.

2 **Table 2-2. Ambient air levels by land use category**

	Formaldehyde exposure by category ^a					
	Agriculture	Commercial	Forest	Industrial	Mobile ^b	Residential
Number of data points	17	166	19	61	16	282
Mean ± standard deviation	2.08 ± 0.98	3.26 ± 2.76	2.79 ± 2.17	6.28 ± 14.45	6.84 ± 7.28	2.75 ± 1.71
Minimum	0.34	0.20	0.40	0.14	2.02	0.17
Maximum	4.34	20.61	7.33	74.72	23.39	12.35

^aValues are µg/m³.

^b“Mobile” is ambient air in locations primarily impacted by mobile sources.

Source: AirData for 2005, 2006, and 2007 (U.S. EPA, 2009b).

3 *This document is a draft for review purposes only and does not constitute Agency policy.*

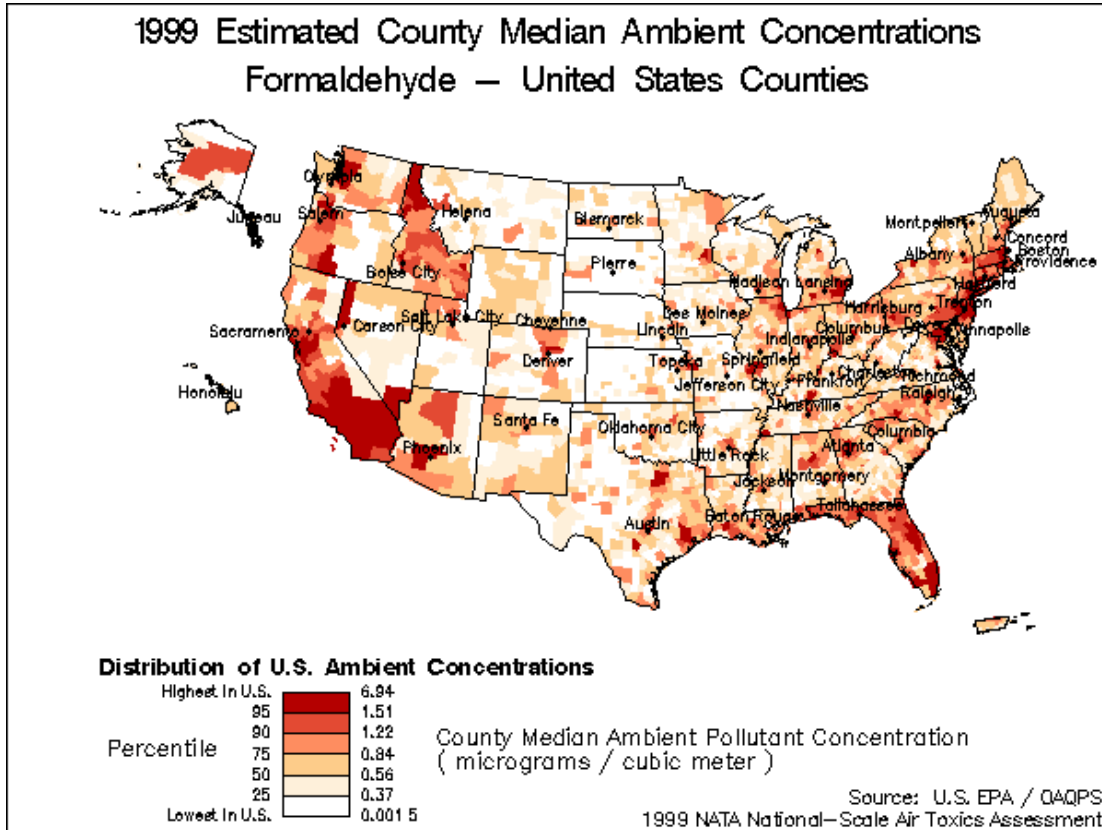


Figure 2-3. Modeled ambient air concentrations based on 1999 emissions.

were found for the year 2002: county concentrations ranged from 0.12 to 9.17 $\mu\text{g}/\text{m}^3$ (0.097–7.38 ppb) with median of 0.78 $\mu\text{g}/\text{m}^3$ (0.63 ppb). NATA has not provided updated concentration maps for 2002. The 1999 map shows the highest levels in the far west and northeastern regions of the U.S. While these modeling results can be useful, it is important to consider their limitations. Some of the geographical differences result from differences in methods used by states supplying the data. For example, the high levels indicated for Idaho result from the large amount of wood burned during forest fires and the relatively high emission factor that Idaho uses (compared with other states) to estimate formaldehyde emissions from forest fires. A comparison of modeling results from NATA to measured values at the same locations is presented in EPA (2006c). For 1999, it was found that formaldehyde levels were underestimated at 76% of the sites ($n = 68$). One possible reason why the NATA results appear low compared to measurements is that the modeling has not accounted for secondary formation of formaldehyde in the atmosphere.

In general, ambient levels of formaldehyde in outdoor air are significantly lower than those measured in the indoor air of workplaces or residences (ATSDR, 1999; IARC, 1995).

This document is a draft for review purposes only and does not constitute Agency policy.

1 Indoor sources of formaldehyde in air include volatilization from pressed wood products,
2 carpets, fabrics, insulation, permanent press clothing, latex paint, and paper bags, along with
3 emissions from gas burners, kerosene heaters, and cigarettes (NLM, 2001). In general, the major
4 indoor air sources of formaldehyde can be described in two ways: (1) those sources that have the
5 highest emissions when the product is new with decreasing emission over time, as with the first
6 set in the examples above; and (2) those sources that are reoccurring or frequent such as the
7 second set of examples above. Gilbert et al. (2006) studied 96 homes in Quebec City, Canada
8 and found elevated levels in homes with new wood or melamine furniture purchased within the
9 previous 12 months. A summary of indoor data is provided in Table 2-3. Results vary
10 depending on housing characteristics and date of study.

11 Salthammer et al. (2010) present a thorough review of formaldehyde sources and levels
12 found in the indoor environment. Based on an examination of international studies carried out in
13 2005 or later they conclude that the average exposure of the population to formaldehyde is 20 to
14 40 $\mu\text{g}/\text{m}^3$ under normal living conditions. They used the diagram shown in Figure 2-4 to
15 summarize data they found on the range of formaldehyde air concentrations (in ppb) in different
16 environments.

17 Data on formaldehyde levels in outdoor and indoor air were collected under Canada's
18 National Air Pollution Surveillance program (IPCS, 2002; Health Canada and Environment
19 Canada, 2001). The effort included four suburban and four urban sites sampled in the period
20 1990–1998. A Monte Carlo analysis applied to the pooled data ($n = 151$) was used to estimate
21 the distribution of time-weighted 24-hour air exposures. This study suggested that mean levels
22 in outdoor air were 3.3 $\mu\text{g}/\text{m}^3$ (2.7 ppb) and mean levels in indoor air were 35.9 $\mu\text{g}/\text{m}^3$
23 (29.2 ppb) (Health Canada and Environment Canada, 2001). The simulation analysis also
24 suggested that general population exposures averaged 33–36 $\mu\text{g}/\text{m}^3$ (27–30 ppb).

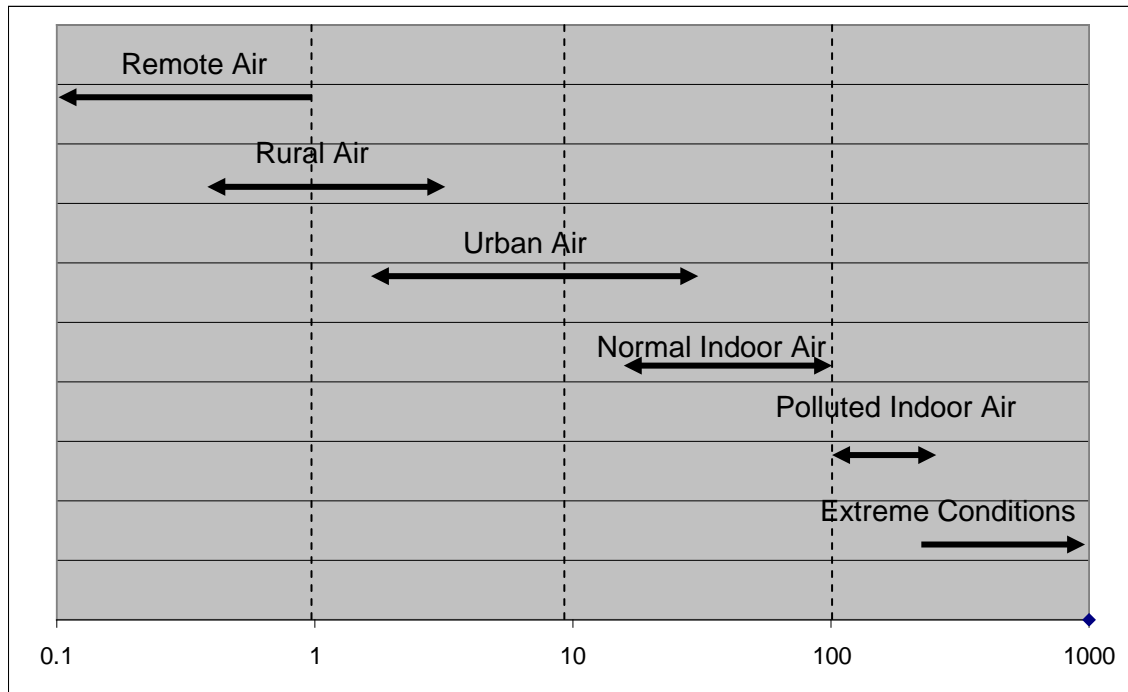
25 Since the early to mid 1980s, manufacturing processes and construction practices have
26 been changed to reduce levels of indoor formaldehyde emissions (ATSDR, 1999). A 2008 law
27 enacted by the California Air Resource Board (CARB, 2008, Final Regulation Order: Airborne
28 Toxic Control Measure to Reduce Formaldehyde Emissions from Composite Wood Products;
29 <http://www.arb.ca.gov/regact/2007/compwood07/fro-final.pdf>) has limited the amount of
30 formaldehyde that can be released by specific composite wood products (i.e., hardwood
31 plywood, particle board, and medium density fiberboard) sold, supplied, or manufactured for use
32 in California. For this reason the mean indoor air levels presented by Health Canada and
33 Environment Canada (2001) (based on samples collected from 1989–1995) may overestimate

1
2

Table 2-3. Studies on residential indoor air levels of formaldehyde (nonoccupational)

Citation	No. of samples	Target population/house type	Mean ($\mu\text{g}/\text{m}^3$)	Range ($\mu\text{g}/\text{m}^3$)
Gold et al., 1993		Complaint homes ¹ Older conventional homes	<60	24–960
Hare et al., 1996		Newly built homes	91	
Hare et al., 1996		30 days after installing pressed wood	42–540	
Gammage and Hawthorne, 1985	>1,200 131 >500 260	Homes with UFFI Homes without UFFI Complaint mobile homes Newer mobile homes Older mobile homes	60–144 30–84 120–1080 1032 300	12–4080 12–204 0–5040
Hawthorne et al., 1986a, b	18 11 11 40	Conventional homes 0–5 yr Conventional homes 5–15 yr Conventional homes >15 yr Conventional homes overall	96 48 36 72	24–480
U.S. EPA, 1987	560	Noncomplaint, conventional, randomly selected Noncomplaint, mobile homes, randomly selected	32–109 109–744	6–576 12–3480
Health Canada and Environment Canada, 2001	151	Residential (Canadian) noncomplaint homes	35	?–148
Zhang et al., 1994a, b	6	Residential, carpeted, nonsmoking homes	66	42–89
Gilbert et al., 2006	96	Residential (Canadian)	29.5	9.6–90.0
Shah and Singh, 1988	315	Residential and commercial	59	23–89
Stock, 1987	43	Conventional homes	84	96–216
Krzyzanowski et al., 1990	202	Conventional homes	31	

¹ The "complaint" homes are ones where the occupants have complained about formaldehyde irritant symptoms.
Note: 1 ppb = 1.2 $\mu\text{g}/\text{m}^3$.



1 **Figure 2-4. Range of formaldehyde air concentrations (ppb) in different**
 2 **environments.**

3
 4 Source: Salthammer et al. (2010).

5 current levels. In addition, the Canadian indoor air data may overestimate formaldehyde levels
 6 in U.S. homes, because many residential homes in Canada use wood burning stoves more
 7 frequently and have tighter construction (due to colder winters), leading to less dilution of indoor
 8 emissions. The outdoor air levels, however, appear to have remained fairly constant over recent
 9 years, and the median outdoor level from the Canadian study ($2.8 \mu\text{g}/\text{m}^3$) (2.3 ppb) is very
 10 similar to the median of the U.S. monitoring data ($2.83 \mu\text{g}/\text{m}^3$) (2.3 ppb) in 1999.

11 Even though formaldehyde levels in construction materials have declined, indoor
 12 inhalation concerns still persist. For example, recent studies have measured formaldehyde levels
 13 in mobile homes/trailers (these terms are used interchangeably here to refer to homes with
 14 wheels that are designed to be moved). ATSDR (2007) reported on air sampling in 96
 15 unoccupied trailers provided by the Federal Emergency Management Agency (FEMA) used as
 16 temporary housing for people displaced by Hurricane Katrina. Formaldehyde levels in closed
 17 trailers averaged $1,250 \pm 828 \mu\text{g}/\text{m}^3$ (mean \pm standard deviation [SD]) (1.04 ± 0.69 ppm), with a
 18 range of $12\text{--}4,390 \mu\text{g}/\text{m}^3$ (0.01–3.66 ppm). The levels decreased to an average of $468 \pm$

This document is a draft for review purposes only and does not constitute Agency policy.

1 324 $\mu\text{g}/\text{m}^3$ (0.39 ± 0.27 ppm), with a range of 0.00–1,960 $\mu\text{g}/\text{m}^3$ (0.00–1.63 ppm) when the air
2 conditioning was turned on. Levels also decreased to an average of 108 ± 96 $\mu\text{g}/\text{m}^3$ ($0.09 \pm$
3 0.08 ppm), with a range of 12–588 $\mu\text{g}/\text{m}^3$ (0.01–0.49 ppm) when the windows were opened.
4 ATSDR (2007) found an association between temperature and formaldehyde levels; higher
5 temperatures were associated with higher formaldehyde levels in trailers with the windows
6 closed. They also noted that different commercial brands of trailers yielded different
7 formaldehyde levels.

8 In December 2007 and January 2008, the Centers for Disease Control and Prevention
9 (CDC) measured formaldehyde levels in a stratified random sample of 519 FEMA-supplied
10 occupied travel trailers, park models, and mobile homes (“trailers”) (CDC, 2008). At the time of
11 the study, sampled trailers were in use as temporary shelters for Louisiana and Mississippi
12 residents displaced by hurricanes Katrina and Rita. The geometric mean level of formaldehyde
13 in sampled trailers was 95 $\mu\text{g}/\text{m}^3$ (77 ppb), and the range was 3.7–730 $\mu\text{g}/\text{m}^3$ (3–590 ppb).
14

15 **2.3.2. Ingestion**

16 Limited U.S. data indicate that concentrations in drinking water may range up to
17 approximately 10 $\mu\text{g}/\text{L}$ in the absence of specific contributions from the formation of
18 formaldehyde by ozonation during water treatment or from leaching of formaldehyde from
19 polyacetyl plumbing fixtures (IPCS, 2002). In the absence of other data, one-half this
20 concentration (5 $\mu\text{g}/\text{L}$) was judged to be a reasonable estimate of the average formaldehyde in
21 Canadian drinking water. Concentrations approaching 100 $\mu\text{g}/\text{L}$ were observed in a U.S. study
22 assessing the leaching of formaldehyde from domestic polyacetal plumbing fixtures, and this
23 concentration was assumed to be representative of a reasonable worst case (IPCS, 2002).

24 Formaldehyde is a natural component of a variety of foodstuffs (IARC, 1995; IPCS,
25 1989). However, foods may be contaminated with formaldehyde as a result of fumigation (e.g.,
26 grain fumigation), cooking (as a combustion product), and release from formaldehyde resin-
27 based tableware (IARC, 1995). Also, the compound has been used as a bacteriostatic agent in
28 some foods, such as cheese (IARC, 1995). There have been no systematic investigations of
29 levels of formaldehyde in a range of foodstuffs that could serve as a basis for estimation of
30 population exposure (Health Canada and Environment Canada, 2001). According to the limited
31 available data, concentrations of formaldehyde in food are highly variable. In the few studies of
32 the formaldehyde content of foods in Canada, the concentrations were within a range of
33 <0.03 –14 mg/kg (Health Canada and Environment Canada, 2001). Data on formaldehyde levels
34 in food have been presented by Feron et al. (1991) and IPCS (1989) from a variety of studies,
35 yielding the following ranges of measured values:

This document is a draft for review purposes only and does not constitute Agency policy.

- 1 • Fruits and vegetables: 3–60 mg/kg
- 2 • Meat and fish: 6–20 mg/kg
- 3 • Shellfish: 1–100 mg/kg
- 4 • Milk and milk products: 1–3.3 mg/kg

5
6 Daily intake of formaldehyde was estimated by IPCS (1989) to be in the range of
7 1.5–14 mg for an average adult. Similarly, Fishbein (1992) estimated that the intake of
8 formaldehyde from food is 1–10 mg/day but discounted this on the belief that it is not available
9 in free form. Although the bioavailability of formaldehyde from the ingestion of food is not
10 known, it is not expected to be significant (ATSDR, 1999). Using U.S. Department of
11 Agriculture (USDA) (1979) consumption rate data for various food groups, Owen et al. (1990)
12 calculated that annual consumption of dietary formaldehyde results in an intake of about
13 4,000 mg or approximately 11 mg/day.

14

15 **2.3.3. Dermal Contact**

16 The general population may have dermal contact with formaldehyde-containing
17 materials, such as some building products and cosmetics (see Section 2.2 for the details on these
18 products). Generally, though, dermal contact is more of a concern in occupations that involve
19 handling concentrated forms of formaldehyde, such as those occurring in embalming and
20 chemical production.

21

3. TOXICOKINETICS

This chapter presents chemical specific information on the toxicokinetics of formaldehyde which helps to inform the potential for health effects from formaldehyde exposure. As a water soluble and reactive gas (see Chapter 2), the chemical reactions of formaldehyde at the site of first contact in biological systems is important to understanding its toxic potential. Therefore, before a discussion of the absorption, distribution, and metabolism of formaldehyde (which normally comprises the heart of the toxicokinetic discussion of an agent) a section is provided which discusses some key issues regarding formaldehyde's reactivity. Section 3.1 provides information regarding the hydration of formaldehyde in biological aqueous systems and the equilibrium which exists between free formaldehyde and methylene glycol. Additional information is provided on what is known of the nature of chemical reactions of free formaldehyde with proteins. These discussions are provided to give context to the following Sections of Chapter 3.

Sections 3.2 and 3.3 present the available studies which describe the absorption and distribution of formaldehyde, including animal studies of radiolabeled formaldehyde. The influence of formaldehyde's reactivity at the site of first contact and effects on the mucociliary apparatus are presented here as well, as these effects may modify the uptake of formaldehyde. Metabolism of formaldehyde is presented in Section 3.4, but the endogenous production of formaldehyde from normal metabolic processes, as well as metabolism of other xenobiotics. The last section of Chapter 3 present the available models which apply to the toxicokinetics of formaldehyde—in this case primarily modeling of the flux of formaldehyde through tissues at the site of first contact using computational fluid dynamics models.

3.1. CHEMICAL PROPERTIES AND REACTIVITY

Formaldehyde (HCHO) is the smallest aldehyde (30 g/mol) and is a gas at room temperature. It is highly water soluble and reactive. In water, less than 0.1% of formaldehyde exists unhydrated, with the majority reported to be in the hydrated form, methylene glycol (CH₂(OH)₂) (Priha et al., 1996). Formaldehyde reacts readily with high and low molecular weight biological constituents.

3.1.1. Hydration of Formaldehyde

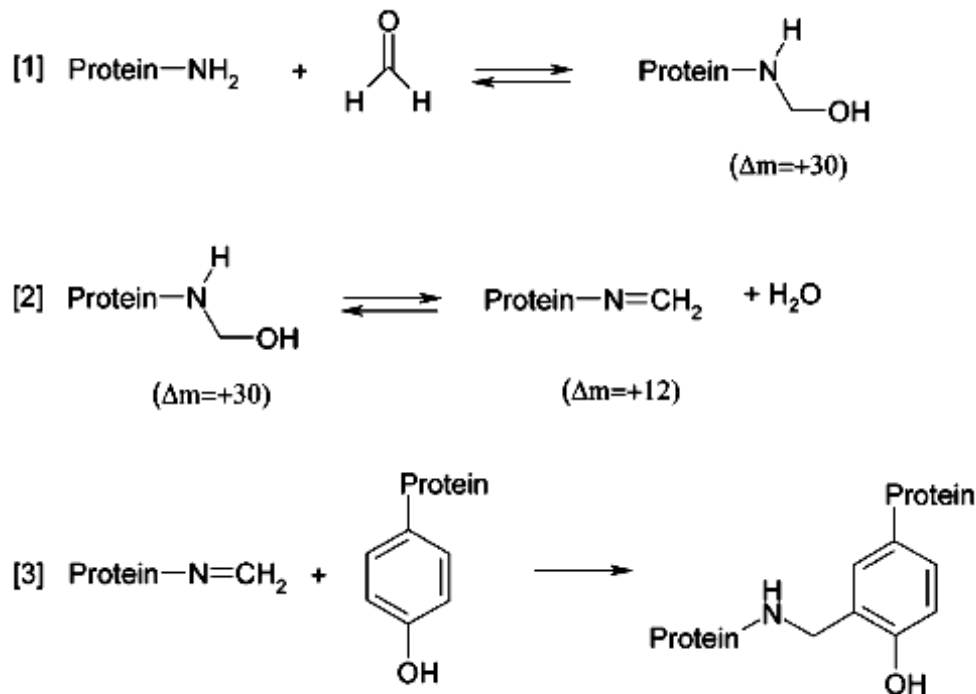
In aqueous solution formaldehyde exists in equilibrium with its hydrated form methanediol (CH₂OH₂) ($K_d = 5.5 \times 10^{-4}$). The equilibrium favors methanediol at physiological

1 temperature and pH (>99.9%) and is readily reversible. In biological systems, as free
2 formaldehyde is removed from aqueous solution through binding with serum proteins and
3 cellular components, the equilibrium is reestablished by dehydration of methanediol to free
4 formaldehyde. The reversible nature of this hydration reaction describes how a pool of free
5 formaldehyde may be sustained in biological systems.

6 7 **3.1.2. Binding of Formaldehyde to Proteins**

8 Formaldehyde is a reactive molecule that is likely to react with both low molecular
9 weight cellular components (e.g., reduced glutathione[GSH]) as well as high molecular weight
10 components. Unlike deoxyribonucleic acid (DNA), which has some additional barriers to
11 exposure (i.e., nucleus), extracellular and intracellular proteins are obvious targets for interacting
12 with formaldehyde. Formaldehyde is a well-known cross-linking agent that is used in the
13 fixation of tissues, preparation of vaccines, and study of protein-protein interactions (Metz et al.,
14 2006). However, the exact nature of the protein modifications used for these purposes is not yet
15 fully characterized (Metz et al., 2006, 2004). Figure 3-1 provides a general reaction scheme for
16 formaldehyde-mediated modifications of amino acids. In step 1, formaldehyde reacts with
17 primary N-terminal amines to form a labile methylol adduct. This adduct can undergo
18 dehydration (step 2) to form an imine, or Schiff base ($-N=CH_2$). Metz et al. (2004) examined
19 the types of formaldehyde-protein reactions that are likely to occur in vivo by synthesizing
20 several identical polypeptides with one varying amino acid (X) within the sequence VELXVLL
21 (V = valine, E = glutamate, L = Leucine, X = varying amino acid). Several peptides with
22 reactive amino acids did not exhibit modifications, suggesting that the peptide sequence/structure
23 affects the ability of formaldehyde to react with amino acids. Peptides that were modified
24 indicated formation of methylol adducts (see Figure 3-1, step 1) or a mixture of methylol and
25 imine adducts (see Figure 3-1, step 2).

26 Mucus is composed of water, electrolytes, polysaccharides, and about 0.5% soluble
27 proteins (Priha et al., 1996; Bogdanffy et al., 1987). Bogdanffy et al. (1987) showed that
28 although human nasal mucus can bind 70% of 100 mM formaldehyde, irreversible binding of
29 [^{14}C]-formaldehyde to serum albumin (the major protein in mucus) was shown to be insignificant
30 after a 1-hour incubation. Irreversible binding (50% or more) did not occur until after about
31 7 hours of incubation. These data suggest that the protein content of mucus may not provide a
32 significant formaldehyde irreversible sink. Nonetheless, the solubility of formaldehyde in mucus
33 along with mucus flow and ingestion likely indicate that much of the inhaled dose is removed—
34 perhaps as much as 42% in rodents (IARC, 2005; Schlosser, 1999).



1 **Figure 3-1. Formaldehyde-mediated protein modifications.**

Note: Formaldehyde reacts with primary *N*-terminal amines to form a methylol adduct [1], which increases the molecular weight by 30 Da (Δm). This labile adduct can rearrange to form an amine, or Schiff base [2], that results in an increase in MW of 12 Da. Schiff bases can react with certain amino acids to form intra- or intermolecular methylene bridges [3]. The two amino acids depicted in step 3 may be within the same protein or possibly from two different proteins.

Source: Metz et al. (2004).

2 In general, formaldehyde interacts with proteins. Studies carried out in cell culture media
 3 containing serum and formaldehyde have shown that such mixtures are quite labile. For
 4 example, during a 60-minute incubation of formaldehyde with complete cell media (i.e., with
 5 fetal calf serum) at 38°C, gas chromatography-mass spectrometry (GC-MS) exhibited very
 6 different peak profiles at different points during the incubation (Proctor et al., 1986). In contrast,
 7 GC-MS chromatograms of cell media containing formaldehyde but no serum proteins appeared
 8 relatively unchanged throughout the incubation. Compared to cell culture medium alone,
 9 complete media were considered to provide a more suitable model for the hypothetical
 10 interactions that formaldehyde could undergo in vivo (including perhaps blood).
 11

This document is a draft for review purposes only and does not constitute Agency policy.

1 **3.2. ABSORPTION**

2 **3.2.1. Oral**

3 Oral absorption of [¹⁴C]-formaldehyde (7 mg/kg) in rats resulted in 40% elimination as
4 ¹⁴C-carbon dioxide (¹⁴CO₂), with 10% excretion in urine, 1% excretion in feces, and much of the
5 remaining 49% retained within the carcass, presumably due to metabolic incorporation (IARC,
6 1995; Buss et al., 1964).

7 **3.2.2. Dermal**

8 Jeffcoat et al. (1983) reported on the disposition of various doses of [¹⁴C]-formaldehyde
9 dermally administered to rats, guinea pigs, and monkeys. Very little (<1% of the applied dose)
10 of the radiolabel was found in the major organs excised during necropsy. As noted by the
11 authors, the disposition of formaldehyde when administered via the dermal route was markedly
12 different to that observed when the compound was administered intravenously or
13 intraperitoneally. In the latter cases, there was much evidence of metabolic activity, and
14 substantial portions of the load were expired as CO₂. The difference appeared to be the result of
15 a reaction of dermally applied formaldehyde with macromolecules at or near the skin surface or
16 of its evaporation. In general, portions of the load that succeed in entering the circulation
17 probably do so bound to macromolecules or by incorporation of the radiolabel via the one-
18 carbon pool. Likewise, Bartnik et al. (1985) who applied [¹⁴C]-formaldehyde to the shaved
19 backs of rats concluded that the overwhelming majority of the formaldehyde load remained
20 sequestered in the outer layers of skin at or near the site of application. At the end of the various
21 measurements, approximately 70% of the dose was found in the treated skin, with a marked
22 localization of the remaining radioactivity in the uppermost layers. This fraction of the load was
23 considered to be permanently sequestered, most likely as a result of irreversible binding to
24 macromolecular components.

25

26 **3.2.3. Inhalation**

27 Studies indicate that the majority of inhaled formaldehyde is absorbed in the upper
28 respiratory tract (URT) but that the extent of the scrubbing in this region varies significantly
29 across species. In dogs, nearly 100% of nasally inhaled formaldehyde is absorbed (Egle, 1972).
30 Lower respiratory tract (LRT) studies designed to collect formaldehyde via a tube inserted into
31 the lower trachea revealed that nearly 95% of formaldehyde was absorbed during the first pass
32 through the upper respiratory tract (Egle, 1972), an effect observed with multiple ventilation
33 rates. The rat nasal passages also scrub nearly all of the inhaled formaldehyde (on average
34 ~97%) (Morgan et al., 1986). In computational dosimetry modeling based on anatomically

This document is a draft for review purposes only and does not constitute Agency policy.

1 realistic representation of the human nasal airways from a single individual, approximately 90%
2 of inhaled formaldehyde was predicted to be absorbed in the nose at resting inspiration. As the
3 inspiratory rate increased, this fraction decreased to about 70% at light exercise and to 58% at
4 heavy exercise conditions (see Figure 1 in Kimbell et al. [2001b]). The normal human breathing
5 mode during heavy exercise is oronasal (with ~54% of airflow being oral) (ICRP 66, 1994).
6 Consequently, it is estimated that during heavy exercise breathing (50 L/minute) the flux of
7 formaldehyde into tissue (or rate of mass transported per mm² of tissue surface area) in the first
8 six to eight generations of the tracheobronchial airways is comparable to that in the nasal region
9 (Overton et al., 2001).

10 It is important to note that the computer simulations mentioned above are based on
11 anatomical representations of a single individual. Significant anatomical variations occur in
12 human nasal airways. For example, the nasal volumes of 10 adult nonsmoking subjects between
13 18 and 50 years of age in a study in the U.S. varied between 15 and 60 mL (Santiago et al.,
14 2001), and disease states can result in considerable further variation (Singh et al., 1998).

15 Species differences in kinetic factors have been argued to be the key determinants of
16 species-specific lesion distributions for formaldehyde and other reactive inhaled gases. Airway
17 geometry is an important determinant of inhaled-formaldehyde dosimetry in the respiratory tract
18 and its differences across species. These issues will be discussed in a later section on dosimetry
19 modeling.

21 **3.2.3.1. Formaldehyde Uptake Can Be Affected by Effects at the Portal of Entry**

22 Certain formaldehyde-related effects have the potential to modulate its uptake and
23 clearance. The mucociliary apparatus of the upper respiratory tract is the first line of defense
24 against airborne toxins. Comprising a thick mucus layer (epiphase), hydrophase, and a ciliated
25 epithelium, the mucociliary apparatus may entrain, neutralize, and remove particulates and
26 airborne chemicals from inspired air. As reviewed by Wolfe (1986), airborne pollutants and
27 reactive gases have been shown to decrease mucus flow rates in several animal models (Mannix
28 et al., 1983; Iravani, 1974; Carson et al., 1966; Dalhamn, 1956; Cralley, 1942). Degradation in
29 the continuity or function of this mucociliary apparatus could result in a lower clearance of
30 inhaled pollutants at the portal of entry.

31 Morgan et al. (1983) first reported defects in mucociliary function in F344 rats exposed
32 to 15 ppm formaldehyde 6 hours/day for 1–9 days. Mucostasis occurred in several regions in all
33 rats after a single 15 ppm exposure. Ciliastasis occurred with greater frequency and across more
34 regions of the nasoturbinate in subsequent days of exposure. The authors observed that
35 mucostasis preceded ciliastasis in most cases, and vigorous ciliary activity was noted in areas

1 without mucus flow. Morgan et al. (1984a) also studied formaldehyde effects on the mucociliary
2 apparatus of isolated frog palates in vitro. Mucostasis was evident as mucus became stiff and
3 eventually rigid with increasing formaldehyde concentration and time of exposure. Ciliary beat
4 continued even after mucostasis, but ciliastasis ultimately occurred when exposure reached 4 and
5 9 ppm.

6 When a rodent is exposed to an irritant, its inhaled dose and pattern of deposition can be
7 profoundly affected by reflex bradypnea, a protective reflex seen in rodents but not in humans.
8 Reflex bradypnea can occur when the trigeminal nerve is exposed to a sufficient concentration of
9 an irritant, such as formaldehyde. It is manifest as markedly decreased activity or prostration,
10 reduced metabolism, hypothermia (as much as 5°C), significantly reduced respiratory rate and
11 minute volume, and altered blood and brain chemistry. Because of their small size, rodents are
12 able to rapidly lower their metabolism and body temperature and therefore their oxygen demand.
13 The consequence is that their inhaled dose of an irritating chemical is dramatically lowered.
14 Reflex bradypnea is quantified as the RD₅₀, which is the concentration of a chemical that results
15 in a 50% decrease in respiratory rate. It can take as much as two hours for rodents to fully
16 recover from the effects of reflex bradypnea. The clinical manifestations of reflex bradypnea can
17 easily be misconstrued as toxicity. None of the studies described in this assessment took into
18 account the fact that reflex bradypnea may have confounded the results. Reflex bradypnea is
19 discussed in depth in Section 4.2.1.1.

20 Sensory irritation studies suggest that formaldehyde activates the trigeminal nerve by
21 activating nociceptors through the modification of receptor amino acids, possibly including thiol
22 groups. Cassee et al. (1996) measured sensory irritation to formaldehyde, acetaldehyde, and
23 acrolein in male Wistar rats, following a 30-minute nose-only exposure. Formaldehyde and
24 acrolein elicited similar responses, whereas acetaldehyde was far less irritating. The authors
25 suggested that the differences in sensitivity to the aldehydes might be explained by differences in
26 physicochemical properties and by regional differences in activities of detoxifying enzymes for
27 each chemical. In addition, it has been suggested that acetaldehyde might interact with sensory
28 nerves via an amino group (Steinhagen and Barrow, 1984), whereas the receptor-binding site for
29 formaldehyde and acrolein is believed to be a thiol group. Differential binding sites for sensory
30 irritants in the trigeminal nerve have been reported (Nielsen, 1991).

31 Sensory irritation effects are discussed in depth in Chapter 4 but are noted here because
32 stimulation of the trigeminal nerve by formaldehyde can result in significantly lower pulmonary
33 ventilation, and formaldehyde exposure in rodents at concentrations that approach the RD₅₀.
34 Barrow et al. (1983) have estimated the “inhaled dose” equivalent to an exposure concentration
35 of 15 ppm in mice and rats used in the chronic formaldehyde bioassays by Kerns et al. (1983)

1 and Monticello and Morgan (1994). Their results indicate that, because mice are observed to
2 decrease their minute volume by approximately 75% as compared to 45% in rats, a twofold
3 greater inhaled dose would be expected in rats versus mice. This difference may be relevant to
4 the increased incidence of squamous cell carcinoma of the nasal cavity in F344 rats as compared
5 to B6C3F1 mice. Chang et al. (1983) estimated a reduction of 25% in the minute volume of
6 F344 rats. Yokley et al. (2008) have recently published a model that accounts for physiological
7 changes in ventilation rate induced by sensory irritation in rats. Thus, the “standard” minute
8 volumes used for rats and mice need to be adjusted downward when calculating dosimetric
9 adjustment factors for extrapolation of adverse effects to humans (Thompson et al., 2008). This
10 question is further discussed in the section on modeling the dosimetry.

11 Another effect that modulates dosimetry is the dynamic tissue remodeling of nasal
12 airways that occurs as a consequence of exposure to reactive gases. For example, formaldehyde
13 dosimetry is influenced by the occurrence of squamous metaplasia, an adaptive tissue conversion
14 to squamous that occurs in nasal epithelium exposed to toxic levels of formaldehyde. The
15 metaplasia has been observed to occur in rats at exposure concentrations of 3 ppm and higher
16 (Kimbell et al., 1997b). Squamous epithelium is known to absorb considerably less
17 formaldehyde than other epithelial types (Kimbell et al., 1997b). Overall, the highest flux levels
18 of formaldehyde in the simulations of the rat nose in Kimbell et al. (2001a) are estimated in the
19 region just posterior to the nasal vestibule. A consequence of squamous metaplasia would be to
20 “push” the higher levels of formaldehyde flux toward the more distal regions of the nose
21 (Kimbell et al., 1997b). Subramaniam et al. (2008) discussed this issue further in the context of
22 uncertainties in the modeling of formaldehyde dosimetry.

23

24 **3.3. DISTRIBUTION**

25 **3.3.1. Transport of Methylene Glycol**

26 In biological systems, formaldehyde is known to exist in equilibrium with its hydrated
27 form, as methanediol (CH_2OH_2) ($K_d = 5.5 \times 10^{-4}$) at physiological temperatures and pH
28 (>99.9%) in the body and is readily reversible. When free formaldehyde is removed from
29 aqueous solution through binding with serum proteins and cellular components, the equilibrium
30 is reestablished by dehydration of methanediol to free formaldehyde. Thus, a pool of free
31 formaldehyde may be sustained in biological systems due to the reversible nature of this
32 hydration reaction.

33 There is strong and consistent evidence in biological testing systems in vitro that treating
34 cells with formaldehyde in an aqueous media results in significant cytotoxicity, cell proliferation,
35 clastogenic effects and clear evidence of mutational events (see Section 4.3). Similarly, animal

This document is a draft for review purposes only and does not constitute Agency policy.

1 bioassays where formaldehyde is administered in drinking water report portal of entry toxicity
2 including hyperplasia, increased cell proliferation, focal lesions and tumors (see Section 4.2.1).
3 It should be noted that URT tissues are covered by an aqueous mucous layer, through which
4 formaldehyde must pass to react the cellular components of the URT. It has been postulated that
5 formaldehyde transports through this mucous layer and the underlying tissues as methanediol
6 (Georgieva et al., 2003).

7 The dynamic equilibrium between the hydrated and unhydrated forms of formaldehyde in
8 biological systems is well understood. Since the hydration reaction favors methanediol, it is
9 expected that exogenous formaldehyde which reaches the blood will primarily exist as
10 methanediol and is subject to physiological elimination. As free, unhydrated formaldehyde
11 continues to react with serum proteins and cellular components, the blood levels of methanediol
12 are expected to reduce as it is dehydrated to maintain equilibrium. Although some attempts to
13 measure significant changes in free formaldehyde levels in blood after inhalation exposure have
14 not been successful, the half-life in blood has been measured after i.v. injection at approximately
15 2 minutes (McMartin et al., 1979). Additionally, the detection of antibodies to formaldehyde-
16 hemoglobin adducts and formaldehyde-albumin adducts in exposures workers, smokers and
17 laboratory animals exposed via inhalation provides direct evidence that formaldehyde is able to
18 react with serum albumin and hemoglobin in biological systems (Li et al., 2007; Varro et al.,
19 1997; Grammer et al., 1993; Dykewicz et al., 1991; Thrasher et al., 1990, Grammer et al., 1990).
20 These data support the hypothesis that exogenous formaldehyde may reach and transport through
21 the blood. If so, formaldehyde (or methanediol) may reach sites distal to the portal of entry.

22 23 **3.3.2. Formaldehyde-GSH Conjugate as a Method of Systemic Distribution**

24 Formaldehyde is primarily metabolized by alcohol dehydrogenase (ADH3) which uses
25 the formaldehyde-glutathione hemiacetal adduct as the substrate. Sanghani et al. (2000) have
26 shown that due to high circulating concentrations (50-fold) of glutathione in human blood, the
27 S-(hydroxymethyl)glutathione (HMGS) adduct, the nonenzymatic product of formaldehyde
28 with glutathione is the major form of formaldehyde seen in vivo (Sanghani et al., 2000). It is
29 likely that the reversibly bound HMGS may be transported to different tissues through
30 circulation, but, specific experimental evidence is lacking.

31 32 **3.3.3. Levels in Blood**

33 Inhalation studies in several species indicate that exposure to formaldehyde does not
34 result in elevated levels in blood. These studies were carried out over a wide range of exposure
35 concentrations and durations. Rats exposed to 14 ppm formaldehyde for 2 hours exhibited no

1 increase in blood formaldehyde levels [$2.25 \pm 0.07 \mu\text{g}/(\text{g blood})$] in treated animals compared
2 with $2.24 \pm 0.07 \mu\text{g}/(\text{g blood})$ in control animals] when measured by GC-MS using a stable
3 isotope dilution technique (Heck et al., 1985, 1982). Similarly, mean formaldehyde blood levels
4 in humans ($n = 6$) exposed to 1.9 ppm formaldehyde for 40 minutes in a walk-in chamber
5 ($2.77 \pm 0.28 \mu\text{g}/\text{g blood}$) were not statistically different from measurements in the same
6 population before exposure (mean of $2.61 \pm 0.14 \mu\text{g}/\text{g}$) (Heck and Casanova-Schmitz, 1984).
7 The variability in the levels was large. At the individual level, the data showed both increase
8 and decrease in blood levels relative to pre-exposure levels, which was attributed by the authors
9 as plausibly due to temporal variations in baseline levels in humans, particularly since the
10 experiment did not control food intake prior to exposure. Studies in rhesus monkeys have
11 revealed endogenous formaldehyde levels ($2.4 \mu\text{g}/\text{g blood}$) comparable to humans and that levels
12 were also unaltered following exposure to 6 ppm formaldehyde via inhalation 6 hours/day for
13 4 weeks, measurements being taken at both 7 minutes and 45 hours post final exposure
14 (Casanova et al., 1988).

15 It is important to keep in mind that the GC-MS method is not capable of detecting
16 irreversibly bound formaldehyde; for example, formaldehyde levels detected by this method,
17 even in the anterior nasal mucosa of rats exposed to 6 ppm of formaldehyde, were not elevated
18 over control levels. Furthermore, the GC-MS method does not differentiate between free and
19 reversibly bound adducts of formaldehyde (Heck et al., 1982). Thus, measured levels represent
20 total formaldehyde concentration that includes free formaldehyde as well as reversibly bound
21 adducts. Based on the known Michaelis-Menten constant, K_m , for formaldehyde dehydrogenase
22 with respect to the GSH adduct formation, Heck et al. (1982) estimated under certain
23 assumptions that free formaldehyde comprised only about 1–2% of the total formaldehyde
24 measured by their method. Furthermore, as shown by Metz et al. (2006, 2004), formaldehyde
25 reactions with primary amino and thiol groups can, in a second step, react with many other
26 amino acids to form stable methylene bridges. Presumably, such reactions would not be
27 detectable by using the methods employed by Heck et al. (1982).⁴ Thus, the limited
28 interpretation of GC-MS measurements of blood levels suggests that formaldehyde does not
29 appreciably reach the blood,
30

⁴ Additionally, note that, although Heck et al. (1982) demonstrated that formaldehyde concentration can be accurately measured from glutathione and tetrahydrofolate adducts, similar experiments were not performed by using protein samples or cellular extracts (i.e., in the presence of various amino acids). In addition, standard curves for predicting formaldehyde concentration in tissues were generated in aqueous solutions rather than biological samples.

1 is rapidly metabolized or interacts with macromolecules when it escapes metabolism, or is
2 otherwise undetected.

3 Results from an earlier experiment using radiolabeled formaldehyde in rats are consistent
4 with the conclusion based on the GC-MS measurements of no appreciable increase in blood
5 levels of formaldehyde. Following a 6-hour exposure of F344 rats to 15 ppm of
6 [¹⁴C]-formaldehyde (Heck et al., 1983), the concentrations of ¹⁴C in the nasal mucosa were
7 28-fold higher than those in the blood. The observed half-life of the terminal phase of the
8 radioactivity was long (55 hours); on the other hand, it is known that the half-life of free
9 formaldehyde in the rat blood is very short. Therefore, the authors concluded that the
10 radioactivity was likely due to modification of macromolecules or metabolic incorporation rather
11 than slow metabolic clearance of formaldehyde. The terminal decline of the radioactivity in the
12 packed cell fraction of the blood was much slower and observed to be consistent with
13 incorporation into erythrocytes.

14 In the same paper, Heck et al. (1983) report on the similarity in the pharmacokinetics of
15 radiolabeled formaldehyde and radiolabeled formate in the rat blood, supporting their hypothesis
16 that oxidation of formaldehyde to formate and subsequent incorporation of this compound
17 through one-carbon metabolism were major factors in the disposition of formaldehyde. Studies
18 by Gottschling et al. (1984) have also established that the main product of metabolic clearance of
19 formaldehyde is formate, which is either further metabolized to CO₂ and water, incorporated into
20 the one-carbon pool, and/or eliminated in the urine as a sodium salt at about 13 mg/L urine.

21

22 **3.3.4. Levels in Various Tissues**

23 The radiolabeling studies indicated high levels of ¹⁴C in the rat nasal mucosa (equivalent
24 concentrations of ¹⁴C-formaldehyde in the nasal mucosa of rats naïvely exposed to 15 ppm
25 ¹⁴C-formaldehyde were 2,148 ± 255 nmol/g compared with 76 ± 11 nmol/g in plasma). In
26 contrast, the GC-MS studies did not detect elevated formaldehyde in this region. This is not to
27 be interpreted as a discrepancy, because the radiolabeling study did not distinguish among
28 radiolabeled species and thus the measured radioactivity could potentially be free or bound
29 formaldehyde, formate, or any [¹⁴C] metabolically incorporated into macromolecules.

30 In concurrent studies, Casanova-Schmitz et al. (1984) resolved the question as to whether
31 the higher [¹⁴C] levels in the nasal mucosa were a consequence of GSH depletion and a
32 subsequent reduction in GSH-dependent clearance of formaldehyde. An important result in
33 these studies was that there was no significant difference in labeling in either the nasal mucosa or
34 in plasma between naïve F344 rats and those pre-exposed to unlabeled 15 ppm formaldehyde
35 6 hours/day for the 9 previous days. These findings indicated little or no apparent effect on the

This document is a draft for review purposes only and does not constitute Agency policy.

1 disposition of formaldehyde following short-term exposure to relatively high levels of
2 formaldehyde. In contrast, Farooqui et al. (1986) reported decreases in GSH in several tissues
3 3 hours after a sublethal I.P. injection of formaldehyde but not after 6 and 9 hours. Taken
4 together, these data suggest that formaldehyde exposure does not result in long-term alterations
5 in cellular GSH levels and that repeated inhalation exposure does not alter the dosimetry to the
6 bloodstream or formaldehyde body burden.

7 Heck et al. (1983) determined the ^{14}C concentrations in different tissues in the F344 rat
8 body by exposing rats in a head-only chamber to various concentrations (5–24 ppm) of
9 radiolabeled formaldehyde for 6 hours. (Concentrations of ^{14}C in internal organs and tissues
10 relative to that in plasma did not appear to vary much as exposure concentrations increased;
11 therefore only averages over the concentration range were reported.) Except for the esophagus,
12 levels in the heart, spleen, lung, intestines, liver, and kidney were 1–3 times higher relative to
13 that in plasma. Labeling in the esophagus was high (fivefold relative to plasma). The authors
14 attributed this relatively higher dose to mucociliary action in the nose and trachea. The data also
15 indicate that the brain, testes, and erythrocytes appear to have about threefold lower ^{14}C levels
16 than plasma. Pre-exposure to formaldehyde (for 9 days) did not alter the measured radioactivity
17 in the nasal mucosa or plasma. Thus, it was concluded that the single exposure findings may
18 also be qualitatively extended to chronic exposures.

19 The total radiolabel measured in the bone marrow (femur) of F344-rats exposed for
20 6 hours to 0.3–15 ppm of radiolabeled formaldehyde in the Casanova et al. (1984) experiment
21 was high (generally within a factor of 0.5 of the total labeling in the nasal respiratory mucosa).
22 Nearly half of the ^{14}C was contained in the DNA in this tissue presumably on account of the high
23 rate of cell turnover in the bone marrow, indicating that the carbon derived from
24 ^{14}C -formaldehyde was utilized for DNA synthesis (Casanova-Schmitz et al., 1984).

25 Chang et al. (1983) described visceral labeling (via autoradiography) in rats, following
26 exposure to 15 ppm [^{14}C]-formaldehyde 6 hours/day for 4 days. The authors attributed this
27 labeling to mucociliary clearance and grooming-related ingestion of formaldehyde.

28 In summary, following exposure to radiolabeled formaldehyde, the radioactivity was very
29 high in the nasal mucosa but was also extensively distributed to various tissues. In particular,
30 levels in the bone marrow were high. On the other hand, formaldehyde levels in the blood
31 measured by GC-MS were not significantly elevated. Thus, the authors considered it unlikely
32 that the elevated ^{14}C in various tissues was due to free formaldehyde. Instead, these levels were
33 thought to arise from either rapid metabolic incorporation or formation of covalent adducts or
34 incorporation via carboxylation reactions of the $^{14}\text{CO}_2$ formed during metabolism.

1 The data presented thus far in this section illustrate that measuring the distribution of the
2 absorbed formaldehyde based on ¹⁴C-radiolabeling and GC-MS studies alone is problematic
3 because it is difficult to resolve (through these studies) whether it is free, reversibly bound,
4 irreversibly bound, formate, one-carbon pool, etc. This is of significance with regard to
5 understanding the availability of the absorbed formaldehyde. More indirect methods had to be
6 developed to further examine the disposition of formaldehyde; however, as discussed below, the
7 interpretation of these approaches may also not be straightforward.

8 9 **3.3.4.1. Disposition of Formaldehyde: Differentiating Covalent Binding and Metabolic** 10 **Incorporation**

11 The motivation in presenting this section is twofold, as follows:

- 12
13 1. As concluded above, subsequent studies were necessary to ascertain whether measured
14 radiolabeling in different experiments was due to formaldehyde adducts or incorporation
15 of [¹⁴C] one-carbon units of formaldehyde into macromolecules via the one-carbon pool.
- 16 2. DNA protein cross-links (DPXs) formed by formaldehyde (covalently bound in this case)
17 have been regarded as a surrogate dose metric for the intracellular concentration of
18 formaldehyde (Hernandez et al., 1994; Casanova et al., 1991, 1989). This is particularly
19 relevant because of the nonlinear dose response for DPX formation due to saturation of
20 enzymatic defenses at high concentrations (Casanova et al., 1991, 1989). Thus, the
21 ability to measure DPX is an important development.

22
23 An important question is whether the formaldehyde disposed in the form of DPX is
24 detected in remote tissues. A set of elegant but complex experiments involving dual isotope
25 labeling (¹⁴C and ³H) was carried out to this end by the Heck and Casanova-Schmitz and their
26 coworkers. Casanova-Schmitz et al. (1984) and Casanova-Schmitz and Heck (1983) used dual
27 isotope labeling of formaldehyde as a way to partially distinguish between formaldehyde adducts
28 formation and metabolic incorporation. In separate experiments, F344 rats were exposed to ³H-
29 and ¹⁴C-formaldehyde at different exposure concentrations (0.3–15.0 ppm), and the ³H/¹⁴C ratios
30 of different phases of DNA were measured. Only the highlights of the results and significant
31 issues are presented here. The overall conclusions from these experiments were as follows:

- 32
33 • Labeling in the nasal mucosa was due to both covalent binding and metabolic
34 incorporation.
- 35 • DPX was formed at 2 ppm and greater concentrations in the respiratory mucosa.
- 36 • In the bone marrow, formaldehyde did not bind covalently to bone marrow
37 macromolecules at any exposure concentration. The labeling of bone marrow

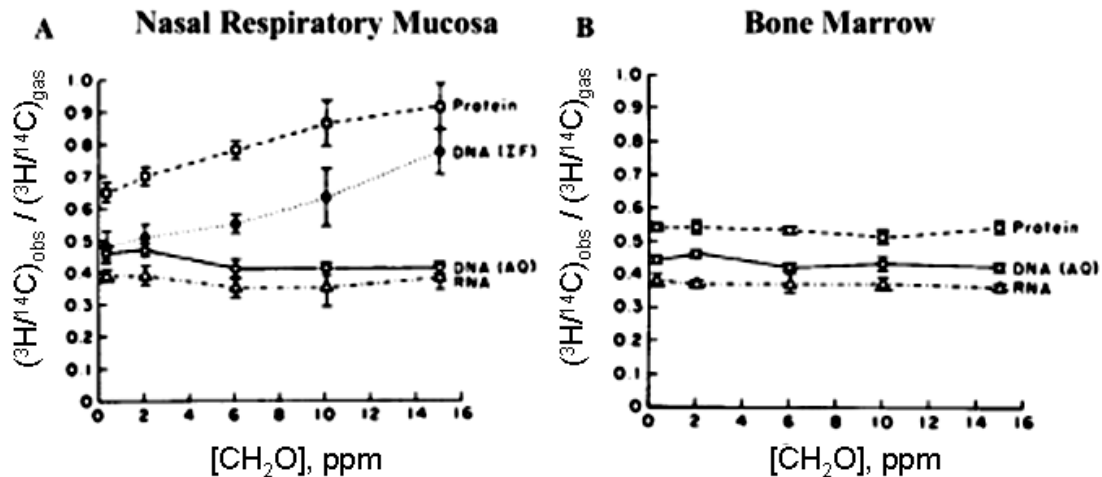
This document is a draft for review purposes only and does not constitute Agency policy.

1 macromolecules was found to be entirely due to metabolic incorporation and not due to
2 covalent binding.

3
4 Macromolecules such as DNA and protein can be isolated from tissue homogenates by
5 extraction into three phases: an organic phase consisting of proteins, an aqueous phase consisting
6 of only double-stranded DNA, and an interfacial phase consisting of both DNA and protein.
7 Single-stranded (but not double-stranded) DNA was particularly likely to form adducts. DNA
8 from this interfacial phase can be further purified and has been shown to consist of DPXs
9 (Casanova-Schmitz and Heck, 1983). Because both [¹⁴C]-formaldehyde and [³H]-formaldehyde
10 can become incorporated into DNA and protein metabolically as well as by cross-linking, the
11 ³H/¹⁴C ratio in such cross-linked material should be higher than in material that primarily
12 contains metabolically incorporated formaldehyde. Figure 3-2 shows the labeling of tissue from
13 the nasal respiratory mucosa and bone marrow (distal femur) in rats exposed to
14 [¹⁴C]-formaldehyde and [³H]-formaldehyde vapor.

15 In the nasal mucosa the interfacial phase has a significantly higher ³H/¹⁴C ratio than the
16 material in the aqueous phase. This suggests that interfacial DNA has significantly more ³H, a
17 phenomenon likely explained by additional [³H]-formaldehyde molecules present as DPXs prior
18 to extraction. The amount of interfacial DNA was found to have a clear dose response. These
19 cross-links were also judged to be due to exogenous formaldehyde. Likewise, the organic phase
20 of the nasal mucosa showed a similar increase in ³H/¹⁴C ratio at higher concentrations, a result
21 that could be attributed to various inter- and intraprotein adducts (Metz et al., 2004; Trezl et al.,
22 2003; Skrzydlewska, 1996).

23 In contrast, analysis of macromolecules at the distal femur location presents a different
24 pattern (see Figure 3-2, part B). First, the interfacial phase was not detected during extraction,
25 suggesting that there were few or no DPXs to be detected. Second, there was no increase in
26 ³H/¹⁴C ratio in the organic (i.e., protein) phase as a function of dose. Therefore, it was concluded
27 that either radiolabeled formaldehyde or formate reached the distal site and was subsequently
28 incorporated into macromolecules. According to the mechanistic interpretation of these studies,
29 the quantity plotted on the ordinate in Figure 3-2 (the ratio of ³H/¹⁴C between the tissue and the
30 exposure gas) should approach unity as metabolism becomes saturated and more adduct
31 formation occurs, particularly for protein. Indeed, this is what is observed (see Figure 3-2,
32 Part A). In contrast, there is no dose effect in the femur, suggesting that the labeling at all doses
33 in that tissue may be due to metabolic incorporation and not due to the parent formaldehyde.



1 **Figure 3-2. ³H/¹⁴C ratios in macromolecular extracts from rat tissues**
 2 **following exposure to ¹⁴C- and ³H-labeled formaldehyde (0.3, 2, 6, 10,**
 3 **15 ppm).**

Note that the small yield of interfacial (IF) phase from bone marrow tissue precluded further analysis; this is *prima facie* evidence for the lack of significant DPXs in this tissue.

Source: Casanova-Schmitz et al. (1984a).

4 (Note: These data were originally shown in the absence of an analysis of isotope effects
 5 on covalent binding and metabolism. Subsequent studies determined that [³H]-formaldehyde is
 6 oxidized less rapidly than [¹⁴C]-formaldehyde and unlabeled formaldehyde. This suggests that
 7 the ³H/¹⁴C ratio, and therefore the amount of formaldehyde covalently bound to tissue, is likely
 8 overestimated because more [³H]-formaldehyde remains unmetabolized, i.e., free to bind [Heck
 9 and Casanova, 1987]. The authors hypothesized that this overestimate was relatively greater at
 10 the lower concentrations.)

11 Similar results were obtained in GSH-depleted rats (Casanova and Heck, 1987). Again,
 12 these authors observed a dose-dependent increase in the ³H/¹⁴C ratio in the interfacial DNA and
 13 organic fractions of disrupted cells of the respiratory and olfactory mucosa and no such increases
 14 in bone marrow. Interestingly, at 10 ppm exposure (only), GSH-depleted rats exhibited a higher
 15 ³H/¹⁴C ratio in the organic phase than did normal rats. Casanova and Heck (1987) posited that
 16 much of the covalent binding at 6 ppm and lower was due to binding to extracellular proteins,
 17 whereas the higher ³H/¹⁴C ratio in GSH-depleted rats at 10 ppm was due to more intracellular
 18 binding.

This document is a draft for review purposes only and does not constitute Agency policy.

1 In their first experiment to measure DPX concentrations, Casanova-Schmidt et al. (1984)
2 and Casanova and Heck (1987) used the dual isotope method ($^3\text{H}/^{14}\text{C}$) mentioned above. In this
3 experiment, DPX was observed only at formaldehyde concentrations ≥ 2 ppm. Subsequently,
4 Casanova et al. (1989) developed a more sensitive method using high-performance liquid
5 chromatography (HPLC) for measuring DPX. In this method, tissue homogenates were digested
6 with a proteolytic enzyme and extracted with a phenolic solvent. DPX was detected in the nasal
7 mucosa of rats at formaldehyde concentrations as low as 0.3 ppm. This method was also used to
8 measure DPX in the nasal region, the larynx, trachea and carina, and major intrapulmonary
9 airways (airway diameters >2 mm) of rhesus monkeys exposed for 6 hours to 0.7, 2.0, and
10 6.0 ppm of formaldehyde. DPX was detected in the nose (including the nasopharynx) at all
11 concentrations and at 2.0 and 6.0 ppm in the larynx, trachea, carina, and other lower airways.
12 However, DPX was not detectable in the bone marrow of these monkeys at any concentration.

13 Overall, Heck and Casanova-Schmitz and their coworkers interpreted the results of these
14 various experiments to mean that inhaled formaldehyde could not reach distant sites in the body.
15 It may be noted in this context that Shaham et al. [1996] reported elevated DPX levels in the
16 white blood cells of laboratory workers exposed to formaldehyde. These data are further
17 reported in Chapter 4.)

18

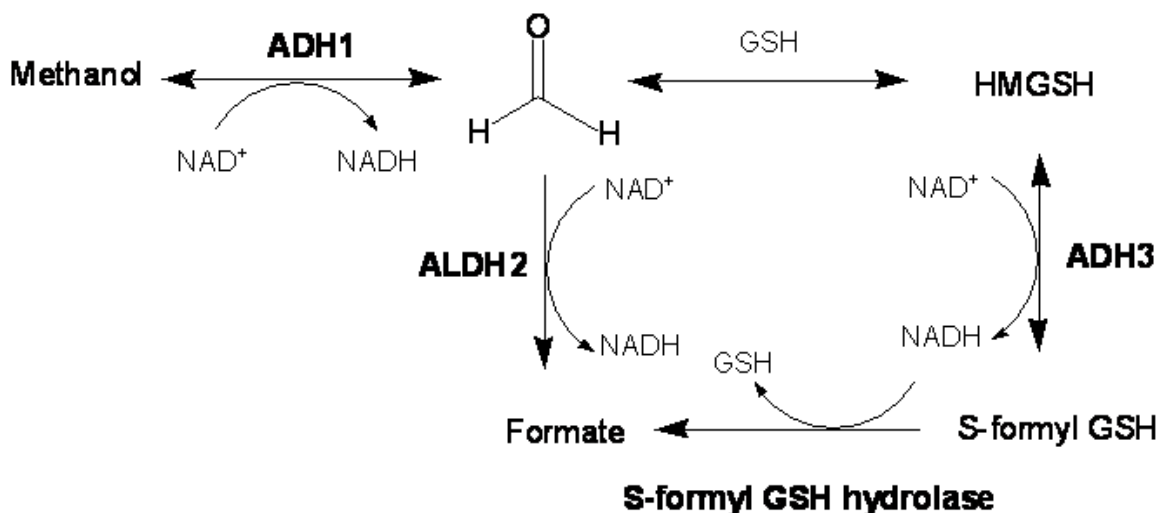
19 **3.4. METABOLISM**

20 Formaldehyde is primarily metabolized by glutathione-dependent formaldehyde
21 dehydrogenase (FALDH) and aldehyde dehydrogenases (ALDHs). Numerous studies now
22 recognize FALDH as a member of the alcohol dehydrogenase (ADH) family, specifically ADH3
23 (Thompson et al., 2009; Liu et al., 2004, 2001; Hedberg et al., 2003; Høgg et al., 2003; and the
24 references in each of these). The remainder of this report will refer to FALDH as ADH3.

25

26 **3.4.1. In Vitro and In Vivo Characterization of Formaldehyde Metabolism**

27 Formaldehyde is oxidized to formate by two metabolic pathways (see Figure 3-3). The
28 first pathway involves conversion of free formaldehyde to formate by the so-called low- K_m
29 ($K_m = 400 \mu\text{M}$) mitochondrial aldehyde dehydrogenase-2 (ALDH2). The second pathway
30 involves a two-enzyme system that converts glutathione-conjugated formaldehyde
31 (S-hydroxymethylglutathione [HMGSH]) to the intermediate S-formylglutathione, which is
32 subsequently metabolized to formate and GSH by S-formylglutathione hydrolase.



1 **Figure 3-3. Formaldehyde clearance by ALDH2 (GSH-independent) and**
 2 **ADH3 (GSH-dependent).**

The K_m value for ALDH2 and free formaldehyde is about 400 μM (Teng et al., 2001), whereas the K_m value for HMGSH and ADH3 is 6.5 μM (Uotila and Koivusalo, 1974a, b). The ADH-mediated reactions are reversible in the presence of excess reduced nicotinamide adenine dinucleotide (NADH).

Source: Adapted from Teng et al. (2001).

3 Though ADH3 is rate limiting in this second pathway, the affinity of HMGSH for ADH3
 4 ($K_m = 6.5 \mu\text{M}$) is about 100-fold higher than that of free formaldehyde for ALDH2. In addition
 5 to the kinetic properties, this member of the ADH gene family (Høgg et al., 2003, 2001; Liu et
 6 al., 2001; Jornvall et al., 2000; Estonius et al., 1996) appears to be ubiquitously expressed in
 7 organ tissues (Molotkov et al., 2002; Ang et al., 1996a, b), exhibits cytoplasmic and nuclear
 8 localization (Fernandez et al., 2003), and is the most abundant ADH family member in the liver
 9 and brain (Galter et al., 2003).

10 In vitro studies have examined the clearance of formaldehyde in several human and rat
 11 tissues (see Table 3-1). Examination of formaldehyde metabolism in the rat nasal and olfactory
 12 mucosa indicates nearly identical pharmacokinetics in the rat liver on a per mg of cell lysate
 13 basis (Casanova-Schmitz et al., 1984b). Similar results have been obtained in the absence of
 14 GSH, where other ALDH family members oxidize formaldehyde, albeit with significantly lower
 15 affinity (i.e., higher K_m). Hedberg et al. (2000) demonstrated that human buccal tissue lysate
 16 kinetics are in close agreement with those reported for purified human liver ADH3 (Uotila and
 17 Koivusalo, 1974a). Additionally, micro-array analysis indicates that these cells express far more
 18 ADH3 and S-formylglutathione hydrolase than ALDH1 or ALDH2 (Hedberg et al., 2001a). The

This document is a draft for review purposes only and does not constitute Agency policy.

1 results of Ovrebo et al. (2002) are not easily compared with the other studies in Table 3-1
 2 because these studies were in intact cell cultures. However, it is apparent that the
 3 pharmacokinetic values in these human cells are comparable to intact rat liver cells.

4 **Table 3-1. Formaldehyde kinetics in human and rat tissue samples**

Source	K _m (μM)	V _{max} (nmol/mg protein × min)	Reference
Purified human liver ADH3	6.5	2.77 ± 0.12	Uotila and Koivusalo (1974a, b)
Rat olfactory mucosa (+ GSH)	2.6 ± 0.5	1.77 ± 0.12	Casanova-Schmitz et al. (1984b)
Rat olfactory mucosa (- GSH)	647 ± 43	4.39 ± 0.14	Casanova-Schmitz et al. (1984b)
Rat respiratory mucosa (+ GSH)	2.6 ± 2.6	0.90 ± 0.24	Casanova-Schmitz et al. (1984b)
Rat respiratory mucosa (- GSH)	481 ± 88	4.07 ± 0.35	Casanova-Schmitz et al. (1984b)
Rat liver (+ GSH)	5.0 ± 1.9	2.0 ± 0.3	Casanova-Schmitz et al. (1984b)
Human bronchial explants ^a	5,100	3.3	Ovrebo et al. (2002)
Human bronchial epithelial ^a	1,400	6.1	Ovrebo et al. (2002)
Rat hepatocytes ^a	1,250	4.2	Ovrebo et al. (2002)
Human buccal tissue (+ GSH)	11 ± 2	2.9 ± 0.6	Hedberg et al. (2000)
Human buccal tissue (- GSH)	360 ± 90	1.2 ± 0.7	Hedberg et al. (2000)
Human keratinocytes	n.d. ^b	14.5 ± 1.8	Hedberg et al. (2000)
Human fibroblasts	n.d.	17.9 ± 1.4	Hedberg et al. (2000)

^aThese studies were carried out in intact cells by measuring the formation of formate. This likely explains the nearly 1,000-fold increase in apparent K_m, since much of the formaldehyde was likely to be bound extracellularly. The remaining studies used either purified enzyme or cell lysates (as indicated) and measured the formation of NADH.

^bn.d. = not determined.

5
6

7 The data in Table 3-2 along with data indicating the ubiquity of ADH3, indicate that
 8 many human tissues and cells, particularly in the respiratory tract, appear to exhibit significant
 9 capacity to metabolize formaldehyde. Molecular biology techniques have demonstrated the
 10 importance of ADH3 in formaldehyde clearance. For example, ADH-knockout studies have
 11 shown that the median lethal dose (LD₅₀) values for formaldehyde in wild type, ADH1^{-/-},
 12 ADH3^{-/-}, and ADH4^{-/-} mice strains were 0.200, 0.175, 0.135, and 0.190 g/kg, respectively
 13 (Deltour et al., 1999). Although the statistical significance was not reported, the data indicate
 14 that deletion of ADH3 increases the sensitivity of mice to formaldehyde.

1

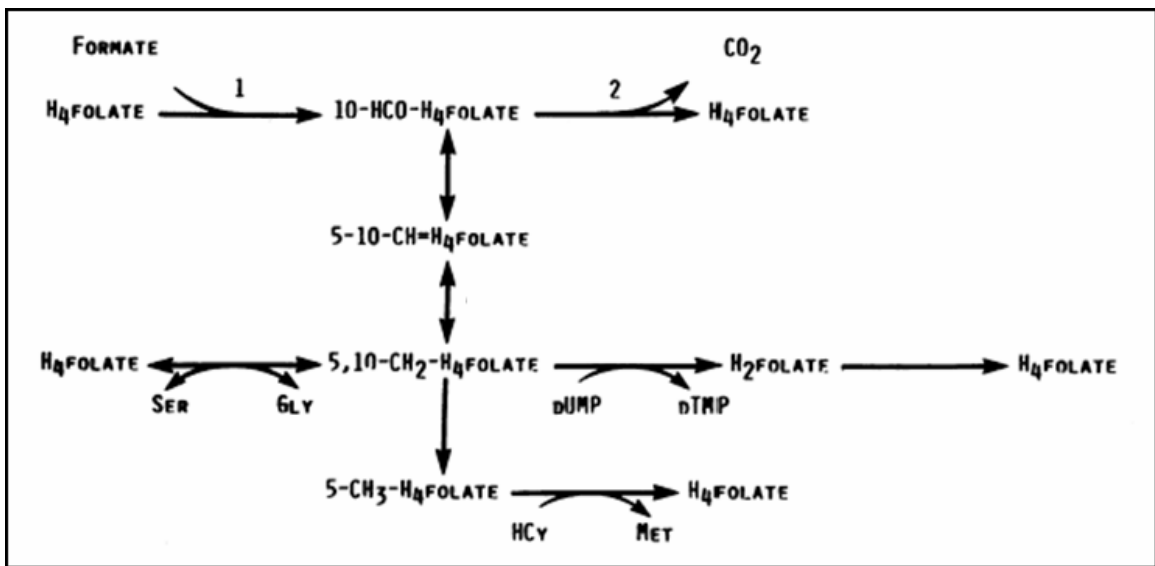
Table 3-2. Allelic frequencies of ADH3 in human populations

Population, <i>n</i>	Allele frequencies (%)							
	<u>AA</u> _{-197/-196}	<u>GG</u> _{-197/-196}		<u>A</u> ₋₇₉	<u>G</u> ₋₇₉		<u>T</u> ₊₉	<u>C</u> ₊₉
Chinese, 83	22	78		100	—		—	100
Spanish, 95	41	59		62	38		—	100
Swedish, 96	47	53		67	33		1.5	98.5

Source: Adapted from Hedberg et al. (2001b).

2 The pharmacokinetics of formate are complex. Formate can undergo adenosine
 3 triphosphate (ATP)-dependent addition to tetrahydrofolate (THF), which can carry either one or
 4 two one-carbon groups. Formate can conjugate with THF to form N¹⁰-formyl-THF and its
 5 isomer N⁵-formyl-THF, both of which can be converted to N⁵,N¹⁰-methenyl-THF and
 6 subsequently to other derivatives that are ultimately incorporated into DNA and proteins via
 7 biosynthetic pathways (see Figure 3-4).

8



9 **Figure 3-4. Metabolism of formate.**

10

11

Note: 1, formyl-THF synthetase; 2, formyl-THF dehydrogenase.

Source: Adapted from Black et al. (1985).

12

1 Elevated levels of formate in urine have been detected following inhalation of methanol
2 or formate under certain conditions (Liesivuori and Savolainen, 1987), although the
3 interpretation of this finding is unclear. There is also evidence that formate generates CO_2^-
4 radicals and can be metabolized to CO_2 via catalase and via the oxidation of N^{10} -formyl-THF
5 (Dikalova et al., 2001, and references therein). The significance of formate in formaldehyde
6 toxicity is unclear. Black et al. (1985) reported that hepatic tetrahydrofolate levels in monkeys
7 are 60% of those in rats and that primates are far less efficient in clearing formate than are rats
8 and dogs. Studies in rats involving [^{14}C]-formate suggest that about 80% is exhaled as $^{14}\text{CO}_2$,
9 2–7% is excreted in the urine, and about 10% undergoes metabolic incorporation (Hanzlik et al.,
10 2005, and references therein). Mice deficient in formyl-THF dehydrogenase exhibit no change
11 in LD_{50} (via I.P. dose) for methanol or in oxidation of high doses of formate (Cook et al., 2001).
12 It has been suggested that rodents efficiently clear formate via folate-dependent pathways,
13 peroxidation by catalase, or an unknown third pathway. Conversely, primates do not appear to
14 exhibit such capacity and are more sensitive to metabolic acidosis following methanol poisoning
15 (Cook et al., 2001).

17 **3.4.2. Formaldehyde Exposure and Perturbation of Metabolic Pathways**

18 The enzyme ADH3 has received renewed attention in recent years because of new
19 functions that have been attributed to it. ADH3 is central to the metabolism of formaldehyde;
20 however, exposure to formaldehyde in turn alters the activity of ADH3 (in multiple dose-
21 dependent ways), thereby leading to perturbation of critical metabolic pathways. These are
22 briefly mentioned below (refer to cited papers for details).

- 24 1. Exposure to formaldehyde increases cell replication. These proliferating epithelial and
25 inflammatory cells are rich in both the messenger ribonucleic acid (mRNA) and protein
26 of ADH3 (Nilsson et al., 2004; Hedberg et al., 2000). Studies in the rodent lung suggest
27 that increases in ADH3 in such cells dramatically alter the biology of other important
28 ADH3 substrates that are involved in protein modification and cell signaling (Que et al.,
29 2005).
- 30 2. ADH3 also participates in the oxidation of retinol and long-chain primary alcohols, as
31 well as the reduction of S-nitrosoglutathione (GSNO) (Staab et al., 2009; Thompson et
32 al., 2009; Hedberg et al., 2003; Høgg et al., 2003; Molotkov et al., 2002; Liu et al., 2001;
33 Jornvall et al., 2000; Jensen et al., 1998). The activity of ADH3 toward some of these
34 substrates has been shown to be significantly increased in the presence of formaldehyde.
35 Staab et al. (2009) showed that (in cultured cells) GSNO can accelerate ADH3-mediated
36 formaldehyde oxidation and, likewise, that formaldehyde increases ADH3-mediated
37 GSNO reduction nearly 25-fold. The following effects may be noted with regard to the
38 relevance of such perturbations.

This document is a draft for review purposes only and does not constitute Agency policy.

- 1 a. GSNO is an endogenous bronchodilator and reservoir of nitric oxide (NO)
2 activity (Jensen et al., 1998). Details on the ADH3-mediated reduction of GSNO
3 are shown in Thompson and Grafstrom (2008).
- 4 b. ADH3 is implicated in playing a central role in regulating bronchiole tone and
5 allergen-induced hyperresponsiveness (Gerard, 2005; Que et al., 2005).
- 6 c. As concluded by California Environmental Protection Agency (CalEPA) (2008),
7 “the dysregulation of NO by formaldehyde [in this manner] helps to explain the
8 variety and variability in the toxic manifestations following formaldehyde
9 inhalation.”

11 3.4.3. Evidence for Susceptibility in Formaldehyde Metabolism

12 Teng et al. (2001) provided evidence that inhibition of ADH1, ALDH2, and ADH3 has
13 significant impact on formaldehyde toxicity. The authors speculated that deficiencies in any of
14 these enzymes would confer an increased susceptibility to formaldehyde toxicity (Teng et al.,
15 2001). Polymorphism in ALDH2 has been shown to have implications in human risk
16 assessment, specifically with regard to acetaldehyde metabolism (Ginsberg et al., 2002). It is
17 worth noting, however, that Teng et al. (2001) only demonstrated the importance of ALDH2 in
18 rat hepatocytes with formaldehyde concentrations of 2.5 mM and greater. Since this
19 concentration is fivefold greater than the 0.5 mM K_m for free formaldehyde, ALDH2
20 involvement is not unexpected at such high concentrations. Teng et al. (2001) also demonstrated
21 the importance of ADH1 in driving the reverse reaction (i.e., formaldehyde to methanol) by
22 coadministration of NADH-generators. This would have the effect of prolonging the life of
23 formaldehyde by continuous recycling. This is not surprising, given that many ADH reactions
24 are reversible. However, levels of nicotinamide adenine dinucleotide (NAD⁺) are normally
25 much higher than NADH.

26 To date, two studies have reported polymorphisms in ADH3, using the new
27 nomenclature.⁵ ADH3 transcription appears to be regulated by specificity protein (Sp1), with a
28 minimal promoter located at positions -34 to +61. The reported polymorphisms in ADH3
29 involve four base-pair substitutions in the promoter region and no polymorphisms in the coding
30 region (Hedberg et al., 2001b). The three polymorphisms include -197/-196 (GG→AA), -79
31 (G→A), and +9 (C→T). The genotype frequencies are shown in Table 3-2. Of these alleles, the
32 +9 (C→T) polymorphism (in the putative Sp1 minimal promoter region) reduced transcriptional

⁵ Other epidemiologic studies investigating links between ADH3 and oral cancer use the older nomenclature and thus refer to Class I ADH (i.e., ADH1) enzymes.

1 activity twofold in in vitro reporter gene experiments. According to Hedberg et al. (2001b), no
2 studies have demonstrated differences in ADH3 enzyme activity in humans. More recently,
3 single nucleotide polymorphisms in ADH3 have been reported to be associated with childhood
4 risk of asthma, although the functional relevance of these polymorphisms has not been published
5 (Wu et al., 2007).

6 Alterations in THF pathways may also have an impact on formaldehyde toxicity. These
7 could result from polymorphisms in various enzymes or differences in folate intake and
8 absorption. Species differences in tetrahydrofolate levels (Black et al., 1985) are thought to play
9 a role in the differential responses to methanol across species. Cook et al. (2001) speculate that
10 rats have redundant pathways for formate clearance that may be absent or less efficient in
11 primates.

13 **3.5. ENDOGENOUS SOURCES OF FORMALDEHYDE**

14 Endogenous formaldehyde is produced through normal cellular metabolism through
15 enzymatic or nonenzymatic reactions, and also as a detoxification product of xenobiotics during
16 cellular metabolism.

18 **3.5.1.1. Normal Cellular Metabolism (Enzymatic)**

19 Formaldehyde is produced during normal metabolism of methanol, amino acids (e.g.,
20 glycine, serine, and methionine), choline, dimethylglycine, and methylamine and through the
21 folate-dependent endogenous one-carbon pool, etc.

- 22
- 23 a) One of the endogenous sources for formaldehyde production is methanol, formed during
24 normal cellular metabolism. However, this fraction may also be derived through
25 consumption of fruits, vegetables and alcohol (Shelby et al., 2004; IPCS, 1997). In
26 studies conducted with healthy humans whose diet was devoid of methanol-containing or
27 methanol-generating foods (such as cereals containing aspartame, a precursor of
28 methanol) and who abstained from alcohol consumption, the background blood levels of
29 methanol range from 0.25–4.7 mg/L (reviewed in Shelby et al., 2004 [CERHR]).
30 Methanol is metabolized to formaldehyde predominantly by hepatic alcohol
31 dehydrogenase-1 (ADH1) in primates and by ADH1 and catalase (CAT) in rodents,
32 ADH1 requiring nicotinamide adenine dinucleotide (NAD⁺) as a cofactor.
- 33 b) Dimethylglycine (DMG), one of the byproducts of choline metabolism endogenously
34 present in the body, is an indirect source of endogenous formaldehyde. Two specific
35 dehydrogenases, (a) dimethylglycine dehydrogenase (DMGDH) which converts DMG to
36 sarcosine (methylglycine) and (b) sarcosine dehydrogenase (SDH) which converts
37 sarcosine to glycine, have been shown to noncovalently bind to the folate enzyme,

1 tetrahydrofolate (THF). Further, these dehydrogenases form “active formaldehyde” by
2 removing the 1-carbon groups from THF (Binzak et al., 2000).

- 3 c) Another source of endogenous formaldehyde is methylamine (MA), an intermediary
4 component of the metabolism of adrenaline, sarcosine, creatine, lecithin, and other
5 dietary sources (Yu and Zuo, 1996). The enzyme semicarbazole-sensitive amine oxidase
6 (SSAO), predominantly present in the plasma membrane of endothelial smooth muscle
7 cells and in circulating blood, converts methylamine to formaldehyde, hydrogen peroxide
8 and ammonia. The formaldehyde thus released has been shown to cause endothelial
9 injury eventually leading to atherosclerosis (Kalasz, 2003). Yu et al. (1997) have shown
10 that adrenaline, released in the body as a response to stress, is known to be deaminated by
11 the enzyme monoamine oxidase, with further conversion of methylamine to
12 formaldehyde by SSAO (Yu et al., 1997). Creatine is another precursor for methylamine
13 which is metabolized by SSAO to form formaldehyde. It has been shown that short-term,
14 high-dose dietary supplementation of creatine in healthy humans causes a significant
15 increase in urinary methylamine and formaldehyde levels (Poortmans et al., 2005).
- 16 d) Endogenous formaldehyde is also a constituent of the one-carbon pool, a network of
17 interrelated biochemical reactions that involve the transfer of one-carbon groups from
18 one compound to another (usually the transfer of the hydroxymethyl group of serine to
19 tetrahydrofolic acid).

20
21 Tyihak et al. (1998) have demonstrated that formaldehyde, but not the methyl radical or
22 methyl cation, is involved in the enzymatic transmethylation and demethylation reactions, and
23 suggested the presence of a formaldehyde cycle in cells for the production and removal of
24 formaldehyde utilizing the transfer through methionine → S-adenosylmethionine →
25 S-adenosyl-homocysteine → homocysteine (Tyihak et al., 1998). However, these studies did not
26 clearly show whether the formaldehyde released in this cycle is in free or bound form.

27 Formaldehyde has been shown to be produced in normal and leukemic leukocytes from
28 N⁵-methyl-THF by enzymatic degradation (Thorndike and Beck, 1977). This is a two-step
29 reaction involving (1) enzymatic conversion of the methyl-THF to formaldehyde followed by (2)
30 nonenzymatic reaction of formaldehyde with an amine. Thorndike and Beck (1977) showed that
31 leukocyte (granulocyte and lymphocyte) cell extracts from normal individuals and patients with
32 chronic lymphocytic leukemia (CLL) or chronic myelocytic leukemia (CML) incubated with
33 ¹⁴C-methyl-THF and saturating amounts of tryptamine produced free formaldehyde which is
34 detected as its corresponding carboline derivative formed with tryptamine. These results
35 demonstrate the activity of the enzyme N⁵, N¹⁰-methylene THF reductase which oxidizes
36 N⁵-methyltetrahydrofolate to N⁵, N¹⁰ methylene THF. The authors noted that the enzyme levels
37 were in the order of normal granulocytes < normal lymphocytes < granulocytes from a CML
38 individual < lymphocytes from a CLL individual (Thorndike and Beck, 1977), suggesting

1 increased activity of formaldehyde producing enzyme in leukemic cells compared to normal
2 leukocytes. Overall, formaldehyde might be a byproduct as well as an intermediary product in
3 several of these reactions.

4 5 **3.5.1.2. Normal Metabolism (Nonenzymatic)**

- 6 i) Formaldehyde can also be formed nonenzymatically by the spontaneous reaction of
7 methanol with hydroxyl radicals, wherein cellular hydrogen peroxide is the precursor for
8 hydroxyl radicals generated through Fenton reaction (Cederbaum and Qureshi, 1982).
- 9 ii) Another mechanism of nonenzymatic production of formaldehyde is through lipid
10 peroxidation of polyunsaturated fatty acids (PUFA) (Shibamoto, 2006; Slater, 1984). In
11 this mechanism, reactive oxygen species (ROS) generated during oxidative stress abstract
12 a hydrogen atom from a methylene group of polyunsaturated fatty acids (PUFA) in cell
13 membranes causing autooxidation of lipids with the eventual production of free radicals
14 (e.g., peroxy radical). It is known that a certain level of oxidative stress and lipid
15 peroxidation does occur in normal individuals, and these cellular metabolic processes are
16 likely to contribute to endogenous formaldehyde production.

17 18 **3.5.1.3. Exogenous Sources of Formaldehyde Production**

19 Microsomal cytochrome P450 enzymes catalyze oxidative demethylation of N-, O- and
20 S-methyl groups of xenobiotic compounds whereby formaldehyde is produced as a primary
21 product, which is subsequently incorporated into the one-carbon pool by reacting with
22 tetrahydrofolic acid or is oxidized to formate (Dahl and Hadley, 1983; Heck et al., 1982). Also,
23 some special peroxidases, such as peroxide-dependent horseradish peroxidase enzymatically
24 catalyze xenobiotics to generate formaldehyde in the body. In particular, an ethyl peroxide-
25 dependent horseradish peroxidase has been shown to act on *N,N*-dimethylaniline and produce
26 equimolar amounts of *N*-methylaniline and formaldehyde (Kedderis and Hollenberg, 1983).

27 The tobacco-specific nitrosamine, 4-(methylnitrosamino)-1-(3-pyridyl)-1-butanone
28 (NNK), is another source of formaldehyde. It has been shown that formaldehyde is also
29 produced during the methyl hydroxylation of NNK by rat liver microsomes (Castonguay et al.,
30 1991). Also recent studies have demonstrated the formation of formaldehyde-DNA adducts in
31 NNK-treated rats using a highly sensitive liquid chromatography-electrospray ionization-tandem
32 mass spectrometry with selected reaction monitoring (Wang et al., 2007), suggesting formation
33 of formaldehyde from nitrosamines. Cigarette smoke is also a source of exogenously produced
34 methylamine which is converted to formaldehyde by SSAO (Yu, 1998).

1 **3.5.1.4. Metabolic Products of Formaldehyde Metabolism (e.g., Formic Acid)**

2 Formate is converted to carbon dioxide (CO₂) in rodents predominantly by a folate-
3 dependent enzyme pathway (Dikalova et al., 2001). Formate is also oxidized to CO₂ and water
4 by a minor pathway involving catalase located in rat liver peroxisomes (Waydhas et al., 1978;
5 Oshino et al., 1973). In the folate-dependent pathway, tetrahydrofolate (THF)-mediated
6 oxidation of formate and the transfer of one-carbon compounds between different derivatives of
7 THF has been described.

8 Endogenous levels of formate also will be affected by dietary intake of methanol-
9 producing or methanol-containing diets since methanol is initially converted to formaldehyde
10 and eventually metabolized to formate. It has been shown in several studies in human subjects
11 who were restricted on consuming methanol producing diets, aspartame or alcohol, that the
12 endogenous blood concentrations of formate ranged from 3.8 to 19.1 mg/L (Shelby et al., 2004
13 [CERHR]). The biological half life of formic acid is 77–90 minutes (Owen et al., 1990b). The
14 levels of formate in the urine of unexposed individuals range from 11.7 to 18 mg/L (Boeniger,
15 1987). One source of formic acid intake is through diet which ranges from 0.4 to 1.2 mg per day
16 (Boeniger, 1987). The half life for plasma formate is ~30 minutes or longer (Boeniger, 1987).
17

18 **3.5.1.5. Levels of Endogenous Formaldehyde in Animal and Human Tissues**

19 Heck et al. (1982) estimated that endogenous levels of formaldehyde (free as well as
20 bound) in rats ranged from 0.05 to 0.5 μmole/g (1.5–15 μg/g) of wet tissue as analyzed by the
21 stable isotope dilution with GC-MS method (Heck et al., 1982). Although the levels of free
22 formaldehyde cannot be measured due to their high reactivity and short half life, they were
23 calculated by Heck et al. (1985) using an indirect method. They added a molar excess of GSH or
24 THF to the test tube containing formaldehyde in aqueous solution enabling complete binding.
25 When estimated, they observed that the amount of formaldehyde detected was equal to the total
26 amount added to the reaction suggesting that the formaldehyde measured contained both free and
27 bound forms. Further, they calculated the free formaldehyde concentration using the
28 dissociation constant of the HMGSH adduct and cellular concentration of GSH. Human
29 formaldehyde dehydrogenase has been shown to have a dissociation constant of 1.5 mM for the
30 formaldehyde-GSH hemithioacetal adduct (Uotila and Koivusalo, 1974), while the folate
31 enzyme product N⁵,N¹⁰-methylene-THF has a dissociation constant of 30 mM (Kallen and
32 Jencks 1966a, b). This could be evaluated using the Michaels-Menton constant (K_m) of
33 formaldehyde dehydrogenase for the GSH adduct (~4 μM at 25°C), whereby they calculated the
34 free formaldehyde level to be around 3–7 μM or 1–2% of the total formaldehyde as measured by
35 GC-MS in rat tissues (Heck 1982).

This document is a draft for review purposes only and does not constitute Agency policy.

1 Cascieri and Clary (1992) estimated the total body content of formaldehyde in human
 2 body based on the following assumptions. For an individual with an average body wt of 70 kg
 3 and with body fluids accounting for 70% of body weight, total formaldehyde content is
 4 distributed in ~49 kg of body mass or 49 L of body fluids, owing to the water solubility and
 5 uniform distribution of formaldehyde in body fluids. It has been shown that the average blood
 6 concentration (mean ± S.E.) of formaldehyde in unexposed rats and humans was 2.24 ± 0.07 and
 7 2.61 ± 0.14 µg/g of blood, respectively (Heck et al., 1985), and in unexposed rhesus monkeys it
 8 was 2.42 ± 0.09 µg/g of blood (Casanova et al., 1988), overall giving an average of
 9 approximately 2.5 ppm (2.5 mg/L) formaldehyde across the species. All these studies used
 10 pentafluorophenyl hydrazine derived formaldehyde using GC-MS analysis (see Table 3-3).
 11 Assuming these values, the body content of total formaldehyde is 122.5 mg (49 L × 2.5 mg/L) or
 12 1.75 mg/kg body wt at any given time. Formaldehyde given intravenously to rhesus monkeys
 13 has been shown to have a half life of ~1.5 minutes in blood, wherein formaldehyde in blood was
 14 measured by the dimedone method (McMartin et al., 1979). Using this information Cascieri and
 15 Clary (1992) calculated that the human body generates approximately 40.83 mg/minute
 16 [(122.5 mg/2 × 1.5)] of formaldehyde. Biotransformation of formaldehyde to carbon dioxide in
 17 the liver alone has been estimated at 22 mg/minute (Owen et al., 1990a).

18 Free formaldehyde is detected in body fluids and tissues using dimedone (Szarvas et al.,
 19 1986) or 2,4-dinitrophenylhydrazine (DNPH) or pentafluorophenyl hydrazine (PFPH) derivative
 20 (Heck et al., 1985) or as a fluorescent derivative (Luo et al., 2001) as trapping agent and detected
 21 by analytical techniques such as thin-layer chromatography (TLC), high-performance liquid
 22 chromatography (HPLC) and gas-chromatography mass spectrometry (GC-MS). Data from
 23 several studies is summarized in Table 3-3. Using ¹⁴C-labeled dimedone, a chemical which
 24 condenses with free formaldehyde forming a product termed “formaldemethone” enabling
 25 radiometric detection, Szarvas et al. (1986) estimated the levels of endogenous formaldehyde in
 26 human blood plasma to be 0.4–0.6 µg/mL and in human urine to be 2.5–4 µg/mL
 27 (Szarvas et al., 1986).

28 Hileman (1984) reported that the endogenous levels of metabolically derived
 29 formaldehyde will be in the range of 3–12 ng/g of tissue (Hileman, 1984). So for an average
 30 70 kg individual, the endogenous level of metabolically derived formaldehyde would be 210 µg
 31 to 840 µg (3–12 ng/g × 0.001 µg/ng × 1,000 g/kg × 70 kg).

32 **Table 3-3. Endogenous formaldehyde levels in animal and human tissues**
 33 **and body fluids**

Tissue	Method	Detected as	Formaldehyde levels	Reference
--------	--------	-------------	---------------------	-----------

Not specified	Not specified	Not specified	0.003–0.012 ppm (3–12 ng/g)	Hileman 1984
Not specified	GC-MS with stable isotope dilution method	As PFPH-derivative	1.5–15 ppm (0.05–0.5 μ mole/g)	Heck et al., 1982a
Blood	GC-MS with select ion monitoring	As PFPH-derivative	2.24 \pm 0.07 ppm (2.24 \pm 0.07 μ g/g)	Heck et al., 1985
Blood	GC-MS with select ion monitoring	As PFPH-derivative	2.61 \pm 0.14 ppm (2.61 \pm 0.14 μ g/g)	Heck et al., 1985
Plasma	Reverse phase HPLC-fluorescent detection	As product of ampicillin	1.65 ppm (1.65 μ g/mL)	Luo et al., 2001
Heart perfusate	HPLC	As DNPH adduct	0.089–0.126 ppm (2.98–4.21 nmol/mL)	Shibamoto 2006
Blood	GC-MS with select ion monitoring	As PFPH-derivative	2.42 \pm 0.09 ppm (2.42 \pm 0.09 μ g/g)	Casanova et al., 1988
Plasma	Radiometric method	As formaldehyde adduct	0.4–0.6 ppm (0.4–0.6 μ g/mL)	Szarvas et al., 1986
Urine	Radiometric method	As formaldehyde adduct	2.5–4.0 ppm (2.5–4.0 μ g/mL)	Szarvas et al., 1986

Values in the parenthesis, originally cited in the references, are converted to parts per million (ppm) as indicated. PFPH, pentafluorophenyl hydrazone derivative; DNPH, dinitrophenyl hydrazine; GC-MS, gas-chromatography mass spectrometry; HPLC, high performance liquid chromatography.

1
2
3
4
5
6
7
8
9
10
11
12
13

3.6. EXCRETION

The main product of metabolic clearance of formaldehyde is formate, which is further metabolized to CO₂ and water, incorporated into the one-carbon pool, or eliminated in the urine. There is also some evidence that formaldehyde is present in exhaled breath; however, it is unclear whether this originates from endogenous sources, or is simply a function of ambient formaldehyde dissolved in fluids lining POEs. The following sections describe first experiments in laboratory species and then available data in humans. Broadly, these studies address two important questions that may be of relevance for risk assessment. First, it may be of interest to know what levels of formaldehyde are exhaled for comparison with inhaled levels, and whether there is any relationship between external exposure and exhaled levels. Second, there are recent studies that have attempted to relate genetic polymorphisms and changes in gene transcription level to levels of putative urinary formaldehyde biomarkers.

1 **3.6.1. Formaldehyde Excretion in Rodents**

2 Heck et al. (1983) determined the relative contributions of various excretion pathways in
3 F344 rats following inhalation exposure to formaldehyde. Table 3-4 indicates that the relative
4 excretion pathways were independent of exposure concentration (at least between 0.63 and
5 15 ppm). Nearly 40% of inhaled [¹⁴C]-formaldehyde appeared to be eliminated via expiration,
6 probably as CO₂ (it should be recalled that nearly 100% of inhaled formaldehyde is absorbed).
7 Within 70 hours of a 6-hour exposure to formaldehyde, about 17 and 5% were eliminated in the
8 urine and feces, respectively. Nearly 40% of inhaled [¹⁴C]-formaldehyde remained in the
9 carcass, presumably due to metabolic incorporation.

10 **Table 3-4. Percent distribution of airborne [¹⁴C]-formaldehyde in F344 rats**

Source	Concentration of formaldehyde (ppm)	
	0.63	13.1
	Distribution (%) ^a	
Expired air	39.4 ± 1.5	41.9 ± 0.8
Urine	17.6 ± 1.2	17.3 ± 0.6
Feces	4.2 ± 1.5	5.3 ± 1.3
Tissues and carcass	38.9 ± 1.2	35.2 ± 0.5

^aValues are means ± standard deviations (n = 4).

Source: Heck et al. (1983).

11 Mashford and Jones (1982) examined elimination pathways of formaldehyde in rats
12 exposed by I.P. injection. Urine and exhaled gases were collected from rats exposed to 4 or
13 40 mg/kg [¹⁴C]-formaldehyde. At 48 hours postinjection, 82 and 78% of the radiolabel were
14 exhaled as ¹⁴CO₂, whereas exhaled [¹⁴C]-formaldehyde was not detected. Mashford and Jones
15 (1982) also further identified the urinary metabolites. Five hours after injection of the higher
16 dose, formate was determined to comprise 80% of the urinary metabolites. The authors were
17 unable to detect cysteine derivatives observed in other studies (see below) in the urine of these
18 rats prior to or after formaldehyde exposure. The authors stated that if formaldehyde were to be
19 excreted in urine containing cysteine, then thiazolidine-4-carboxylate (TZCA) would likely be
20 produced. They speculated that species differences in urinary compounds may produce
21 formaldehyde conjugates (or artifacts).

This document is a draft for review purposes only and does not constitute Agency policy.

1 Hemminki (1982) reacted formaldehyde and acetaldehyde with cysteine,
2 N-acetylcysteine, and GSH and found that formaldehyde reacted most rapidly with cysteine to
3 form TZCA. Similarly, acetaldehyde reacted preferentially with cysteine, albeit slower than
4 formaldehyde, to form a thiazolidine derivative. However, when each aldehyde was
5 administered I.P. (10% formaldehyde, 50% acetaldehyde), thioether concentrations (nmol/mol
6 creatinine) significantly increased in the 24 and 48 hour urine of acetaldehyde-treated rats but
7 not formaldehyde-treated rats. These data suggest that formaldehyde is not appreciably excreted
8 in urine and thus cysteine conjugates are not likely to represent formaldehyde exposure.

9 Most recently, Shin et al. (2007) attempted to show that formaldehyde inhalation
10 increased urinary TZCA levels in Sprague-Dawley rats. Treated rats were exposed to 3.1 and
11 38.1 ppm formaldehyde for 6 hours/day for 2 weeks, and urine was collected for 3 days. The
12 TZCA level in four control rats was 0.07 ± 0.02 mg/L, whereas levels in the 3 and 38 ppm
13 groups were 0.18 ± 0.045 and 1.01 ± 0.36 , respectively. Notably, the concentrations in the four
14 highest exposed animals (0.71, 0.70, 1.20, and 1.43 ppm) exhibited a nearly twofold range.
15 However, these comparisons are confounded if the exposures have any influence on urine
16 production and urine cysteine levels. The study does not provide any data that might allow one
17 to examine this issue.

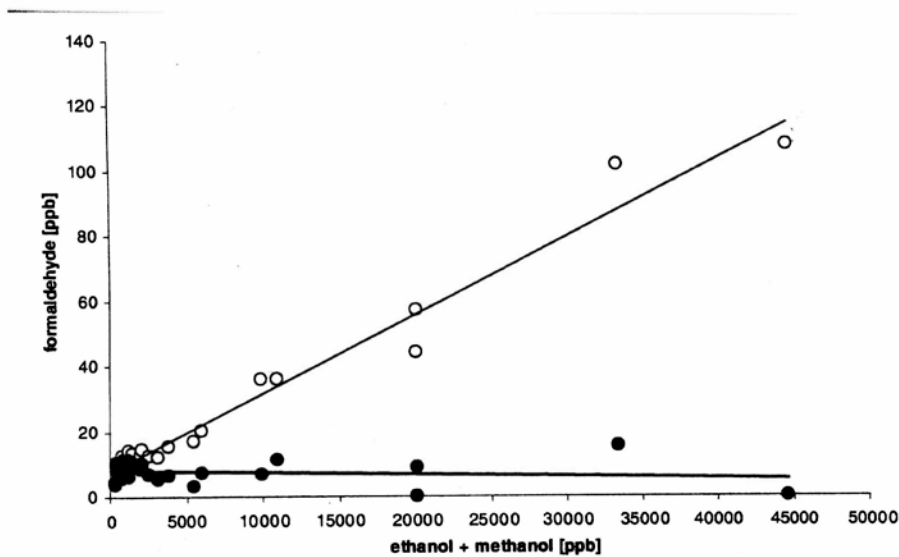
18 19 **3.6.2. Formaldehyde Excretion in Exhaled Human Breath**

20 Several human and animal studies have attempted to measure the concentration of
21 formaldehyde in exhaled breath. However, study design and limitations of available analytical
22 techniques have resulted in little data which provide a basis for determining levels of
23 formaldehyde in exhaled breath either from normal metabolism (in humans), or when
24 formaldehyde is administered (animal study). The two major limitations of studies of human
25 breath include the potential for false positives for formaldehyde from the primary analytical
26 technique for breath analysis and the need for concurrent room air controls.

27 A recent study has illustrated that the use of proton transfer reaction in SIFT-MS may
28 result in false positive results for formaldehyde as the characteristic analytical product ion for
29 formaldehyde is also produced from methanol and ethanol found in exhaled breath (Španěl and
30 Smith, 2008). Proton transfer reaction mass spectrometry (PTR-MS) has been applied to
31 measure trace compounds in exhaled breath including volatile organics and specifically
32 formaldehyde. The basic method of PTR-MS is based on the transfer of protons from H_3O^+ to
33 gases in exhaled breath and the in-line monitoring of products where gases are tentatively
34 identified by the mass to charge ratio (m/z) where an m/z of 31 is consistent with protonated
35 formaldehyde (Hansel et al., 1995; Lindinger et al., 1998). It is important to note that reaction

This document is a draft for review purposes only and does not constitute Agency policy.

1 products from methanol and ethanol may also produce fragments with an m/z ratio of 31 (Kusch
2 et al., 2008). Selected ion flow tube mass spectrometry (SIFT-MS) is an application of PTR-MS
3 developed for real-time analysis of trace gases in breath (Smith and Španěl, 2005; Španěl and
4 Smith, 2007). As shown in Figure 3-5 up to 1% of the mass of ethanol and methanol in exhaled
5 breath may be detected with a mass-to-charge ratio (m/z ratio) of 31—which may have been
6 reported as formaldehyde in earlier publications (Kusch et al., 2008; Španěl and Smith, 2008).
7 The authors have improved the SIFT-MS software used in exhaled breath analysis to adjust the
8 reported formaldehyde levels by accounting for the contribution of methanol and ethanol to the
9 characteristic analytical product ion for formaldehyde ($m/z = 31$). No published articles were
10 available on formaldehyde in exhaled breath which adjusted for methanol and ethanol levels in
11 exhaled breath. Therefore, the available articles discussed below will be evaluated with respect
12 to the potential for ethanol or methanol to influence the reported formaldehyde levels.
13



14
15 **Figure 3-5. Detection of the characteristic analytical product ion for**
16 **formaldehyde (m/z ratio of 31) by proton transfer reaction mass**
17 **spectrometry (PTR-MS) in gas samples spiked with only methanol and**
18 **ethanol.** Open circles show the reported formaldehyde without adjustment for
19 the methanol and ethanol present (each of which produces a small fraction of the
20 analytical product with an m/z ratio of 31). Closed circles represent the same
21 data, corrected by the SIFT-MS software to control for methanol and ethanol.
22

23 Source: Španěl and Smith (2008).

1 Six articles were located which reported formaldehyde levels in exhaled breath, three of
2 which provide level of methanol and ethanol in exhaled breath in the same individuals or study
3 group and are further discussed below (Wang et al., 2008; Cap et al., 2008; and Moser et al.,
4 2005). Although Wehinger et al., (2007) report a compound tentatively identified as
5 formaldehyde correlated with a diagnosis of lung cancer, the PTR-MS was not controlled for any
6 contribution of ethanol and methanol, and the levels of these compounds were not provided for
7 comparison so it is not further discussed here. Turner et al. (2008) measured levels of volatile
8 compounds including formaldehyde in exhaled breath five healthy males. The subjects fasted
9 overnight, and measurements were taken before and after ingesting 75 g of glucose. The source
10 of the inhaled air was laboratory air which contained an unreported concentration of
11 formaldehyde. Formaldehyde was not detected in the exhaled breath of any subjects (5 ppb limit
12 of detection) ethanol and methanol levels were not reported.

13 In a study designed to compare volatile organics in exhaled breath of smokers and
14 nonsmokers, compounds tentatively identified as formaldehyde and methanol were not different
15 between the populations (Kushch et al., 2008). The authors acknowledge that the reported
16 formaldehyde ($m/z = 31$) might also represent fragments of reaction products from methanol and
17 ethanol. Reported formaldehyde levels were approximately 5% of the methanol (e.g., mean of
18 9.9 ppb versus 208 ppb respectively).

19 Wang et al. (2008) measured the concentrations volatile organics, including
20 formaldehyde, in the exhaled breath through the nose or mouth, and oral cavity during breath
21 holding of three healthy male laboratory workers. Measurements were taken in each individual
22 over a period of a month, 20 workdays. Formaldehyde levels (4–7 ppb) were lower than the
23 inspired laboratory air (9.6 ppb) (see Table 3-5). Formaldehyde in the mouth during breath
24 holding, did not differ from the exhaled air (nose or mouth). The SIFT-MS analysis did not
25 adjust for any contribution of ethanol or methanol to the tentatively identified formaldehyde
26 levels. Although only means are reported, a comparison of results in Table 3-5 does indicate that
27 1% of the reported ethanol and methanol may have contributed significantly to the reported
28 formaldehyde levels.

29 Cáp et al. (2008) evaluated relationships between volatile organic compounds measured
30 in exhaled breath and exhaled breath condensate. Exhaled breath condensate consists of
31 aerosolized particles of airway lining fluid evolved from the airway wall by turbulent airflow
32 that serve as seeds for substantial water vapor condensation, which then serves to trap water
33 soluble volatile gases. This study also attempted to ascertain whether the source of each
34 compound was endogenous or exogenous. According to the published article and electronic

1 communication with Dr. Patrik Španěl, a coauthor for this study, the limit of quantification was 3
 2 ppb or better.

3 **Table 3-5. Measurements of exhaled formaldehyde concentrations in the**
 4 **mouth and nose, and in the oral cavity after breath holding in three healthy**
 5 **male laboratory workers.** The median levels are estimated as the geometric
 6 mean with the associated standard deviation (σ).
 7

Subject		Methanol (median ppb/ σ)	Ethanol (median ppb/ σ)	Formaldehyde (median ppb/ σ)
A	Mouth	178/1.2	236/1.6	5/2.3
	Nose	167/1.2	28/1.3	7/2.1
	Oral cavity	149/1.2	412/1.4	5/2.3
B	Mouth	300/1.4	64/1.6	7/2.3
	Nose	396/1.4	27/1.4	5/2.1
	Oral cavity	358/1.4	93/1.4	6/1.9
C	Mouth	228/1.5	153/1.5	4/2.5
	Nose	229/1.5	26/1.4	6/1.9
	Oral cavity	162/1.7	163/1.4	6/1.9
Laboratory air		44 \pm 9	101 \pm 52	9.6 \pm 1.5

Notes: The limit of quantification for formaldehyde was not reported.
 Source: Wang et al. (2008).

8 However, the SIFT-MS protocol used in this study did not adjust for any contribution of ethanol
 9 or methanol to reported formaldehyde levels. Unadjusted reported formaldehyde levels in the
 10 direct exhaled breath of 34 subjects (25 to 62 years; 11 males; 2 smokers) varied from 0 to 12
 11 ppb with a mean of 2 ppb and a median of 1 ppb (see Table 3-6). Measurements of
 12 formaldehyde in exhaled breath condensate ranged from 0 to 12 ppb with a mean of 2 ppb and a
 13 median of 0 ppb. All but one measurement was below the average ambient room air
 14 concentration of 9.6 \pm 1.5 ppb. Although comparisons on the individual level could not be made
 15 from the data as reported, the range of ethanol and methanol levels in exhaled breath indicate
 16 that 1% of the reported ethanol and methanol may have contributed significantly to the reported
 17 formaldehyde levels in exhaled breath (see Table 3-6). It is unclear if the reported formaldehyde
 18 may represent in part inhaled formaldehyde, reduced by absorption in the upper respiratory tract,
 19 or is an artifact of the reported methanol and ethanol levels.

This document is a draft for review purposes only and does not constitute Agency policy.

1
2

Table 3-6. Formaldehyde, methanol and ethanol levels reported in the exhaled breath of 34 subjects (25 to 62 years; 11 males; 2 smokers)

Chemical	Minimum (ppb)	Maximum (ppb)	Mean (ppb)	Median (ppb)
Methanol	102	2319	297	189
Ethanol	27	10262	447	82
1% of the reported levels of both ethanol and methanol	1.3	125	7.3	2.6
Formaldehyde (tentatively identified with a m/z ratio $n = 31$)	0	12	2	1

Source: Cáp et al. (2008).

3 Moser et al. (2005) measured levels of 179 volatile organic compounds (VOCs) in the
4 exhaled breath of 344 individuals. This study was not designed to ascertain whether exhaled
5 formaldehyde is of endogenous origin, but rather to demonstrate that proton transfer reaction-
6 mass spectrometry can be used as a new method for rapid screening of large collectives for risk
7 factors (e.g., smoking behavior), potential disease biomarkers, and ambient air characterization.
8 The study was conducted at a health fair. The test subjects had a mean age of 61.6 years; 63%
9 were males and 14% were smokers. Samples of room air were collected and evaluated in
10 parallel with exhaled breath samples. The authors note that formaldehyde was detected in room
11 air, but did not report the levels; rather they stated that the background concentrations were
12 negligible. Of the 179 volatile organic compounds measured, data were reported for 14,
13 including formaldehyde and formic acid. The report by Moser et al. (2005) does not provide the
14 limit of detection for any of the compounds measured or details of the analytical method. Moser
15 et al. (2005) do note that significant differences in exhaled breath composition could be found
16 between smokers and nonsmokers for 32 of the 179 chemicals measured, but the 32 chemicals
17 were not named and no substantiating data were provided.

18 The formaldehyde levels in exhaled breath spanned from 1.2 to 72.7 ppb with a median
19 of 4.3 ppb and 75th percentile of 6.3 ppb (see Table 3-7) (Moser et al., 2005). The reported
20 levels of formaldehyde (m/z ratio = 31) we not adjusted for any potential contribution from
21 methanol or ethanol in exhaled breath. The levels of methanol and ethanol in exhaled breath
22 were reported by Moser et al. (2005). Although the summary statistics do not allow comparison

1 of individual results, it is possible that reaction fragments from methanol and ethanol may have
2 contributed to the reported formaldehyde levels (see Table 3-7).

3 **Table 3-7. Apparent formaldehyde levels (ppb) in exhaled breath of**
4 **individuals attending a health fair, adjusted for methanol and ethanol levels**
5 **which contribute to the detection of the protonated species with a mass to**
6 **charge ratio of 31 reported as formaldehyde ($m/z = 31$)**

Chemical	Minimum	25 th percentile	Median	75 th percentile	97.5 th percentile	Maximum
Methanol	13.367	106.227	161.179	243.185	643.614	1536.499
Ethanol	11.583	23.1	34.664	64.24	549.24	9779.768
1% of the reported levels of both ethanol and methanol	0.25	1.29	1.96	3.07	11.93	113.16
Mass of $m/z = 31$ reported as formaldehyde	1.23	3.1	4.26	6.33	39.8	72.7

Source: Moser et al. (2005).

7 .
8 The range of reported formaldehyde is much greater in this study of the general
9 population (attendees at a health fair) than that observed in healthy volunteers discussed above
10 (Wang et al., 2008; Cap et al., 2008; Turner et al., 2008; Kushch et al., 2008). Moser et al.
11 (2005) do not discuss potential causes for this wide range in values, and there was no distinction
12 of the data by sex, age, or health. However, reported formaldehyde in exhaled breath
13 (unadjusted) has been correlated to lung cancer diagnosis with a median of 7.0 ppb and upper
14 95th CI greater than 30 ppb (Wehinger et al., 2007). Although it is unknown if these results
15 represent only formaldehyde, or are in part an artifact of increased ethanol and methanol in
16 exhaled breath, the higher levels reported by Moser et al. (2005) may reflect volatile levels in
17 unhealthy individuals who attended the public health fair.

18 Selected ion flow tube mass spectrometry (SIFT-MS), with the recent improvements by
19 Španěl and Smith (2008) to account for the fragments of methanol and ethanol reaction products,
20 have the ability to detect formaldehyde in exhaled breath. However, to date, no data has been
21 published which makes this adjustment for reporting formaldehyde levels. Therefore all of the
22 above reports of formaldehyde in exhaled breath should be carefully interpreted as the mass
23 reported as formaldehyde—is only tentatively identified as formaldehyde. A careful review of
24 the data where methanol and ethanol levels are also provided, indicate that levels of
25 formaldehyde (tentatively identified as $m/z = 31$) may reflect a significant contribution from

This document is a draft for review purposes only and does not constitute Agency policy.

1 reaction products of methanol and ethanol. In summary, there are insufficient data at this time to
2 confidently establish a concentration of formaldehyde in exhaled breath that can be attributed to
3 endogenous sources. Additional research is needed to further clarify.

4 5 **3.6.3. Formaldehyde Excretion in Human Urine**

6 Gottschling et al. (1984) examined urinary formic acid in 35 veterinary students.
7 Personal monitoring badges were worn and returned after class, and urine samples were taken
8 prior to class and within 2 hours after the class. Mean exposure levels were about 100 ppb.
9 Baseline averages of urinary formic acid (as a sodium salt) were 12.47 mg/L and ranged from
10 2.43 to 28.38 mg/L among subjects. Post exposure formate levels were slightly elevated but
11 were not statistically significant. Moreover, formate levels decreased in several individuals
12 relative to pre-exposure levels. The authors concluded that variability in urinary formate may
13 mask any changes and that monitoring formate within 2 hours of exposure is not informative. It
14 is worth noting, however, that interpretation of this finding is confounded due to the fact that diet
15 was not controlled and because no markers for urinary normalization were employed (Boeniger,
16 1987).

17 Boeniger (1987) reviewed previously published data on formate in urine (some of which
18 were in German). In one occupational study, workers were exposed to an average formaldehyde
19 exposure of 1.28 mg/m³ over a 6-hour work shift. This implies an average intake of 6 mg;⁶
20 Boeniger reported a range of 2.5 to 13 mg. However, the original study reported that post-shift
21 formate levels were 152 mg/L, whereas the levels were only 24 mg/L 6 days later (no exposure).
22 Considering that only a small percentage of inhaled formaldehyde would be excreted in urine, it
23 is unclear how (or whether) formaldehyde exposure, with the highest total dose of 13 mg, could
24 be responsible for the observed increase.

25 In the previously described study by Shin et al. (2007), human urine samples were shown
26 to contain TZCA, although variability was not reported. A subsequent study reported that urine

27 TZCA levels were higher in individuals living in newer apartments (0.18 ± 0.121 mg/g
28 creatinine) as compared to older apartments (0.097 ± 0.040 mg/g creatinine) (Li et al., 2007).⁷

29 The authors cited this as evidence that TZCA is a urinary marker for formaldehyde exposure,
30 even though TZCA levels were not correlated to measured (or estimated) formaldehyde
31 exposures. The individuals also differed significantly in age (21.5 vs. 28.6, $p = 0.053$) and

⁶ $1.28 \text{ mg/m}^3 / 1,000 \text{ L/m}^3 \times 13.8 \text{ L/minute} \times 60 \text{ minutes/hour} \times 6 \text{ hours}$.

⁷ This study is described in greater detail in Chapter 5.

1 differed in smoking percentage (10 vs. 27%). Clearly these two studies do not establish a
2 relationship between human formaldehyde exposure and urine TZCA levels.
3

4 **3.7. MODELING THE TOXICOKINETICS OF FORMALDEHYDE AND DPX**

5 **3.7.1. Motivation**

6 Airway geometry is expected to be an important determinant of inhaled formaldehyde
7 dosimetry in the respiratory tract and its differences across species. The uptake of formaldehyde
8 in the upper respiratory tract is highly nonhomogeneous and spatially localized and exhibits
9 strong species differences. Species differences in kinetic factors have been argued to be the key
10 determinants of species-specific lesion distributions for formaldehyde and other reactive inhaled
11 gases. Section 3.7.2 details the benefits to the quantitative risk assessment of modeling these
12 dosimetric differences in the upper respiratory tract. While frank effects were seen only in the
13 upper respiratory tract in rodents, mild lesions were also present in the major bronchiolar region
14 of the rhesus monkey. Therefore, with regard to extrapolation of cancer risk from animal
15 bioassays to humans, it appears that the upper and lower human respiratory tract should both be
16 considered potentially at risk of developing formaldehyde-induced squamous cell carcinoma.
17 Therefore, formaldehyde dose to the lower human respiratory tract also needs to be quantified in
18 order to develop a dose-response relationship that considers the entire respiratory tract.

19 This assessment uses internal dose metrics computed by using fluid dynamic models to
20 compute regional formaldehyde uptake in the F344 rat and human nasal passages and in the
21 human lower respiratory tract. The assessment also uses estimates of DPX levels in the nasal
22 lining predicted by physiologically-based pharmacokinetic models which use the fluid dynamic
23 model derived estimates of formaldehyde flux to the tissue as input. These computational
24 models enable the derivation of more accurate human equivalent concentrations from the animal
25 bioassays than would be obtained by averaging over the respiratory surface area. The following
26 sections provide the motivation for these calculations, and discuss the strengths and uncertainties
27 associated with the data and the models and their relevance to the hypothesized mode of action
28 are discussed in some length.
29

30 **3.7.2. Species Differences in Anatomy: Consequences for Gas Transport and Risk**

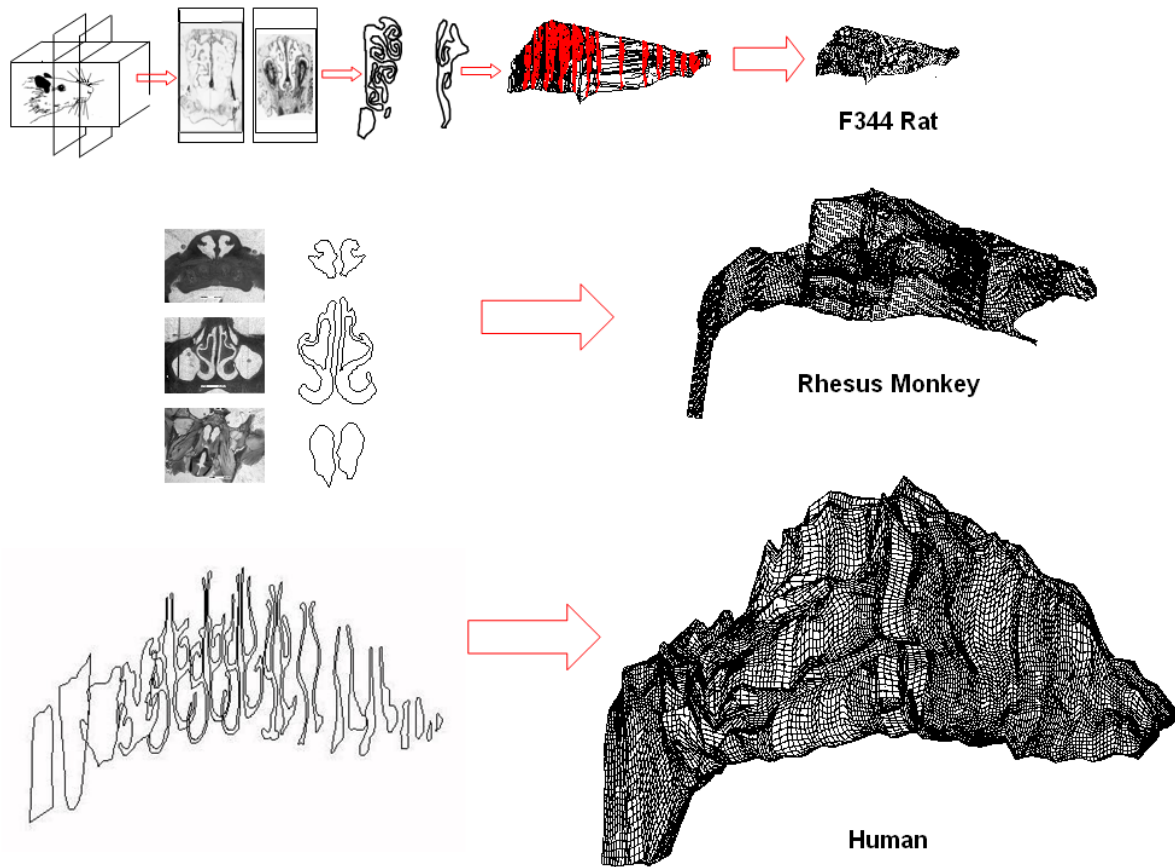
31 As discussed earlier, formaldehyde is highly reactive and water soluble (categorized as a
32 category 1 gas), thus its absorption in the mucus layer and tissue lining of the upper respiratory
33 tract is known to be significant. The regional inhaled dose of formaldehyde to the respiratory
34 tract of a given species depends on the amount of formaldehyde delivered by inhaled air, the
35 absorption characteristics of the nasal lining, and reactions in the tissue. The amount delivered

This document is a draft for review purposes only and does not constitute Agency policy.

1 by inhaled air is a function of the major airflow patterns, air-phase diffusion, and absorption at
2 the airway-epithelial tissue interface. The dose of formaldehyde to the epithelial tissue, which is
3 different from the amount delivered, depends on the amount absorbed at the airway-tissue
4 interface, water solubility, mucus-to-tissue phase diffusion, and chemical reactions, such as
5 hydrolysis, protein binding, and metabolism. It has been argued strongly that species differences
6 in these kinetic factors are determinants of species-specific lesion distributions for formaldehyde
7 and other inhaled gases (Moulin et al., 2002; Bogdanffy et al., 1999; Ibanes et al., 1996;
8 Monticello et al., 1996; Monticello and Morgan, 1994; Morgan et al., 1991).

9 Because of the convoluted nature of the airways in the upper respiratory tract, the
10 absorption of such gases in the upper respiratory tract is highly nonhomogeneous. There are
11 large differences across species in the anatomy of the upper respiratory tract (see Figure 3-6) and
12 in airflow patterns (see Figure 3-7). Therefore, as shown in the simulations in Figure 3-8, it may
13 be expected that the uptake patterns, and thus risk due to inhaled formaldehyde, will also show
14 strong species dependence. Morgan et al. (1991) concluded that airflow-driven dosimetry plays
15 a critical role in determining the site specificity of various formaldehyde-induced responses,
16 including tumors, in the nose of the F344 rat. The convoluted geometry of the airway passages
17 in the upper respiratory tract, as seen from the cross sections of the nose in Figure 3-6, renders an
18 idealized representation of fluid flow and uptake profiles almost impossible. For these reasons,
19 Kimbell et al. (1998, 1993), Kepler et al. (1998), and Subramaniam et al. (1998) developed
20 anatomically realistic finite-element representations of the noses of humans, F344 rats, and
21 rhesus monkeys. These representations were subsequently used in physical and computational
22 models (see Figure 3-6). This assessment utilizes dosimetry derived from these representations.

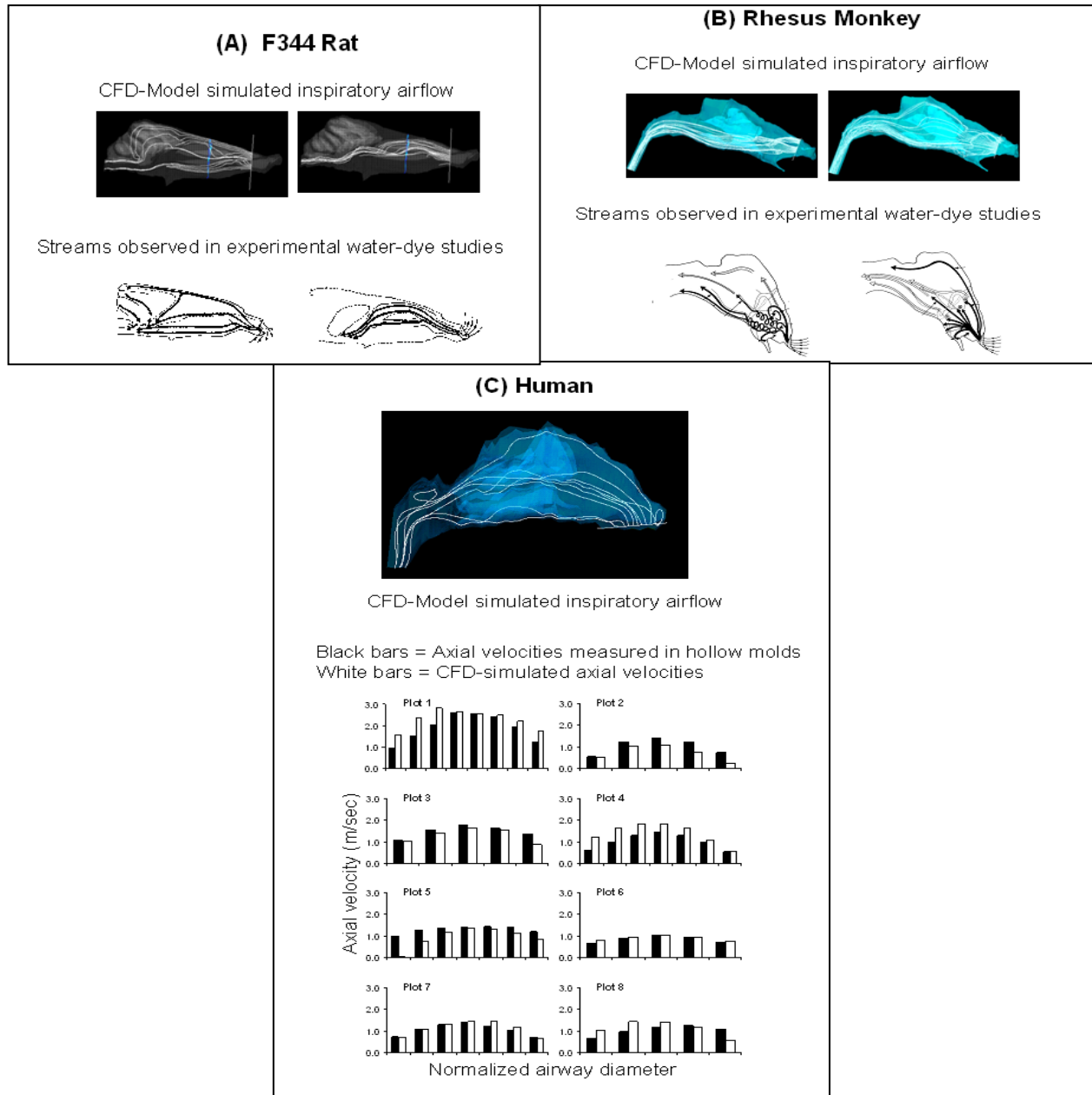
23 An accurate calculation of species differences in formaldehyde dosimetry in the upper
24 respiratory tract is important to the extrapolation problem for another reason. The upper
25 respiratory tract in rats is an extremely efficient scrubber of reactive gases (97% uptake)
26 (Morgan et al., 1986), thereby protecting the lower respiratory tract from gaseous penetration.
27 On the other hand, there is considerably more fractional penetration of formaldehyde into the
28 lower respiratory tract of the rhesus monkey than in the rat (see Figure 3-8). Therefore, an
29 accurate determination of scrubbing in the upper respiratory tract is important to delineate
30 species differences in dosimetry in both the upper and lower respiratory tract. Thus, in the case
31 of the rhesus monkey, the model by Kepler et al. (1998) included the trachea. It is important to
32 note that the models mentioned above represent nasal passages reconstructed from a single
33 individual from each species (Kimbell et al., 2001a, b; Conolly et al., 2000; CIIT, 1999;
34 Subramaniam et al., 1998). This is discussed later in the context of intraspecies variability.



1
2
3

Figure 3-6. Reconstructed nasal passages of F344 rat, rhesus monkey, and human.

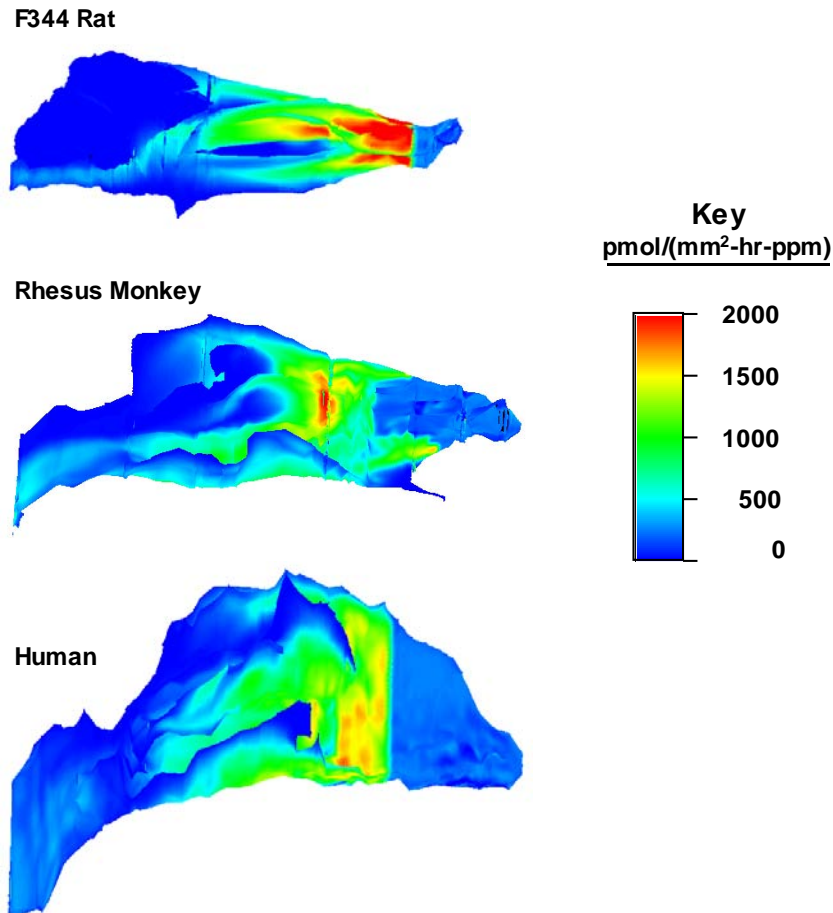
Note: Nostril is to the right, and the nasopharynx is to the left. Right side shows the finite element mesh. Left-hand side shows tracings of airways obtained from cross sections of fixed heads (F344 rat and rhesus monkey) and magnetic resonance image sectional scans (humans). Aligned cross sections were connected to form a three-dimensional reconstruction and finite-element computational mesh. Source: Adapted from Kimbell et al. (2001a). Additional images provided courtesy of Dr. J.S. Kimbell, CIIT Hamner Institutes.



1 **Figure 3-7. Illustration of interspecies differences in airflow and verification**
 2 **of CFD simulations with water-dye studies.**

Note: Panels A and B show the simulated airflow pattern versus water-dye streams observed experimentally in casts of the nasal passages of rats and monkeys, respectively. Panel C shows the simulated inspiration airflow pattern, and the histogram depicts the simulated axial velocities (white bars) vs. experimental measurements made in hollow molds of the human nasal passages. Dye stream plots were compiled for the rat and monkey over the physiological range of inspiration flow rates. Modeled flow rates in humans were 15 L/minute. Source: Adapted from Kimbell et al. (2001a).

This document is a draft for review purposes only and does not constitute Agency policy.



1 **Figure 3-8. Lateral view of nasal wall mass flux of inhaled formaldehyde**
 2 **simulated in the F344 rat, rhesus monkey, and human.**

Note: Nostrils are to the right. Simulations were exercised in each species at steady-state inspiration flow rates of 0.576 L/minute in the rat, 4.8 L/minute in the monkey, and 15 L/minute in the human. Flux was contoured over the range from 0–2,000 $\text{pmol}/(\text{mm}^2\text{-hour-ppm})$ in each species.

Source: Kimbell et al. (2001a).

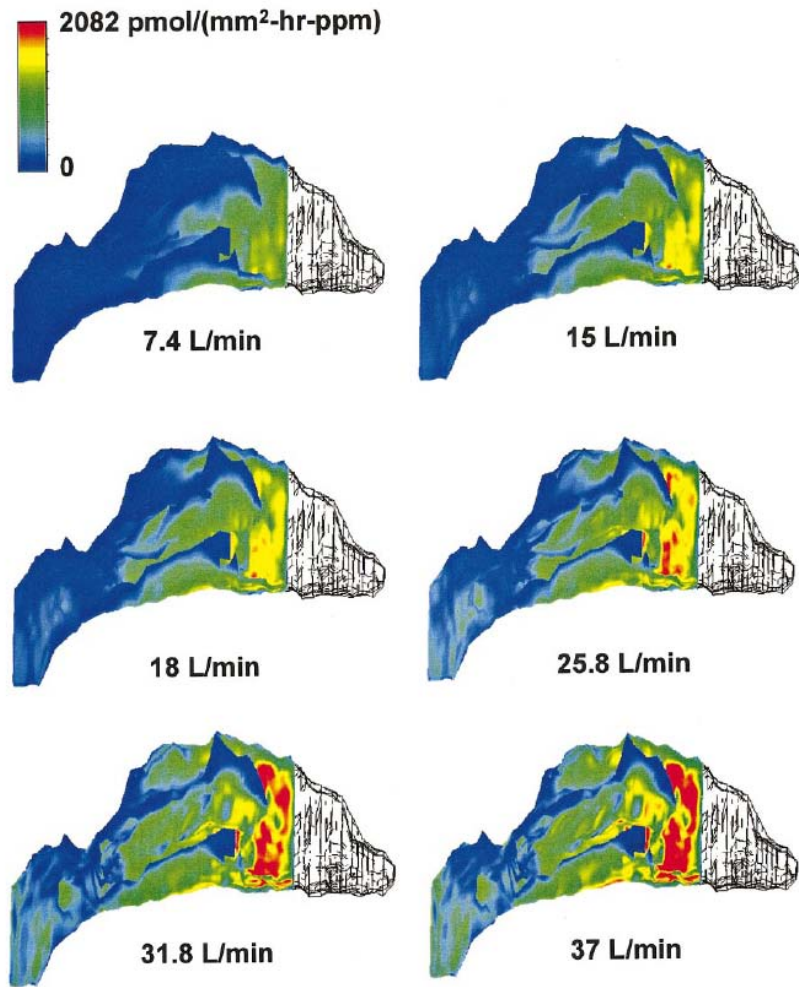
3 The highly localized nature of uptake patterns shown in Figure 3-8 means that averaging
 4 uptake over the entire nasal surface area would dilute the regional dose over areas where
 5 response was observed and that an extrapolation based on such averaging would clearly not be
 6 accurate.

7 Another factor to consider in the extrapolation is that monkeys and humans are oronasal
 8 breathers while rats are obligate nose-only breathers. Thus, for humans and monkeys, oronasal
 9 or oral breathing implies a significantly higher uptake in the lower respiratory tract. It is known

This document is a draft for review purposes only and does not constitute Agency policy.

1 that a significant fraction of the human population breathes normally through the mouth.
2 Finally, activity profiles are also determinants of extraction efficiency (see Figure 3-9) and of
3 breathing route (Niinimaa et al., 1981). Given the fact that formaldehyde-induced lesions were
4 observed as far down the respiratory tract as the first bifurcation of the lungs in exposed
5 monkeys, the entire human respiratory tract should be considered when extrapolating data from
6 rats. Thus, for the human, Overton et al. (2001) attached an idealized single-path model of the
7 lower respiratory tract to a model of the upper respiratory tract.

8



9 **Figure 3-9. CFD simulations of formaldehyde flux to human nasal lining at**
10 **different inspiratory flow rates.**

11 Note: Right lateral view. Uptake is shown for the nonsquamous portion of the
12 epithelium. The front portion of the nose (vestibule) is lined with keratinized
13 squamous epithelium and is expected to absorb relatively much less
14 formaldehyde.

15 Source: Kimbell et al. (2001b).

This document is a draft for review purposes only and does not constitute Agency policy.

3.7.3. Modeling Formaldehyde Uptake in Nasal Passages

Computational models for air flow and formaldehyde uptake in the F344 rat, rhesus monkey, human nose, and human lung were developed by several scientists (Kimbell et al., 1998, 1993; Kepler et al., 1998; Subramaniam et al., 1998; Kimbell et al., 2001a, b). The F344 strain of the rat was chosen since it was assumed to be anatomically representative of its species and because it is widely used experimentally, most notably in bioassays sponsored by the National Toxicology Program. The approximate locations of squamous, mucus-coated, and nonmucus epithelial cells were mapped onto the reconstructed nasal geometry of the computer models. Taken together, these regions of nonmucus and mucus-coated cells comprise the entire surface area of the nasal passages (see original papers and CIIT [1999] for further details on reconstruction and morphometry). Types of nasal epithelium overlaid onto the geometry of the models were assumed to be similar in characteristics across all three species (rat, monkey, and human) except for thickness, surface area, and location. Species-specific mucosal thickness, surface area, and location were estimated from the literature or by direct measurements (Conolly et al., 2000; CIIT, 1999). The nasal passages of all three species were assumed to have a continuous mucus coating over all surfaces except specific areas in the nasal vestibule. As discussed at the beginning of this chapter, formaldehyde hydrolyzes in water and reacts readily with a number of components of nasal mucus. Absorption rates of inhaled formaldehyde by the nasal lining were therefore assumed to depend on where the epithelial lining is coated by mucus and where it is not.

To calculate an airflow rate that would be comparable among species, the amount of inspired air (tidal volume, V_T) was divided by the estimated time involved in inhalation (half the time a breath takes, or $(1/2)(1/[\text{breathing frequency, } f])$). Thus, an inspiratory flow rate was calculated to be $2V_T f$, or twice the minute volume. Predicted flux values represent an average of one nasal cycle. Minute volumes were allometrically scaled to 0.288 L/minute for a 315 g rat from data given by Mauderly (1986). Simulations were therefore carried out at 0.576 L/minute for the rat.

The fluid dynamics modeling in the respiratory tract comprises two steps: modeling the airflow through the lumen (solution of Navier-Stokes equations) and modeling formaldehyde uptake by the respiratory tract lining (solution of convective-diffusion equations for a given airflow field). Details of these simulations, including boundary conditions for air flow and mass transfer, are provided in Kimbell et al. (2001a, b; 1998, 1993) and Subramaniam et al. (1998). Formaldehyde absorption at the airway-to-epithelial tissue interface was assumed to be proportional to the air-phase formaldehyde concentration adjacent to the nasal lining layer in

1 monkeys and humans (see the original paper [Kimbell et al., 2001a, b] for a more detailed
2 elaboration of the calculations for these coefficients).

3 Because formaldehyde is highly water soluble and reactive, Kimbell et al. (2001a)
4 assumed that absorption occurred only during inspiration. Thus, for each breath, flux into nasal
5 passage walls (rate of mass transport in the direction perpendicular to the nasal wall per mm² of
6 the wall surface) was assumed to be zero during exhalation, with no backpressure to uptake built
7 up in the tissues. Overton et al. (2001) estimated the error due to this assumption to be small,
8 roughly an underestimate of 3% in comparison to cyclic breathing. Also, this assumption is the
9 same as that used in default methods for reference concentration determination and has been
10 used in other PBPK model applications to describe nasal uptake (Andersen and Jarabek, 2001).

11 **3.7.3.1. Flux Bins**

12 A novel contribution of the CIIT biologically motivated dose-response model is that cell
13 division rates and DPX concentrations are driven by the local concentration of formaldehyde.
14 These were determined by partitioning the nasal surface by flux, resulting in 20 “flux bins.”
15 Each bin was comprised of elements (not necessarily contiguous) of the nasal surface that
16 receive a particular interval of formaldehyde flux per ppm of exposure concentration (Kimbell et
17 al., 2001a, b). The spatial coordinates of elements comprising a particular flux bin were fixed
18 for all exposure concentrations, with formaldehyde flux in a bin scaling linearly with exposure
19 concentration (ppm). Thus, formaldehyde flux was expressed as pmol/(mm²-hour-ppm).

20 **3.7.3.2. Flux Estimates**

21 Formaldehyde flux was estimated for the rat, monkey, and human over the entire nasal
22 surface and over the portion of the nasal surface that was lined by nonsquamous epithelium.
23 Formaldehyde flux was also estimated for the rat and monkey over the areas where cell
24 proliferation measurements were made (Monticello et al., 1991, 1989) and over the anterior
25 portion of the human nasal passages that is lined by nonsquamous epithelium. Figure 3-8 shows
26 the mass flux of inhaled formaldehyde to the lateral wall of nasal passages in the F344 rat, rhesus
27 monkey, and human (Kimbell et al., 2001a, b).

28 Maximum flux estimates for the entire upper respiratory tract were located in the mucus-
29 coated squamous epithelium on the dorsal aspect of the dorsal medial meatus near the boundary
30 between nonmucus and mucus-coated squamous epithelium in the rat, at the anterior or rostral
31 margin of the middle turbinate in the monkey, and in the nonsquamous epithelium on the
32 proximal portion of the mid-septum near the boundary between squamous and nonsquamous
33
34

1 epithelium in the human (see Kimbell et al. [2001a, b] for tabulations of comparative estimates
2 of formaldehyde flux across the species).

3 The rat-to-monkey ratio of the highest site-specific fluxes in the two species was 0.98. In
4 the rat, the incidence of formaldehyde-induced squamous cell carcinomas in chronically exposed
5 animals was high in the anterior lateral meatus (Monticello et al., 1996). Flux predicted per ppm
6 in this site and flux predicted near the anterior or proximal aspect of the inferior turbinate and
7 adjacent lateral walls and septum in the human were similar, with a rat-to-human ratio of 0.84.
8

9 **3.7.3.3. Mass Balance Errors**

10 Overall uptake of formaldehyde was calculated as $100\% \times (\text{mass entering nostril} - \text{mass}$
11 $\text{exiting outlet})/(\text{mass entering nostril})$. Mass balance errors for air, $100\% \times (\text{mass of air entering}$
12 $\text{nostril} - \text{mass exiting outlet})/(\text{mass entering nostril})$, and inhaled formaldehyde, $100\% \times (\text{mass}$
13 $\text{entering nostril} - \text{mass absorbed by airway walls} - \text{mass exiting outlet})/(\text{mass entering nostril})$,
14 were calculated. Mass balance errors associated with simulated formaldehyde uptake from air
15 into tissue ranged from less than 14% for the rat, monkey, and human at 7.4 and 15 L/minute to
16 approximately 27% at the highest inspiratory flow rates of 31.8 and 37 L/minute (Kimbell et al.,
17 2001b). Kimbell et al. (2001b) corrected the simulation results for these errors by evenly
18 distributing the lost mass over the entire nasal surface.
19

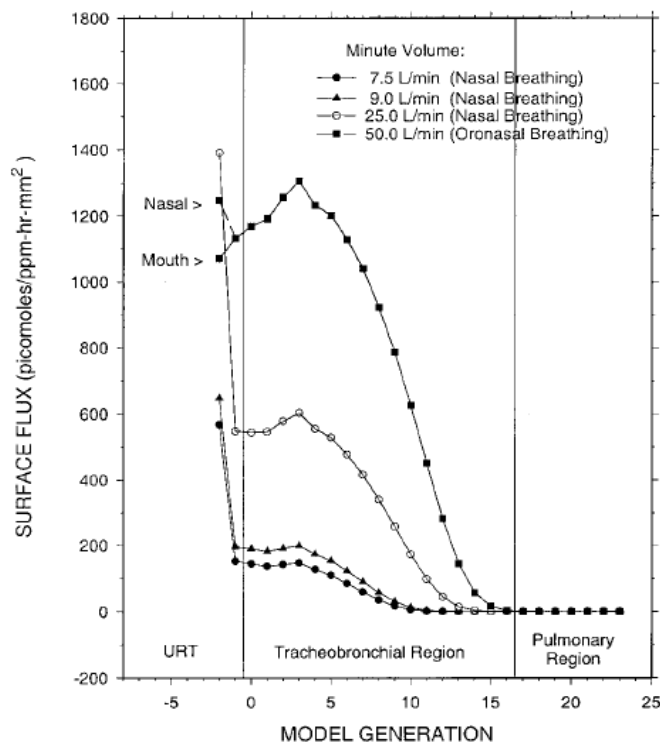
20 **3.7.4. Modeling Formaldehyde Uptake in the Lower Respiratory Tract**

21 Lesions were observed in the lower respiratory tract of rhesus monkeys exposed to 6 ppm
22 formaldehyde. Therefore it is appropriate to consider the human lower respiratory tract as
23 potentially at risk for formaldehyde-induced cancer. Accordingly, fluid flow and formaldehyde
24 uptake in the lower respiratory tract were also modeled for the human in the CIIT approach by
25 using dosimetry estimates for the human lower respiratory tract.

26 The single-path idealization of the human lung anatomy captures the geometrical
27 characteristics of the airways for a given lung depth, and of airflow through these airways, in an
28 average, homogeneous sense. For particulates, this has provided a reasonable representation of
29 the average deposition in a given generation of the lung airways for a normal human population.

30 The one-dimensional model by Weibel (1963) is generally considered adequate unless the fluid
31 dynamics at airway bifurcations need to be explicitly modeled, and such an idealization of the
32 lung geometry has been successfully used in various models for the dosimetry of ozone and
33 particulate and fibrous matter. Most likely, the lung geometries of the susceptible population,
34 such as those with chronic obstructive pulmonary disease, would depart significantly from the
35 geometry described in Weibel (1963). Unlike the accurate representation of the nasal anatomy

1 used in the CFD modeling, the lung geometry is idealized in the CIIT approach as a typical path
2 Weibel geometry. The single-path model used to calculate formaldehyde uptake in the human
3 respiratory tract (Overton et al., 2001; CIIT, 1999) applied a one-dimensional equation of mass
4 transport to each generation of an adult human symmetric, bifurcating Weibel-type respiratory
5 tract anatomical model, augmented by an upper respiratory tract. The detailed CFD modeling of
6 the upper respiratory tract was made consistent with the upper respiratory tract in the single-path
7 model by requiring that the one-dimensional version of the nasal passages have the same
8 inspiratory air-flow rate and uptake during inspiration as the CFD simulations for four daily
9 human activity levels. The reader is referred to Overton et al. (2001) for further details of the
10 simulations. Results most relevant to this assessment are shown in Figure 3-10.
11



12 **Figure 3-10. Single-path model simulations of surface flux per ppm of**
13 **formaldehyde exposure concentration in an adult male human.**

Source: Overton et al. (2001).

14
15
16 The primary predictions of the model, as shown in Figure 3-10, were that more than 95%
17 of the inhaled formaldehyde would be retained and formaldehyde flux in the lower respiratory

This document is a draft for review purposes only and does not constitute Agency policy.

1 tract would increase for several lung airway generations from that in the posterior-most segment
2 of the nose and then decrease rapidly, resulting in almost zero flux to the alveolar sacs.

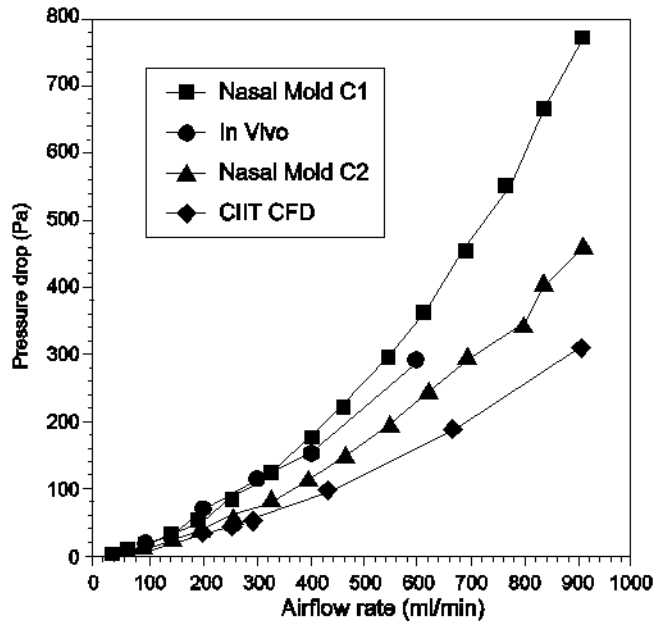
3 Overton et al. (2001) modeled uptake at higher inspiratory rates, including those at
4 50 L/minute of minute volume (well beyond levels where the oronasal switch occurs in the
5 normal nasal breathing population). At these rates Figure 3-8 indicates that formaldehyde flux in
6 the mouth cavity is comparable (but a bit less) to that occurring in the nasal passages. Overton et
7 al. (2001) did not model uptake in the oral cavity at minute volumes less than 50 L/minute. This
8 would be of interest because mouth breathers form a large segment of the population.
9 Furthermore, at concentrations of formaldehyde where either odor or sensory irritation becomes
10 a significant factor, humans are likely to switch to mouth breathing even at resting inspiration.
11 At a minute volume of 50 L/minute, Overton et al. (2001) assumed, citing Niinimaa et al. (1981),
12 that 0.55 of the inspired fraction is through the mouth. Therefore, based on the results in
13 Figure 3-8, it is not unreasonable to assume that for mouth breathing conditions at resting or
14 light exercise inspiratory rates, average flux across the human mouth lining would be
15 comparable to the average flux across the nasal lining computed in Kimbell et al. (2001a, b).

16 17 **3.7.5. Uncertainties in Formaldehyde Dosimetry Modeling**

18 **3.7.5.1. Verification of Predicted Flow Profiles**

19 The simulated streamlines of steady-state inspiration airflow predicted by the CFD model
20 agreed reasonably well with experimentally observed patterns of water-dye streams made in
21 casts of the nasal passages for the rat and monkey as shown in panels A and B in Figure 3-7.
22 The airflow velocity predicted by CFD model simulations of the human also agreed well with
23 measurements taken in hollow molds of the human nasal passages (panel C, Figure 3-8) (Kepler
24 et al., 1998; Subramaniam et al., 1998; Kimbell et al., 1997a, 1998, 1993). However, the
25 accuracy and relevance of these comparisons are limited. The profiles were verified by video
26 analysis of dye streak lines in the molds of rats and rhesus monkeys, although this method is
27 reasonable for only the major airflow streams.

28 Plots of pressure drop vs. volumetric airflow rate predicted by the CFD simulations
29 compared well with measurements made in rats in vivo (Gerde et al., 1991) and in acrylic casts
30 of the rat nasal airways (Cheng et al., 1990) as shown in Figure 3-11. This latter comparison
31 remains qualitative due to differences among the simulation and experiments as to where the
32 outlet pressure was measured and because no tubing attachments or other experimental apparatus
33 were included in the simulation geometry. The simulated pressure drop values were somewhat
34 lower, possibly due to these differences.



1 **Figure 3-11. Pressure drop vs. volumetric airflow rate predicted by the CIIT**
 2 **CFD model compared with pressure drop measurements made in two hollow**
 3 **molds (C1 and C2) of the rat nasal passage (Cheng et al., 1990) or in rats**
 4 **in vivo (Gerde et al., 1991).**

Source: Kimbell et al. (1997a).

5 Inspiratory airflow was assumed to be constant in time (steady state). Subramaniam et al.
 6 (1998) considered this to be a reasonable assumption during resting breathing conditions based
 7 on a value of 0.02 obtained for the Strouhal number. Unsteady effects are insignificant when
 8 this number is much less than one. However, this assumption may not be reasonable for light
 9 and heavy exercise breathing scenarios.

10

11 **3.7.5.2. Level of Confidence in Formaldehyde Uptake Simulations**

12 Unlike the airflow simulations, it was not possible to evaluate the formaldehyde uptake
 13 calculations directly. Since the mass transfer boundary conditions were set by fitting overall
 14 uptake to the average experimental data for various exposure concentrations, it was not possible
 15 to independently verify even the overall uptake values with empirical data. This assessment has
 16 relied on several indirect qualitative and quantitative lines of evidence listed below to provide
 17 general confidence in the uptake profile for the F344 rat nasal passages, as modeled in CIIT
 18 (1999), when gross averages are considered over certain regions of the nasal lining.

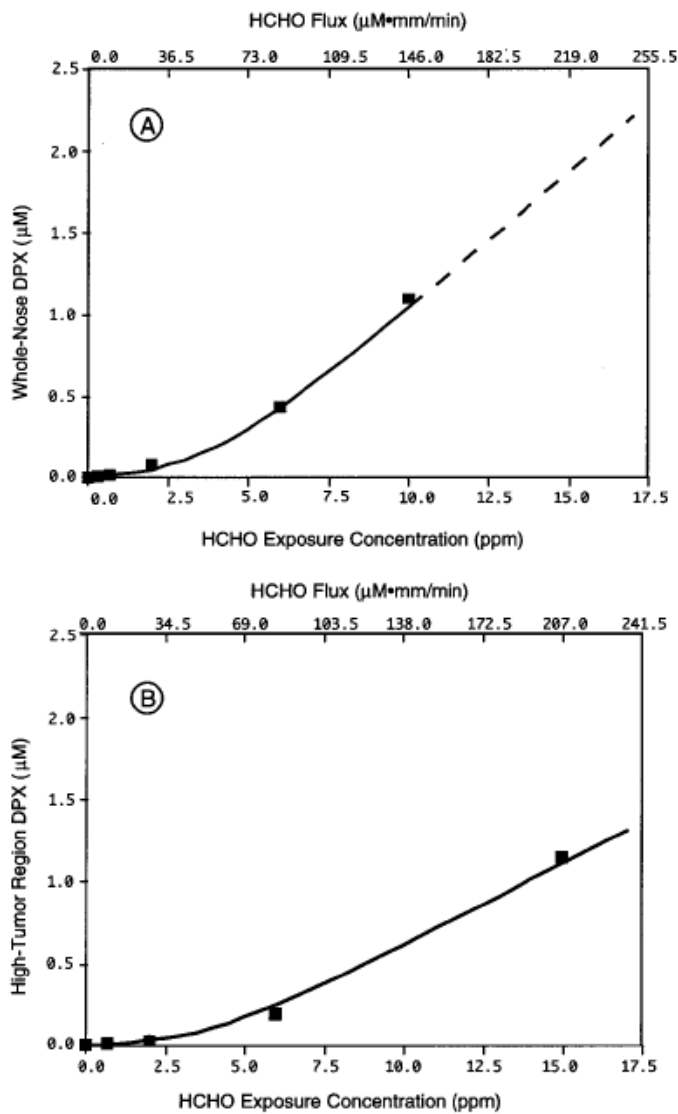
1 In an earlier simulation, where the nasal walls were set to be infinitely absorbing of
2 formaldehyde, uptake of inhaled formaldehyde in the upper respiratory tract was predicted to be
3 90% in the rat for simulations corresponding to the resting minute volume in the F344 rat. This
4 estimate compared reasonably well with the range of 91–98% observed by Morgan et al.
5 (1986a).

6 Morgan et al. (1991) showed general qualitative correspondence between the main routes
7 of flow and lesion distribution induced by formaldehyde in the rat nose. In their initial work
8 with a CFD model that represented a highly reactive and soluble gas, Kimbell et al. (1998, 1993)
9 described similarities in computed regional mass flux patterns and lesion distribution due to
10 formaldehyde. When the results from this work in the coronal section immediately posterior to
11 the vestibular region were considered, simulated flux levels over regions such as the medial
12 aspect of the maxilloturbinate and the adjacent septum (where lesions were seen) were an order
13 of magnitude higher than over other regions, such as the nasoturbinate (where lesions were not
14 seen).⁸

15 The results of a PBPK model by Cohen-Hubal et al. (1997) provide a reasonable level of
16 confidence in regional uptake simulations for the F344 rat when gross averages over nasal sites
17 are carried out. Cohen-Hubal et al. (1997) linked the CFD dosimetry model for formaldehyde to
18 a PBPK model for formaldehyde-DPX concentration in the F344 rat. This PBPK model was
19 calibrated by optimizing the model to combined DPX data from all regions of the rat nose (high-
20 tumor and low-tumor incidence regions) that were obtained in separate experiments by Casanova
21 et al. (1991, 1989). These data were obtained at 0.3, 0.7, 2.0, 6.0, and 10 ppm for both regions.
22 DPX data were also obtained at 15 ppm exposure from the high-tumor region; however these
23 were not included for the calibration. Model prediction of DPX concentrations were then
24 compared with data for the high-tumor region only and compared well with the experimental
25 data, including the 15 ppm data for which the model had not been calibrated. This is shown in
26 Figure 3-12. Such a verification, albeit indirect, is not available for the simulation of uptake
27 patterns in the human.

28 The CFD simulations do not model reflex bradypnea, a protective reflex seen in rodents
29 but not in humans. As discussed at length in Sections 3.2.3.1 and 4.2.1.1, it is reasonable to

⁸ However, this 1993 CFD model differed somewhat from the subsequent model by Kimbell et al. (2001a) used in this assessment. In the 1993 model, the limiting mass-transfer resistance for the gas was assumed to be in the air phase; that is, the concentration of formaldehyde was set to zero at the airway lining. Furthermore, this same boundary condition was used on the nasal vestibule as well, while, in the more recent model, the vestibule was considered to be nonabsorbing. Unfortunately, Kimbell et al. (2001a) did not report on correspondences between flux patterns and lesion distribution.



1 **Figure 3-12. Formaldehyde-DPX dosimetry in the F344 rat.**

Panel A: calibration of the PBPK model using data from high and low tumor incidence sites. Panel B: model prediction compared against data from high tumor incidence site. Dashed line in panel A shows the extrapolation outside the range of the calibrated data.

Source: Cohen-Hubal et al. (1997).

- 2 expect a range of 25% (Chang et al., 1983) to 45% (Barrow et al., 1983) decrease in minute
 3 volume in F344 rats at the exposure concentration of 15 ppm. Explicit omission of this effect in
 4 the modeling is, however, not likely to be a source of major uncertainty in the modeled results

This document is a draft for review purposes only and does not constitute Agency policy.

1 for uptake of formaldehyde in the rat nose for the following reason. The CFD model for the
2 F344 rat was calibrated to fit the overall experimental result for formaldehyde uptake in the F344
3 rat at 15 ppm exposure concentration. This was carried out by adjusting the mass transfer
4 coefficient used as boundary condition on the absorbing portion of the nasal lining. Thus, the
5 reflex bradypnea occurring in those experimental animals is phenomenologically factored into
6 the value used for the boundary condition. Nonetheless, some error in the localized distribution
7 of uptake patterns may be expected, even if the overall uptake is reproduced correctly.
8 Furthermore, since the same value for the mass transfer coefficient was used in human
9 simulations (as obtained from calibration of the rat model), there is additional uncertainty in the
10 modeled human flux estimates. This issue was not addressed by Kimbell et al. (2001a, b),
11 Conolly et al. (2004), or Schlosser et al. (2003), and we are unable to assess the extent of this
12 error more accurately.

13

14 **3.7.6. PBPK Modeling of DNA Protein Cross-Links (DPXs) Formed by Formaldehyde**

15 **3.7.6.1. PBPK Models for DPXs**

16 As can be seen from the previous sections, measuring the distribution of the absorbed
17 formaldehyde and identifying its form have proven difficult. Because of the high reactivity of
18 formaldehyde, rapid metabolism of formaldehyde, and complexity of formate clearance, dose
19 surrogates (or biomarkers) of exposure have been used to characterize the extent of absorption
20 and distribution of formaldehyde. As with other soluble and reactive gases, typical PBPK
21 models that predict steady-state blood concentrations are not useful for predicting formaldehyde
22 dosimetry at this time. As noted previously, inhalation exposure to formaldehyde has not been
23 shown to increase blood formaldehyde levels. Thus, most modeling efforts for formaldehyde
24 have focused on disposition at the site of contact.

25 As discussed earlier, the concentration of DPXs formed by formaldehyde has been
26 treated as a surrogate for the tissue dose of formaldehyde in earlier efforts by Casanova et al.
27 (1991) and in EPA's efforts to update its health assessment of formaldehyde (Hernandez et al.,
28 1994). These efforts used data from rats and rhesus monkeys (Casanova et al., 1991, 1989).
29 Using DPXs in this manner allowed the incorporation of both clearance and metabolism of
30 formaldehyde and the incorporation of the effect of saturation on detoxification of formaldehyde
31 at higher doses. Calculation of the average DPX concentration from these data was seen as a
32 surrogate for the area under the curve (AUC) of the reactive formaldehyde species in the
33 epithelium. Based on these data, Casanova et al. (1991) developed a PBPK model for predicting
34 DPXs in these species and for extrapolating to the human.

1 The Casanova et al. (1991) model consists of three anatomical compartments
2 representing different parts of the upper respiratory tract of the rhesus monkey. The results
3 indicated a 10-fold difference in DPX formation between rats and monkeys, due primarily to
4 species differences in minute volume and differing quantities of DNA in the nasal mucosa.
5 Casanova et al. (1991) then developed a monkey/rat scaling factor for these parameters by taking
6 the ratio of nasal mucosa tissue between the two species, a determinant that was proportional to
7 the total body weight differences between the two species. Using these scaling factors in their
8 model, the authors' predictions in monkey (based on the rat data) were in close agreement with
9 observed DPXs in monkey, particularly at higher formaldehyde concentrations. However, the
10 model overpredicted DPX formation in the monkey at lower formaldehyde concentrations.
11 Subsequent rat-human and monkey-human scaling results predicted much lower DPX formation
12 in man. Again, the values obtained at lower concentrations may have been overpredicted, as was
13 the case for the rat-monkey extrapolation.

14 Georgieva et al. (2003) developed a model for the uptake and disposition of
15 formaldehyde in the rat nasal lining. This model was designed to predict the distribution of
16 formaldehyde in the nasal mucosa. The model indicated that, at 6 ppm exposure, a steady-state
17 elevation of 15–20 μM formaldehyde would be achieved within 30 seconds. Furthermore, this
18 same elevation was predicted when the exposure was 6 ppm formaldehyde for 60 minutes.
19 Given that human blood formaldehyde levels are predicted to be about $100 \pm 15 \mu\text{M}$ (Heck et al.,
20 1985) and assuming that blood formaldehyde concentration is roughly equivalent to the
21 concentration predicted at the basement membrane of the epithelium, this model predicts roughly
22 a 15–20% increase in blood formaldehyde. However, it should be noted that a 40-minute
23 inhalation exposure of humans to 1.99 ppm formaldehyde did not lead to a measurable increase
24 in blood formaldehyde (Heck et al., 1985).

25 Franks (2005) published a mathematical model for predicting the disposition of
26 formaldehyde in the human nasal mucosa and blood. The calculated concentrations of
27 formaldehyde in the mucus, the epithelium, and the blood attained steady-state profiles within a
28 few seconds of exposure. The increase of the formaldehyde concentration in the blood was
29 predicted to be insignificant compared with the existing pre-exposure levels in the body: an
30 increase of 0.00044 mg/L in blood formaldehyde following exposure to 1.9 ppm formaldehyde
31 for up to 8 hours. The model described formaldehyde concentration gradients across the mucus,
32 epithelial, and submucosal compartments in the human nose. Transport of formaldehyde was
33 governed by the following processes: diffusional (in the mucus); a combination of diffusional,
34 two first order terms representing intrinsic reactivity of formaldehyde and binding to DNA, and
35 Michaelis-Menten kinetics representing enzymatic metabolism (in the epithelial layer); a first-

1 order term representing nonenzymatic removal governed by the blood perfusion rate (in the
2 submucosal compartment). The model used the values for the first order reaction rate constants
3 and the Michaelis-Menten parameters (V_{\max} and K_m) estimated by Conolly et al. (2000) in their
4 model for extrapolating the rat and rhesus monkey data to the human. The modeling in Franks
5 (2005) was not calibrated or validated against experimental data, but the predictions of
6 negligible penetration of free formaldehyde to the blood are qualitatively in agreement with the
7 conclusions in Heck et al. (1985).

8 Following the efforts by Casanova and coworkers, Cohen-Hubal et al. (1997), Conolly et
9 al. (2000), and Georgieva et al. (2003) developed models that linked local formaldehyde flux
10 from CFD models to DPX predictions. The focus here will be on the Conolly et al. (2000) effort
11 for the following two reasons: it explicitly incorporates regional formaldehyde dosimetry in the
12 nasal lining by using results from CFD modeling of airflow and gas uptake and it brings data
13 across species (rat and rhesus monkey) to bear on model calibration, such a situation being
14 relatively rare in chemical health risk assessments.

15 16 ***3.7.6.2. A PBPK Model for DPXs in the F344 Rat and Rhesus Monkey that Uses Local*** 17 ***Tissue Dose of Formaldehyde***

18 In earlier risk assessment efforts (Hernandez et al., 1994; Casanova et al., 1991; U.S.
19 EPA, 1991b), the average DPX concentration was considered a surrogate tissue dose metric for
20 the AUC of the reactive formaldehyde species. Conolly et al. (2003) assigned a more specific
21 role for DPXs, treating local DPX concentration as a dose surrogate indicative of the
22 intercellular concentration of formaldehyde, leading to formaldehyde-induced mutations. These
23 authors indicated that it was not known whether DPXs directly induced mutations (Conolly et
24 al., 2003; Merk and Speit, 1998). This is discussed in detail in the mode-of-action sections in
25 this document. The Conolly et al. (2000) model for the disposition of inhaled formaldehyde gas
26 and DPX in the rat and rhesus nasal lining is relatively simple in terms of model structure
27 because it consists of a single well-mixed compartment for the nasal lining as follows:

- 28
29
- 30 1. Formaldehyde flux to a given region of the nasal lining is provided as input to the
31 modeling and is obtained in turn as the result of a CFD model. This flux is defined as the
32 amount of formaldehyde delivered to the nasal lining per unit time per unit area per ppm
33 of concentration in the air in a direction transverse to the airflow. It is locally defined as
34 a function of location in the nose and the inspiratory flow rate and is linear with exposure
concentration.
 - 35 2. The clearance of formaldehyde from the tissue is modeled as follows:

- a. a saturable pathway representing enzymatic metabolism of formaldehyde, which is primarily by formaldehyde dehydrogenase (involving Michaelis-Menten parameters V_{\max} and K_m)
 - b. a separate first-order pathway, which is assumed to represent the intrinsic reactivity of formaldehyde with tissue constituents (rate constant k_f)
 - c. first-order binding to DNA that leads to DPX formation (rate constant k_b)
3. The clearance or repair of this DPX is modeled as a first order process (rate constant k_{loss}).

DPX data. DPX concentrations were estimated from a study by Casanova et al. (1994) in which rats were exposed 6 hours/day, 5 days/week, plus 4 days for 11 weeks to filtered air (naive) or to 0.7, 2, 6, or 15 ppm (0.9, 2.5, 7.4, or 18 mg/m³) formaldehyde (pre-exposed). On the 5th day of the 12th week, the rats were then exposed for 3 hours to 0, 0.7, 2, 6, or 15 ppm ¹⁴C-labeled formaldehyde (with pre-exposed animals exposed to the same concentration as during the preceding 12 weeks and 4 days). The animals were sacrificed and DPX concentrations determined at two sites in the nasal mucosa. Conolly et al. (2000) used these naive rat data to develop a PBPK model that predicted the time-course of DPX concentrations as a function of formaldehyde flux at these sites.⁹

3.7.6.3. Uncertainties in Modeling the Rat and Rhesus DPX Data

3.6.6.3.1. Half-life of DPX repair. In the development of the PBPK model for DPXs, Conolly et al. (2000) assumed a value of 6.5×10^{-3} minute⁻¹ for k_{loss} , the first-order rate constant for the clearance (repair) of DPXs, such that the DPXs predicted at the end of a 6-hour exposure to 15 ppm were reduced to exactly the detection limit for DPXs in 18 hours (the period between the end of 1 day's 6-hour exposure and the beginning of the next). This determination of rapid clearance was based on an observation by Casanova et al. (1994) that the DPX concentrations observed in the pre-exposed animals were not significantly higher than those in naïve animals (in which there was no significant DPX accumulation). However, in vitro data (Quievryn and Zhitkovich, 2000) indicate a much slower clearance, with an average k_{loss} of 9.24×10^{-4} minute⁻¹.

Subramaniam et al. (2007) examined the Casanova et al. (1994) data and argued that there was a significantly decreased (~ 40%) level of DPXs in high tumor regions of pre-exposed animals vs. naive animals at 6 and 15 ppm and that the weight of the tissues dissected from those

⁹ Subramaniam et al. (2007) who also used the same data verified that they were on naïve rats; however, Conolly et

1 regions increased substantially, indicating a thickening of the tissues. After testing the outcome
2 of changing the tissue thickness in the PBPK model for DPXs, it was apparent to these authors
3 that such a change alone could not account for the dramatic reduction in DPX levels after
4 pre-exposure, even with the higher value of k_{loss} used by Conolly et al. (2000). Therefore, in
5 addition to the gross increase in tissue weight, these data indicated either an induction in the
6 activity of enzymes that remove formaldehyde (aldehyde and formaldehyde dehydrogenase) or
7 other changes in the biochemical properties of the highly exposed tissue that must have occurred.
8 Given such a change, Subramaniam et al. (2007) concluded that the experimental results in
9 Casanova et al. (1994) were consistent with the smaller experimental value of k_{loss} indicated by
10 the Quievryn and Zhitkovich (2000) data. In particular, they argued that if V_{max} increased with
11 exposure (in a tissue region- and dose-specific manner), then it was possible to explain the naïve
12 vs. pre-exposed data of Casanova et al. (1994), with the value of k_{loss} effectively measured in
13 vitro by Quievryn and Zhitkovich (2000). Furthermore, this value was measured directly, rather
14 than obtained by indirect interpretation of measurements made at only two time points where
15 significant changes in the tissue had occurred. Therefore, Subramaniam et al. (2007) considered
16 the use of this lower value for k_{loss} to be more appropriate. The same lower value of k_{loss} was
17 also used by Georgieva et al. (2003). Consequently, they reimplemented and reoptimized the
18 Conolly et al. (2000) model with this modification and found that the fit so obtained to the acute
19 DPX data was excellent. The reimplemented model will be used in this assessment, and more
20 details can be found in Subramaniam et al. (2007).

21 It should be noted that this slower DPX repair rate was obtained in an in vitro study by
22 using human cell lines that were transformed and immortalized. However, it appears that DPX
23 repair in normal cells would be even slower. When nontransformed freshly purified human
24 peripheral lymphocytes were used instead, the half-life for DPX repair was about 50% longer
25 than in the cultured cells (Quievryn and Zhitkovich, 2000).

26

27 **3.6.6.3.2. Statistical uncertainty in parameter estimates and extrapolation.** Klein et al. (2010)
28 developed methods for deriving statistical inferences of results from PBPK models, and used the
29 structure of the Conolly et al. (2000) model for demonstrating their methods, specifically
30 because of the sparse time-course information in the above DPX data. However, they used the
31 value of k_{loss} deduced from Quievryn and Zhitkovich (2000) and fitted the model simultaneously
32 to both the rat and rhesus monkey data, as opposed to the sequential fitting in Conolly et al.
33 (2000). They found that the predicted DPX concentrations were extremely sensitive to V_{max} and

al. (2000) state that they used data on pre-exposed rats.

1 tissue thickness as was also concluded by Georgieva et al. (2003) and Cohen-Hubal et al. (1997).
2 K_m was seen to be substantially different across species, a finding that was attributed plausibly
3 to the involvement of more than one enzyme (Klein et al., 2010; Georgieva et al., 2003). Klein
4 et al. (2010) concluded that the two efforts (Conolly et al. [2000] vs. Klein et al. [2010]) resulted
5 in substantially different predictions outside the range of the observed data over which the
6 models were calibrated.

7 The differences between these models occur in spite of the fact that both methods use all
8 the available DPX data in both species and the same model structures. At the 0.1 ppm exposure
9 concentration, in general these authors obtained three- to fourfold higher DPX concentrations
10 averaged over a 24-hour period after exposure. Furthermore, the standard deviations in Klein et
11 al. (2010) for V_{max} and K_m were an order of magnitude higher and that for k_f was 35-fold lower
12 than the corresponding standard deviations reported in Conolly et al. (2000). The relatively
13 larger standard deviation for k_f resulted in this parameter becoming negative in Conolly et al.
14 (2000) at half the standard deviation below the maximum likelihood estimate (MLE) value. Note
15 that, at a negative value of k_f , formaldehyde would be produced as opposed to being cleared
16 through its intrinsic reactivity.

17 Klein et al. (2010) concluded that these “remarkable differences outside the range of the
18 observed data suggest caution in the use of these models in a predictive sense for extrapolating to
19 human exposures.”

21 **3.7.7. Uncertainty in Prediction of Human DPX Concentrations**

22 Conolly et al. (2000) used both the rat and rhesus monkey data to predict human DPX
23 concentrations and constructed a PBPK model for the rhesus monkey along similar lines as for
24 the F344 rat. In the rhesus monkey model, they maintained the same values of k_b , k_{loss} , and k_f as
25 in the rat model but optimized the values of V_{max} and K_m against the rhesus monkey data from
26 Casanova et al. (1994). The rat and rhesus monkey parameters were then used to construct a
27 human model (see Conolly et al. [2000] for a more detailed report of implementing the rhesus
28 monkey model and the extrapolating to humans).

29 For the human, the model used the value of K_m obtained in the rhesus monkey model and
30 the epithelial thickness averaged over three regions of the rhesus monkey nose. The maximum
31 rate of metabolism, V_{max} , which was estimated independently for the rat and rhesus monkey by
32 fitting to the DPX data available for these species, was then extrapolated to the human by
33 assuming a power law scaling with body weight (BW) (i.e., $V_{max} = a \times BW^b$), and the coefficient
34 “a” and exponent “b” were derived from the independently estimated values of $(V_{max})_{RAT}$ and

1 (V_{\max})_{MONKEY}. Table 3-8 gives the values of V_{\max} and K_m in the Conolly et al. (2000)
2 extrapolation.

3 **Table 3-8. Extrapolation of parameters for enzymatic metabolism to the**
4 **human**

Parameter	F344 rat	Rhesus monkey	Human
V_{\max} (pmol/min- mm ³)	1,008.0	91.0	15.7
K_m (pmol/mm ³)	70.8	6.69	6.69

Source: Conolly et al. (2000).

5
6
7 The above scale-up procedure was an attempt to use both the rodent and primate DPX
8 data. However, laws for allometric scaling across species, such as how enzymatic metabolic
9 rates vary across organisms, are empirical regression relationships whose strength is that they are
10 based on data from multiple species and usually multiple sources of data points. For example,
11 West and Brown (2005) demonstrate that metabolic rates scale with mass^{3/4} using data from
12 organisms ranging over 27 orders of magnitude in mass (intracellular up to the largest
13 organisms). In Conolly et al. (2000) the power-law relationship is derived using two data points
14 (F344 rat and rhesus monkey for a single chemical) with log BW as x-axis and V_{\max} on y-axis.
15 Since such a regression does not have the power to delineate the curvature in the scaling
16 function, the empirical strength of the allometric relationship derived in Conolly et al. (2000) is
17 extremely weak for use in extrapolating from the rat to the human on the basis of body-weight.

18 The following observations point to the uncertainty in the values of the parameters V_{\max}
19 and K_m in the Conolly et al. (2000) models for predicting DPXs. First, K_m varies by an order of
20 magnitude across the rat and monkey models but is then considered invariant between the
21 monkey and human models (Conolly et al., 2000). Second, the values in Conolly et al. (2000)
22 for V_{\max}/K_m , the low-dose limit of the rate of enzymatic metabolism, is roughly similar between
23 the rat and monkey but lower by a factor of six in the human.

24 Another factor that can substantially influence the above extrapolation of DPXs in the
25 human is that Conolly et al. (2000) assumed the tissue to be a well-mixed compartment with
26 regard to formaldehyde interaction with DNA and used the amount of formaldehyde bound to
27 DNA per unit volume of tissue as the DPX dose metric. Considering formaldehyde's highly
28 reactive nature, the concentrations of formaldehyde and DPX are likely to have a sharp gradient
29 with distance into the nasal mucosa (Georgieva et al., 2003). Given the interspecies differences
30 in tissue thickness, there is consequent uncertainty as to whether DPX per unit volume or DPX

1 per unit area of nasal lining is the more appropriate dose metric to be used in the extrapolation.
2 In particular, it may be assumed that the cells at risk for tumor formation are only those in the
3 epithelium and that measured DPX data (in monkeys and rats) are an average over the entire
4 tissue thickness. Since the epithelial DPXs in monkeys (and presumably humans) would then be
5 more greatly “diluted” by lower levels of DPX formation that occur deeper into the tissue than in
6 rats, it could be predicted that the ratio of epithelial to measured DPXs in monkeys and humans
7 would be much higher than the ratio in rats.

8 9 **3.7.8. Modeling Interindividual Variability in the Nasal Dosimetry of Reactive and** 10 **Soluble Gases**

11 Garcia et al. (2009) used computational fluid dynamics to study human variability in the
12 nasal dosimetry of reactive, water-soluble gases in 5 adults and 2 children, aged 7 and 8 years
13 old. The sample size in this study is too small to consider the results representative of the
14 population as a whole (as also recognized by the authors). Nonetheless, various comparisons
15 with the characteristics of other study populations add to the strength of this study (see
16 Appendix B). The authors considered two model categories of gases, corresponding to maximal
17 and moderate absorption at the nasal lining. We focus here only on the “maximum uptake”
18 simulations in Garcia et al. (2009). In this case, the gas was considered so highly reactive and
19 soluble that it was reasonable to assume an infinitely fast reaction of the absorbed gas with
20 compounds in the airway lining. Although such a gas could be reasonably considered as a proxy
21 for formaldehyde, these results cannot be fully utilized to inform quantitative estimates of
22 formaldehyde dosimetry (and it does not appear to have been the intent of the authors either).
23 This is because the same boundary condition corresponding to maximal uptake was applied on
24 the vestibular lining of the nose as well as on the respiratory and transitional epithelial lining on
25 the rest of the nose. This is not appropriate for formaldehyde as the lining on the nasal vestibule
26 is made of keratinized epithelium which is considerably less absorbing than the rest of the nose
27 (Kimbell et al., 2001b).

28 The Garcia et al. (2009) study and the results of their analyses have been further
29 described and evaluated in Appendix B. Overall uptake efficiency, average flux (rate of gas
30 absorbed per unit surface area of the nasal lining) and maximum flux levels over the entire nasal
31 lining did not vary substantially between adults (1.6-fold difference in average flux and much
32 less in maximum flux), and the mean values of these quantities were comparable between adults
33 and children. These results are also in agreement with conclusions reached by Ginsberg et al.
34 (2005) that overall extrathoracic absorption of highly and moderately reactive and soluble gases
35 (corresponding to Category 1 and 2 reactive gases as per the scheme in EPA [1994]) is similar in

1 adults and children. On the other hand, Figure 6A of the paper (reproduced as Figure B-1 in
2 Appendix B), provides a different perspective on variations between the adults in flux values at
3 specific points on the nasal walls. The plot indicates that local flux of formaldehyde may vary
4 among individuals by a factor of 3 to 5 at various distances along the septal axis of the nose;
5 such an evaluation of inter-individual variability in the spatial distribution of formaldehyde flux
6 over the nasal lining is important for a highly reactive and soluble gas whose regional absorption
7 is highly nonhomogeneously distributed (see text surrounding Figure 3-8).

8

1
2
3
4
5
6
7
8
9
10
11
12

End of Volume I